THE

LONDON, EDINBURGH, AND DUBLIN

PHILOSOPHICAL MAGAZINE

AND

JOURNAL OF SCIENCE.

[SEVENTH SERIES.]

SUPPLEMENT, FEBRUARY 1934.

XXIX. *The Scattering of Homogeneous X-rays of* 0·25 to 0·4 Å.

By IVOR BACKHURST, *M.Sc., Physics Department, National Physical Laboratory, Teddington, Middlesex* *.

Introduction.

IT is well known, that on scattering, X-rays may in part, or wholly, be changed in wave-length. Theoretical expressions for the intensities of the modified and unmodified components of scattered radiation have been built up by Compton, Woo, Jauncey, Wentzel, Waller, Dirac, and others. Good agreement has been found between experiment and theory when short X-rays or γ-rays are scattered by light elements. The scattered rays are then practically completely modified and incoherent, and a relative angular distribution of intensity is found exactly similar to that calculated for scattering by a single electron.

For X-rays of medium wave-length or for scattering by substances consisting of other than very light atoms, the process of scattering is complicated (*a*) by interference between the unmodified or coherent radiation scattered by electrons belonging to the same atom, resulting in

* Communicated by Dr. G. W. C. Kaye, O.B.E.

"atomic scattering" and (*b*) by interference between coherent radiation scattered by atoms of the same molecule. With a gaseous scatterer, interference of type (*a*) alone may be appreciable, as in the work of Wollan[1] and Herzog[2], or with longer wave-lengths type (*b*) may become evident, as shown by Debye[3], Bewilogua[4], and Gajewski[5]. The additional interference phenomena occasioned by the crystalline structure of solids are well known, and from them consistent values of atomic scattering have been deduced. The wave-lengths and angles of scattering then employed have been such that the intensity of incoherent scattered radiation has been nearly or quite negligible.

The question calls for attention as to how far agreement between experiment and theory may be obtained when crystalline solids are made to scatter radiation under conditions such that neither coherent nor incoherent constituents are of negligible intensity. Attempts to answer this question are naturally beset with a number of experimental complications, the neglect of any of which may make satisfactory comparison between experiment and theory impossible. Also, a considerable degree of uncertainty must be inseparable from results obtained in experiments involving measurement of wave-length change when primary, or filtered primary, X-rays are used, and, in the present investigation, homogeneous rays produced by crystal diffraction have alone been employed. Some important features of the work are enumerated below :—

(1) Sensitive control maintained of current and voltage of X-ray tube, held in continuous operation throughout each experiment.

(2) Automatic time measurement of X-ray exposure.

(3) Reduction of stray radiation, except for small scattering angles, to under 1 per cent. of total measured intensity.

(4) Use of very small scatterers in order to reduce error occasioned by double scattering.

(5) Correction made for differential absorption of modified and unmodified radiation in material of scatterer, ionization chamber window, and in filter used to eliminate characteristic radiation excited from scatterer.

(6) Absorption of rays in ionization chamber measured in order to obtain good estimation of change of sensitivity of chamber with change of wave-length.

(7) Measurement made of the proportion of polarized radiation present in the incident beam.

(8) Absolute value of angular scattering determined by direct comparison of intensities of incident and scattered beams.

Apparatus and General Method of Experiment.

The full-wave rectification constant potential X-ray plant used has previously been described[6], [7]. In part of the work the supply current and voltage were maintained constant by means of potentiometers [7], but it was afterwards found equally satisfactory to use a shunted moving coil galvanometer to measure the high tension current directly and to rely on the readings of an attracted disk high tension voltmeter. The image produced by a beam of light reflected from the voltmeter mirror travelled 2 cm. (at 1·5 metres distance) for 1 per cent. change of voltage and the image from the galvanometer mirror 21 cm. for 1 per cent. change of high tension current. This degree of sensitivity of the galvanometer was secured by means of an initial twist on the suspension. Under the conditions of use the instrument was practically aperiodic and rapidly followed any supply fluctuations. The valves of the constant potential plant were of the glass bulb pattern and, in order to reduce the Wellauer [8] effect, it was found a definite advantage to use metal cone screens around those valves connected to the positive high tension lead. Details of such an arrangement have been given by Albrecht [9].

The X-ray exposures were automatically timed, either by the exposure meter previously described[7] or by a sector wheel in the case of the absolute measurements. The method of mounting the X-ray tube filament was altered from that previously shown diagrammatically[7]. In order to avoid the effects of vibration due to the forced oil cooling of the anticathode it was found better to clamp the filament ends in a small steel mount, having mica insulation for one end, and to screw this unit to the tubular cathode stem, the insulated filament end being connected by copper flex to the inner cathode rod. This

has proved quite effective, the filament now in use having been mounted over a year ago. The primary X-ray beam, after being limited by a lead slit system clamped to the X-ray tube, passed through an aluminium crystal 3 mm. thick, cut with two plane faces each parallel to the same (110) crystal plane. The crystal mount was clamped to the X-ray tube and the crystal turned so that a beam of the desired wave-length was diffracted from a (111) plane situated perpendicular to the cut faces. The diffracted beam passed through two lead slit apertures forming part of the spectrometer on which was mounted the scatterer. The scattered beam also passed through two lead apertures, the second of which defined the cone of rays entering the ionization chamber. Great care was taken to exclude stray scattered radiation from incidence on the scatterer or entry into the ionization chamber. The X-ray tube was exhausted through a curved lead pipe 2 feet long and the pump end of the pipe was further shielded with lead sheet. The ionization chamber was lead covered, except for an aperture at each end, and carefully counterpoised. The ionization current was received by a small air condenser coupled to a potentiometer, a Compton electrometer being used as a null instrument.

The amount of the X-ray beam absorbed by the ionization chamber was measured, by means of a gold leaf electroscope, for zero scattering angle. The change of sensitivity of the ionization chamber with scattering angle could then be calculated using Compton's [10] [11] formulæ :—

$$R=1-0\cdot85\epsilon^{-\mu''\bar{x}}(\omega\tau/\mu)_{Br}\,.\,\lambda/\lambda''-\epsilon^{-\mu'\bar{x}}\,.\,\sigma/\mu \quad . \quad (1)$$

and

$$\lambda'-\lambda=\frac{h}{mc}.\,\text{vers}\,\phi \quad . \quad . \quad . \quad . \quad . \quad (2)$$

where

μ, μ', μ'' are linear absorption coefficients in Br of the incident rays, rays scattered in the ionization chamber, and BrK rays respectively;

λ, λ', λ'' wave-lengths of incident, modified, and BrK rays respectively;

$\bar{x}$ effective distance from the path of the X-ray beam to the walls of the ionization chamber;

ω fluorescence yield,

R fraction of absorbed rays utilised in producing ionization.

The ionization chamber contained a mixture of air and methyl bromide and μ_ϕ, the absorption coefficient appropriate to rays modified by scattering at the angle ϕ, was calculated using equation (2) from the experimental value of μ. Fortunately, R did not change rapidly as ϕ was altered and, as the ratio R_ϕ/R_0 was the quantity that mattered, it was not necessary to know $\bar{x}$ accurately. Compton's value of 0·565 for ω_{Br} was assumed.

Correction was made, when obtaining relative angular intensities, for the circumstance that the average scattering angle corresponding to a given setting of the ionization chamber aperture (rectangular) was not quite the same as the scattering angle proper to the centre of the aperture. Taking rectangular coordinates x and y in the plane of the aperture, with origin at the centre,

$$\sin^2\phi_{(x,\,y)} = \frac{y^2+(a\sin\phi+x\cos\phi)^2}{a^2+x^2+y^2},$$

where "a" is the distance scatterer to aperture and $\phi_{(x,\,y)}$ is the scattering angle proper to the point $(x,\,y)$. For a particular ionization chamber angle the average value, with x varying, of $\phi_{(x,\,y)}$ may be found for each of a number of y values, and the mean of these averages gives the effective value of ϕ. The greatest difference occurring between effective and ionization chamber angle, *i. e.*, that at 30° and 150°, was 0° 39′. For the absolute measurement of scattering coefficients, use was made of a circular aperture too small for such a correction to be needed. The rectangular aperture used for the relative measurements was 2·8 cm. high and 1·0 cm. wide, distant 9·0 cm. from the spectrometer axis. The centre part of the aperture thus included an angular range of scattering of 6° 22′.

Distribution of Intensity of Scattered Radiation with Angle.

Fig. 1 shows the relation between intensity and scattering angle when using a beryllium scatterer in the form of powder contained in a cylindrical celluphane cell 2 mm.

in diameter and 2 cm. high. The intensities are relative, that at 90° being taken as unity. The full curve (1) is experimental, the dotted curve (2) is that calculated from Dirac's[12] equation,

$$I_\phi = ZI_e(1+\alpha \text{ vers } \phi)^{-3} \quad . \quad . \quad . \quad . \quad (3)$$

where

$$\alpha = h\nu/mc^2, \quad I_e = \frac{I_0 e^4}{2m^2c^4} \cdot (1+\cos^2\phi) \cdot f_P.$$

Fig. 1.

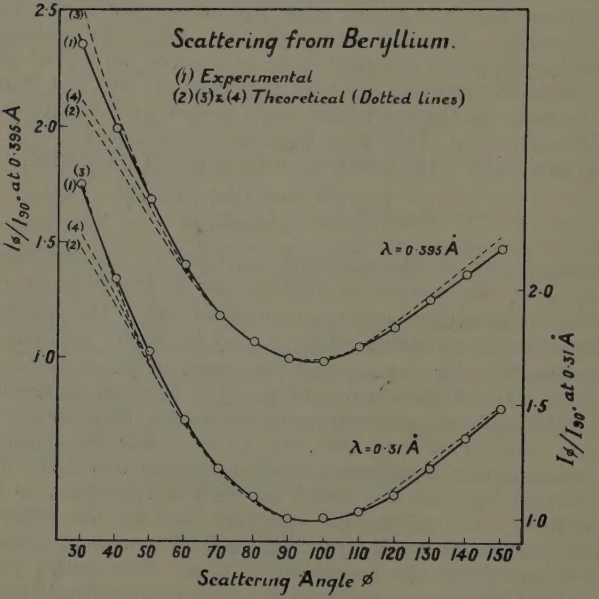

and f_P (see below) is an added factor allowing for partial polarization of the incident rays, while curve (3) is obtained from Compton's[13] equation (with relativity correction added)

$$I_\phi = I_e\left\{ F^2 + \left(Z - \frac{F^2}{Z}\right)(1+\alpha \text{ vers } \phi)^{-3} \right\}. \quad . \quad (4)$$

and curve (4) from Woo's [14] equation

$$I_\phi = I_e \left\{ F^2(1-e^{-2M}) + \left(Z - \frac{F^2}{Z}\right)(1+\alpha \text{ vers } \phi)^{-3} \right\} \quad . \quad (5)$$

where

$$F = \int_0^\alpha U(r) \frac{\sin kr}{kr} \, . \, dr, \quad k = \frac{4\pi}{\lambda} \sin(\phi/2), \quad U(r) \text{ is}$$

the radial charge density of the atom measured in electrons per unit distance and e^{-2M} is the temperature factor. In Table I., columns (1), (2), and (3) correspond to curves (1), (2), and (3) respectively. The percentage differences shown are between (1) and (3) for angles less than 60° and between (1) and (2) for larger angles, (3) being then practically indistinguishable from (2).

For angles greater than 60° it seems probable that what difference exists between curves (1) and (2) may quite reasonably be attributed to error involved in correcting for change of sensitivity of the ionization chamber at different scattering angles. Equation (3) is only applicable to the incoherent modified radiation scattered by an atom ; on account of the incoherency, the radiation intensity from each of the Z electrons of the atom may then be regarded as simply additive, and the result is the same as that obtained on J. J. Thomson's classical theory, multiplied by the approximate relativity correction factor $(1+\alpha \text{ vers } \phi)^{-3}$. Dirac's theory takes no account of the simultaneous existence of any coherent scattered radiation and may be expected to apply only when conditions of atomic number, scattering angle, and wave-length are such as to minimize coherent scattering. The proportion of coherent unmodified radiation scattered by beryllium at 0·31 and 0·395 Å. was found (see below) to be very small, so that it forms quite a suitable scattering substance with which to test equation (3).

Compton's equation (curve 3) is intended to take into account the unmodified radiation, as well as the modified, but strictly only for a gaseous scatterer, that is, no account is taken of interference between coherent radiation scattered by different atoms.

Equation (5) relates to scattering from crystalline solids and expresses the combined intensities of diffusely scattered coherent radiation and of incoherent scattered radiation. It has been derived from equation (4) by

TABLE I.

Ratio $I\phi/I_{90°}$.

	λ=0·31 Å.				λ=0·395 A.			
		Theory.				Theory.		
ϕ.	Expt. (I).	(2).	(3).	Diff. Per cent.	Expt. (I).	(2).	(3).	Diff. Per cent.
30°	2·453	2·178	2·471	0·7	2·355	2·066	2·527	7·3
40	2·044	1·923	2·019	−1·2	1·994	1·836	2·048	2·7
50	1·729	1·653	..	..	1·690	1·596	1·687	−0·2
60	1·429	1·413	..	−1·1	1·407	1·372	..	−2·5
70	1·220	1·212	..	−0·7	1·185	1·189	..	0·3
80	1·099	1·072	..	−2·5	1·073	1·063	..	−0·9
90	1·000	1·000	..	..	1·000	1·000	..	..
100	1·002	0·993	..	−0·9	0·989	1·001	..	1·2
110	1·033	1·044	..	1·1	1·051	1·057	..	0·6
120	1·107	1·137	..	2·7	1·132	1·154	..	1·9
130	1·225	1·254	..	2·4	1·256	1·277	..	1·7
140	1·356	1·379	..	1·7	1·367	1·408	..	3·0
150	1·484	1·496	..	0·8	1·475	1·530	..	3·7

subtracting from the right-hand side the quantity $I_e F^2 e^{-2M}$ to allow for the intensity diverted to the regularly reflected spectra. The radiation received by the ionization chamber, however, includes the regularly reflected intensity, which is averaged over the angular range of ϕ of the aperture, in this case about $6\frac{1}{2}°$. Assuming that equation (5) is correct, this averaged intensity, if no maxima remain, cannot be greater than $I_e F^2 e^{-2M}$ although, on account of interference, it may be less. The experimental curves (1), on this reasoning, should thus fall on, or somewhat below, curves (3) representing equation (4), but should be definitely above curves (4) representing equation (5). It will be seen that, within a few per cent., this is, in fact, the case. Rather similar results to this (see below) have recently been obtained by Jauncey and Williams[15], Coven [16], and Harvey[17] in comparing the scattering from powdered salts, such as NaF and KCl with that from neon and argon.

It is difficult to evaluate the right-hand side of equation (5) satisfactorily, on account of the uncertainty of the temperature factor, but the approximation yielding curves (4) was obtained as follows. According to Waller's[18] modification of Debye's[19] theory,

$$M = -P \cdot \text{vers}\,\phi \cdot \frac{f(x)}{x} \quad . \quad . \quad . \quad . \quad (6)$$

or assuming zero-point energy,

$$M = -P \cdot \text{vers}\,\phi \cdot \left\{ \frac{1}{4} + \frac{f(x)}{x} \right\} \quad . \quad . \quad . \quad (7)$$

$$P = \frac{3Nh^2}{k\lambda^2 A \Theta}, \quad x = \frac{\Theta}{T},$$

A is atomic weight, Θ is characteristic temperature, λ is wave-length in cm., T is absolute temperature, k is Boltzmann's gas constant, and $f(x)$ is evaluated by Debye. For beryllium, Θ was found to be 1033° abs. by F. Simon[20] from low temperature specific heat measurements, and similar measurements at high temperatures by Magnus and Holzmann[21] have been found to give good agreement with the specific heat theory of Born and Brody[22], if this value of Θ is taken. Debye's theory was worked out for a simple cubic lattice, but although beryllium has

a hexagonal structure, equations (6) and (7) should furnish an approximation for the temperature factor. Equation (7) has been used to obtain curves (4), since it has been found[23] to agree best with experiment. Values for F for beryllium have been taken from the tables given by James and Brindley[24].

The incident rays were only slightly polarized (see below) and the maximum alteration produced by the correction factor f_p in the ordinates of the curves (2), for example, amounted to an increase at 30° and 150° of 2·5 per cent. at 0·31 Å. and 1·2 per cent. at 0·395 Å. It was ascertained by absorption measurements that the wave-length change of the scattered rays was that given by equation (2). The size of the scatterer and mass irradiated (approximately 0·017 grams) were therefore sufficiently small for the effect of twice scattered radiation to be inappreciable.

In order that equation (5) should correspond more closely with the expression for scattering from a gas atom derived by Wentzel [25] and independently by Waller and Hartree [26], [27] on the basis of wave-mechanics, Woo[28] has suggested that the part of (5) representing intensity of incoherent scattering, viz. :

$$I_e\left\{\left(Z-\frac{F^2}{Z}\right)(1+\alpha \text{ vers } \phi)^{-3}\right\}$$

should be replaced by

$$I_e\left\{(Z-\sum_{r=1}^{z}E_r^2)(1+\alpha \text{ vers } \phi)^{-3}\right\},$$

where E_r is the average amplitude of waves scattered by the rth electron of the atom, the atomic structure factor F being equal to $\sum_{r=1}^{z}E_r$. Since $\sum_{r=1}^{z}E_r^2$ is greater than F^2/Z[29], the effect of this would be to slightly decrease the ordinates of curves (4). It has further been suggested by Woo[14], that when scattering from powdered crystals takes place, there is additional coherent diffuse scattering similar to that calculated by Debye[30] for amorphous materials, and the total intensity of the coherent radiation should be equal to

$$I_e\{[1-e^{-2M}]+[1-f(u)]\} \cdot F^2$$

instead of

$$I_e(1-e^{-2M})F^2, \quad \text{where} \quad f(u)=\left(\frac{3}{u^3}\right)(\sin u - u\cos u),$$

$$u=\frac{8\pi a}{\lambda}\ .\ \sin(\phi/2),$$

and "a" is the effective radius of the scattering unit.

If ϕ is not less than about 40°, $f(u)$ for both 0·31 and 0·395 Å. has a maximum value less than 0·01 if an effective atomic radius not less than 1 Å. is assumed, hence the effect of the term $[1-f(u)]$ would be practically to double the theoretical value of the diffuse coherent scattering. This would bring curves (4) considerably nearer to curves (1), but measurements of the proportion of modified to unmodified radiation (see below) are in complete disagreement with the inclusion of a term such as $[1-f(u)]$ and it has accordingly been regarded as inapplicable under the conditions of experiment.

The main object of this part of the work was, however, to test equation (3) with homogeneous incident radiation, and it is hoped to publish later an account of some experiments, still in progress, dealing with the simultaneous existence, at a given scattering angle, of regularly reflected, diffusely scattered coherent, and incoherent radiation. Assuming that equations (4) and (5) are in the main correct, it would follow that provided λ and ϕ are such as to make F^2 negligible compared with $Z(1+\alpha \text{ vers } \phi)^{-3}$, then on account of the incoherent nature of the modified radiation, the scattering should be independent of the state of molecular aggregation.

Angular intensity measurements were made, with an incident wave-length of 0·31 Å., on paraffin wax, water, turpentine, benzene, alcohol, and benzophenone. At angles greater than 60°, the relative angular intensities were, within about 2 per cent., the same for all these scattering materials as for beryllium and may therefore be regarded as identical within the limits of experimental error. Each liquid scatterer was contained in an extremely thin glass tube of about 2 mm. diameter, contracted to a capillary at the upper end to check evaporation and joined at the lower end to a thicker glass tube of similar bore with a rubber extension containing mercury and compressed by an adjustable clip. The scattering was measured with the liquid level at a mark just at the lower

edge of the X-ray beam and also at a mark just above the upper edge of the beam. The effect of scattering from the container could then be eliminated from the result.

Measurement was made of the scattering from benzophenone in both the liquid and solid state. Change of state was conveniently brought about by condensing on the scatterer rays from an arc lamp ; this avoided any increase in stray scattering. At large angles, change of state produced no change in relative angular scattering. In all these experiments the stray scattering was kept to quite a small fraction of the total intensity measured, and the appropriate correction made.

Relative Proportion of Modified and Unmodified Radiation.

The proportion of radiation modified on scattering was found, for a number of elements, by absorption measurements on the incident and scattered beams, it being assumed that the modified radiation at a given scattering angle consisted entirely of one wave-length, *i. e.*, that given by equation (2). The excited characteristic radiation of a scatterer, when too penetrating to be absorbed in the aluminium window of the ionization chamber, was absorbed by a filter placed between the scatterer and the ionization chamber slit next to the scatterer. The amount of radiation scattered from the filter and able to enter the ionization chamber was small enough to be negligible. In every case the filter was sufficiently thick to reduce the intensity of the transmitted characteristic radiation to an amount negligible compared with that of the combined modified and unmodified scattered radiation. Account was taken of the different absorption of the modified and unmodified beams in the scatterer, filter, and ionization chamber window, and the extent of the necessary corrections may be gauged from Table V., given for 0·31 Å. as an example. As a result of preliminary measurements it was decided to use a copper absorbing screen to determine wave-length. Aluminium, although very convenient for the measurement of thickness, has at wave-lengths near 0·3 Å. a less rapid rate of change of absorption coefficient than copper, and existing values for the total absorption coefficient of aluminium were found to be insufficiently exact for the purpose. Lead proved too inconvenient on account of lack of rigidity and difficulty of measuring effective thickness.

Each scatterer was in the form of a narrow flat strip of sufficient width to ensure that all the scattered rays received by the ionization chamber passed through the plane face of the strip when it was placed so that this plane bisected the scattering angle. Since the angle of the scattered cone of rays entering the ionization chamber was small, the intensity ratio of the two beams on leaving the scatterer was taken to be

$$\frac{s_2\int_0^d e^{-2\mu_1 x \operatorname{cosec}\phi/2}\,.\,dx}{s_1\int_0^d e^{-(\mu_1+\mu_2)x\operatorname{cosec}\phi/2}\,.\,dx} = \frac{s_2k_2(1-e^{-k_1d})}{s_1k_1(1-e^{-k_2d})},$$

where s_1 and s_2 are the scattering coefficients, μ_1 and μ_2 the linear absorption coefficients, for the scatterer, of the unmodified and modified beams respectively,

$$k_1=2\mu_1 \operatorname{cosec}\phi/2, \quad k_2=(\mu_1+\mu_2)\operatorname{cosec}\phi/2, \quad \text{and} \quad \text{“}d\text{”}$$

is the thickness of the scatterer. The ionization current was measured (1) without an absorbing screen, (2) with an absorbing screen in the incident beam, (3) with the same screen in the scattered beam. Denoting these current values by I_1, I_2, I_3 respectively, the ratio s_2/s_1 was obtained from the relation

$$\frac{s_2}{s_1}=\frac{R_2(R_3-R_1)}{R_1(R_2-R_3)}\cdot\frac{k_2(1-e^{-k_1d})}{k_1(1-e^{-k_2d})}\cdot\frac{1}{f_{Br}}e^{(\mu_2'-\mu_1')t_F+(\mu_2''-\mu_1'')t_W},$$

where $$R_1=I_2/I_1 \quad \text{and} \quad R_3=I_3/I_1.$$

R_2, the corresponding absorption ratio for the modified part of the scattered beam alone and not directly measurable, was calculated from R_1 by means of equation (2); μ_2', μ_1', t_F are the absorption coefficients for and thickness of the filter used to stop the excited characteristic radiation and μ_2'', μ_1'', t_W are similar quantities for the ionization chamber window; f_{Br} is the sensitivity of the ionization chamber to the modified beam divided by its sensitivity to the unmodified beam, the variation in sensitivity being obtained in the same manner as that described above for the modified and incident beams. A series of measurements for wave-lengths of 0·25, 0·31, and 0·395 Å. were made at a scattering angle of 150°, and the results are shown in fig. 2 and Table II. It may be remarked that at large

scattering angles error due to the presence of twice scattered radiation is minimized.

Fig. 2.

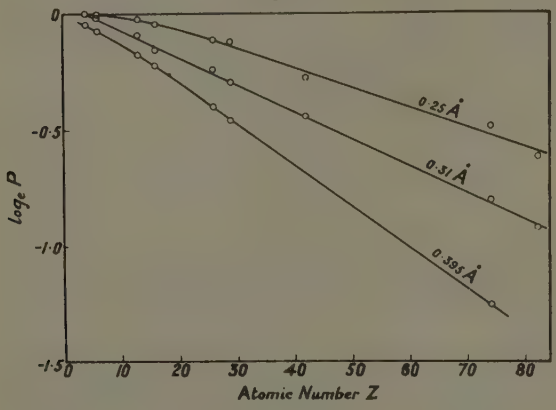

TABLE II.

Percentage of Modified Radiation at $\phi = 150°$.

Element.	0·25 Å.	0·31 Å.	0·395 Å.
Be (4)	100	100	95·2
C (6)	99	98·8	92·6
Al (13)	97·6	91·2	84·0
S (16)	95·2	85·7	80·2
Fe (26)	89·5	78·5	67·1
Cu (29)	88·7	74·6	63·5
Mo (42)	75·8	64·4	—
W (74)	61·3	44·9	28·6
Pb (82)	54·0	39·8	—

In fig. 2, $\log_e P$ where $P = s_2/(s_1+s_2)$ is plotted against atomic number Z, and it is seen that the relation is practically linear for $Z > 20$. The expression

$$\log_e P = -8{\cdot}3\frac{(Z-g)}{(74-g)} \cdot \lambda^2$$

then holds where "g" is a function of λ and lies between 4 and 14 for $0{\cdot}25<\lambda<0{\cdot}395$ Å. For this wave-length range it may be assumed that at $\phi=150°$ the temperature factor e^{-2M} of equation (5) is negligible. The incoherent part of the scattered intensity is represented by

$$I_e\left(Z-\frac{F^2}{Z}\right)(1+\alpha\,.\,\text{vers}\,\phi)^{-3},$$

so that s_2/s_1 should be equal to

$$\left(Z-\frac{F^2}{Z}\right)(1+\alpha\,.\,\text{vers}\,\phi)^{-3}/F^2.$$

TABLE III.

Percentage of Modified Radiation at $\phi=150°$.

Element.	Wave-length in Å.	Experiment (from fig. 2).	Theory. Woo.	Diff.	Heisenberg.	Diff.
Na (11)	0·395	86·5	92·3	5·8	92	5·6
Cl (17)		78·7	89·0	10·3	88·5	9·8
Rb (37)		55·3	62·3	7·0	59·4	4·1
Pb (82)		24·8	29·6	4·8	24·8	0·0
Rb (37)	0·25	81·3	84·0	2·7	83·6	2·3
Pb (82)		55·4	52·2	−3·2	50·0	−5·4

For sodium, chlorine, and rubidium, values of $U(r)$ the atomic radial charge density, obtained by Hartree[31] from "self-consistent field" solutions of the wave-mechanics equation, have been used to calculate F^2 and thence P (Table III., column 4). For heavy atoms a general expression for $U(r)$ has been given by Fermi[32], and using this,

$$F=\frac{Z}{k\mu}\int_0^x f^{-3/2}\,.\,x^{-1/2}\,.\,\sin k\mu x\,.\,dx$$

where

$$\mu^3=9\pi^2a_H/128Z, \quad a_H \text{ is } h^2/4\pi^2me^2$$

and "f" is the function of "x" satisfying

$$\frac{d^2f}{dx^2}=f^{3/2}\,.\,x^{-1/2}$$

with boundary conditions

$$f(0)=1, \quad \int_0^\infty f^{3/2} \cdot x^{1/2} \cdot dx=1.$$

Values of "f" obtained by Bush and Caldwell [33] with a differential analyser have been used in obtaining P for lead (Table III., column 4).

Heisenberg[34] has recently calculated the modified scattering, taking the spin-coordinate of the electron into account as well as the space coordinates, so that the modified scattering is then not solely dependent on the charge density. For atoms of sufficiently high atomic number for the Fermi field to be a good enough approximation, Heisenberg obtains an expression for the modified scattering on the assumption that the wave-length of the incident radiation is short compared with that required for the excitation of the shortest simultaneously produced characteristic radiation. Bewilogua[35] has developed Heisenberg's equation numerically, and expresses the total scattered radiation as proportional to the sum of $Z^2\Phi^2$ unmodified and ZS modified, where

$$S=1-\int_0^{x_0} x^2\left[\left(\frac{f(x)}{x}\right)^{1/2}-v\right]^2\left[\left(\frac{f(x)}{x}\right)^{1/2}+\frac{v}{2}\right]^2 dx$$

and

$$\left(\frac{f(x_0)}{x_0}\right)^{1/2}=v.$$

He gives tables of Φ and S in which Φ (equivalent to F/Z) is a function of

$$u=\frac{4\pi a}{\lambda} \cdot \sin(\phi/2) \quad \text{and S of} \quad v=\frac{4\pi b}{\lambda} \cdot \sin(\phi/2),$$

where

$$"\ a\ "=Z^{-1/3}\left(\frac{3}{32\pi^2}\right)^{2/3} \cdot \frac{h^2}{2me^2} \doteq 0{\cdot}47Z^{-1/3}.\ \text{Å}.$$

and

$$"\ b\ "=\frac{a}{(6\pi Z)^{1/3}} \doteq 0{\cdot}176\ Z^{-2/3} \cdot \text{Å}.$$

Bewilogua's "S" table has been used to obtain the amount of modified radiation in calculating column (6) of Table III. in which experiment and theory are compared. His Φ table, however, does not extend to values of "u"

required here, and intensity values of unmodified scattering used in obtaining column (6) have been the same as for column (4). The experimental values were deduced from the curves of fig. 2. It should be mentioned that the self-consistent fields, worked out by Hartree and used here, were for ions. Since, however, the scattering at large angles and short wave-lengths depends mainly on the central part of the atomic charge distribution, it is, within the limits of error of measurement, independent of the state of ionisation.

As will be seen from the difference columns (5) and (7)

Fig. 3.

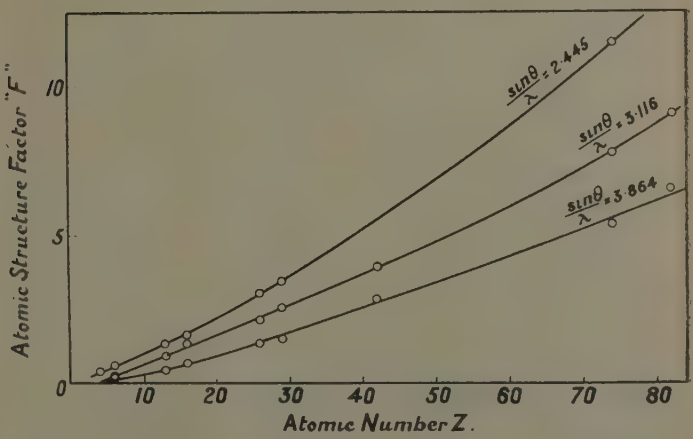

the experimental results are in somewhat better agreement with the theory of Heisenberg than of Woo. The difference between theory and experiment is probably within the limits of experimental error, except possibly for chlorine, for which the difference seems rather large. Small variations in the measured ratios lead unfortunately to larger changes in P, especially when P is 90 per cent. or over, so that in fig. 2 the region of the origin is likely to contain the greatest experimental percentage error.

A similar observation applies to fig. 3 (Table IV.), in which the atomic structure factor F, deduced from the experimentally determined proportion of modified radiation, is plotted against atomic number. Since F, for

any atom, is very nearly a function of $(\sin\theta)/\lambda$ alone, where $\theta=\phi/2$, values of this quantity are shown against the curves. Although this method of obtaining F, even supposing the theory to be exact, appears incapable of furnishing results of similar accuracy to those deducible from measurement of regularly reflected rays, it is of interest, since it gives F for a range of $(\sin\theta)/\lambda$ outside the limits of crystal spectra and independent of any uncertainty due to temperature effect.

TABLE IV.

Experimental Values of Atomic Structure Factor "F."

Element.	$(\sin\theta)/\lambda$. 2·445.	3·116.	3·864.
Be (4)	0·38	—	—
C (6)	0·59	0·22	0·19
Al (13)	1·33	0·91	0·45
S (16)	1·68	1·33	0·70
Fe (26)	3·02	2·15	1·36
Cu (29)	3·45	2·56	1·50
Mo (42)	—	3·91	2·85
W (74)	11·41	7·71	5·31
Pb (82)	—	9·03	6·50

Absolute Value of Angular Scattering at 150°.

The direct measurement of the absolute value of angular scattering, involving the measurement of intensity ratios of the order of 10^5, was conveniently effected by limiting the time of exposure of the incident beam, when measuring its intensity, to approximately 0·02 sec. by means of a rotating disk having a sector cut away. A ball-bearing lead-covered brass disk was used, having adjustable lead slits. After adjustment by means of a brass template, these were screwed into position and the disk then balanced with extra lead to put the C. G. at the axis. The disk was coupled by means of a belt to a synchronous motor driven from the A.C. mains, which for this part of the work were used to feed the high tension transformer. The mass of the disk was sufficient to keep the rotation steady, and the exposure time of one A.C. cycle obviated

the production of irregularities through "ripple" left over from the "constant potential" high tension smoothing. The disk, of 7″ diameter, rotated once in 0·69 sec., the sector being 10° 18′. With the aid of a pea lamp arranged behind the disk so that the lamp was exposed to view through the sector immediately after the latter had traversed the X-ray beam, no difficulty was experienced in operating an auxiliary lead shutter by hand, so that an effective exposure occurred only when required. Intensity measurements of the incident beam made in this way were found to vary over a total range of about 2 per cent. Eight or ten readings were taken to obtain a mean value. The width of the sector, relative to its thickness, at the position of the X-ray beam, was too large for error in the calculation of the exposure time to be occasioned through the slight divergence of the beam.

When measuring the intensity of the scattered rays, a circular diaphragm limited the solid angle of the cone of rays entering the ionization chamber to 0·004115. Exposures were of 2 or 2½ minutes, automatically timed. The divergence of the rays passing through the chamber in this case was greater than when measuring the incident beam obtained by crystal reflexion, but it was considered undesirable to reduce the solid angle further on account of loss of intensity. In order to ascertain what error might be due to obliquity of the rays, measurement of the ionization produced by the incident beam was made with the ionization chamber placed in various positions, so that the rays passed through the chamber in directions the same as those taken in the other case by constituent rays of the scattered cone. It was found that the limiting rays of the cone would occasion 5 per cent. less ionization than the central rays, although there was little decrease in the ionization produced by rays nearer the axis of the cone. It was estimated that, on account of the divergence, the total ionization produced was about 2 per cent. less than it otherwise would have been.

Scatterers of natural graphite and aluminium were used. The aluminium was of 99·85 per cent. purity (0·10 per cent. Fe, 0·05 per cent. Si). Beryllium was also tried, but on account of the low effective density of powdered beryllium, and since it was necessary to limit the dimensions of the scatterer so that the obliquity of the rays passing through the ionization chamber aperture should not be

too great, it was found that the scattered intensity was inadequate. The scatterers were cut in the form of rectangular blocks, approximately 4 mm. wide, 3 mm. thick, and 12 mm. high, and held in position by hollow rectangular prisms of thin celluloid cemented to the lower edges, or by very light boxwood rods. The 4×12 mm. faces were placed parallel to the bisector of the scattering angle, and the scattered rays measured all passed through the 4×12 mm. face first encountered by the incident beam.

If no account is taken of polarization or double scattering the intensity ratio of scattered to incident beams will, since the solid angle subtended by the ionization chamber aperture of area "A," at any point in the scatterer, is small and the width of the incident beam (1·1 mm.) is sufficiently small, be given by

$$R_\phi = A \cdot s_1 \int_0^{d \operatorname{cosec} \phi/2} e^{-2\mu_1 x} \cdot (b - x\cos\phi)^{-2} \cdot dx + A \cdot s_2 \cdot e^{-(\mu'_w - \mu_w)d_w} \cdot f_{Br} \int_0^{d \operatorname{cosec} \phi/2} e^{-(\mu_1+\mu_2)x} \cdot (b - x\cos\phi)^{-2} \cdot dx, \quad . \quad . \quad (8)$$

where s_1, s_2, are respectively the unmodified and modified linear scattering coefficients for the angle ϕ, μ_1, and μ_2 are the unmodified and modified absorption coefficients for the scatterer, μ_w' and μ_w are similar coefficients for the ionization chamber window of thickness d_w, "d" is the thickness of the scatterer, $b = r_0 + \frac{d}{2} \cdot \cos\phi \cdot \operatorname{cosec}\phi/2$, r_0 is the distance from the spectrometer axis to the ionization chamber aperture and f_{Br} is the factor allowing for the increased sensitivity of the chamber to the modified rays.

On integrating by parts, the above integrals reduce to exponential integrals, which although tabulated are troublesome, since many significant figures are necessitated by the narrowness of the integration limits. It was found, however, that with the values of the constants used, the result obtained from the above expression differed by not more than 0·3 per cent. from that obtained from the following more approximate one, viz. :

$$R_\phi = q \cdot s_1 \left\{ \frac{1 - e^{-2\mu_1 d \operatorname{cosec}\phi/2}}{2\mu_1} \right\} + q \cdot s_2 \cdot f_{Br} \cdot e^{-(\mu'_w - \mu_w)d_w} \left\{ \frac{1 - e^{-(\mu_1+\mu_2)\, d \operatorname{cosec}\phi/2}}{\mu_1 + \mu_2} \right\}. \quad (9)$$

TABLE V.

Effect of Correction Factors at $\lambda = 0{\cdot}31$ Å. and $\phi = 150°$.

Element.	Dimensions of scatterer (cm.).	Filter for excited characteristic rays.	$\frac{R_2(R_3-R_1)}{R_1(R_2-R_3)}$.	Correction factors.			Intensity Ratio R.
				Sensitivity of ionization chamber.	Differential absorption in window and filter.	Differential absorption in scatterer.	
Be (4) ...	2·4×0·63×0·356	..	∞	..	..	..	∞
C (6)	4·0×0·30×0·075	..	113·8	0·726	1·013	..	84·0
Al (13) ...	4·0×0·40×0·055	..	13·77	0·729	1·013	1·018	10·37
S (16) ...	4·0×0·35×0·060	..	8·05	0·718	1·013	1·022	5·96
Fe (26) ...	4·0×0·20×0·097	0·01 cm. Al	3.938	0·721	1·019	1·212	3·711
Cu (29) ...	4·0×0·60×0·0110	0·10 cm. Al	3·360	0·731	1·081	1·102	2·932
Mo (42) ...	4·0×0·32×0·051	0·021 cm. Cu	1·220	0·751	1·598	1·232	1·807
W (74) ...	4·0×0·34×0·051	0·150 cm. Al	0·8055	0·738	1·112	1·232	0·816
Pb (82) ...	4·0×0·6×0·065	0·200 cm. Al	0·630	0·734	1·152	1·244	0·661

where " q " is the solid angle of the scattered rays measured. A scattering angle of 150° was chosen, for which the ratio s_2/s_1 had been experimentally determined as described above, so that by combining these results s_1 and s_2 could be found.

In order to compare results with theory, F^2 may be obtained by inserting the experimental value of s_2/s_1 in the expression

$$s_2/s_1=\left(\frac{Z}{F^2}-\frac{1}{Z}\right)(1+\alpha \cdot \text{vers}\,\phi)^{-3},$$

TABLE VI.

Absolute Values of R_ϕ.

Scatterer.	Graphite. $3{\cdot}255\times4{\cdot}38\times12{\cdot}620$ mm.		Aluminium. $2{\cdot}976\times3{\cdot}976\times11{\cdot}905$ mm.
λ	0·31 Å.	0·395 Å.	0·31 Å.
K	0·007514	0·007514	0·0042115
ρ	2·145	2·145	2·70
μ_1	0·4075	0·5195	1·593
μ_2	0·452	0·5885	2·203
b	8·249	8·249	8·262
f_{Br}	1·390	1·187	1·380
f_P	0·996	0·998	0·996
f_{ss}	1·06	1·06	1·074
s_1	(Neglected).	0·002533	0·003912
s_2	0·0300	0·03227	0·03627
R_ϕ(exper.).	$5{\cdot}13\times10^{-5}$	$5{\cdot}08\times10^{-5}$	$4{\cdot}36\times10^{-5}$
R_ϕ (calc.) .	$5{\cdot}237\times10^{-5}$	$4{\cdot}93\times10^{-5}$	$4{\cdot}317\times10^{-5}$
Per cent. diff..	2·1	−3·0	−1·0

and then inserting this value for F^2 in the expressions for the scattering coefficients

$$s_1=KF^2 \text{ and } s_2=K\left(Z-\frac{F^2}{Z}\right)(1+\alpha \cdot \text{vers}\,\phi)^{-3},$$

where

$$K=\frac{Le^4}{2m^2c^4}\cdot\frac{\rho}{W}\cdot(1+\cos^2\phi)\cdot f_e,$$

L being Avogadro's number and W atomic weight. Putting s_1 and s_2 so found into the expressions (8) or (9), comparison may be made with the observed ratio R_ϕ. No appreciable polarization correction (see below) was required at this scattering angle. Results are shown in

Table VI. The constants $r_0 = 8{\cdot}395$ cm., $q = 0{\cdot}004115$, $A = 0{\cdot}28984$ cm.^{2}, $e^{(\mu_w' - \mu_w)d_w} = 1{\cdot}012$, were the same throughout.

Double Scattering.

An approximate allowance for the effect of twice scattered radiation has been made following the treatment of the subject by Du Mond[36]. For a spherical scatterer of radius "r," he has obtained the expression $\frac{9}{32} \cdot \sigma \cdot r \cdot R(\phi)$ for the ratio of the intensity of twice scattered to once scattered radiation, where σ is Thomson's scattering coefficient and $R(\phi)$ is a function which varies little from 2·5 for any value of ϕ. Absorption is not taken into account in this formula, but it is useful in obtaining an estimate of the maximum double scattered intensity to be expected. Since the scatterers used in the present research were not spherical and the X-ray beam was of rectangular cross-section, an accurate equivalent of "r" is not readily estimated. A value 0·2 cm. for "r" has actually been taken in calculating the double scattering correction factor f_{ss} shown in Table VI. The effect of absorption must be to reduce f_{ss}, since the twice scattered radiation will on the average be of longer wave-length than the once scattered, while the extension of the scatterer in height, as compared with a sphere of diameter equal to the width of the scatterer, will tend to increase f_{ss}. As the total correction does not amount to more than about 7 per cent., it seems probable that the error made on this account should not exceed about $2\frac{1}{2}$ per cent. The double scattering correction, however, would appear to be the least satisfactory to estimate of all the correction factors necessary in the present work.

Polarization of Incident Rays.

The amount of polarization present in the incident beam was obtained by using natural graphite scatterers in the form of rectangular blocks, the scattering at $\phi = 90°$ being measured in the horizontal plane containing the cathode stream and also in the vertical direction. The wire connecting the ionization chamber electrode with the electrometer passed through a 2″ diameter brass tube system which had a number of swivel joints.

The part of the tube system rigidly connected to the ionization chamber formed the only support for the latter, and could be removed from the spectrometer arm by undoing four screws. The ionization chamber could thus be quickly removed from its position for measurements in a horizontal plane, and the swivel joints were so arranged that the chamber could be swung round and immediately clamped into position for measurements of vertical scattering without any change occurring in the electrostatic capacity of the connecting tube system. It was ascertained that, without the scatterer, no measurable ionization occurred in either position of the ionization chamber. In order to obviate error, which might be occasioned by redistribution of weight on the spectrometer altering the position of the latter slightly relative to the X-ray tube when the ionization chamber was moved for vertical measurements, the intensity of the incident beam was measured in each case with a gold leaf electroscope. Care was taken that the beam passed through the electroscope in such a position that a slight relative lateral displacement produced negligible alteration of the reading.

The cross-section of the X-ray beam was 1·1 mm.× 6·5 mm., so that even with a graphite scatterer 2·43× 3·26× 8·64 mm. the absorption correction was important. The graphite block was set with a 2·43 × 8·64 mm. face perpendicular to the incident rays and an 8·64 mm. edge vertical. The cone of scattered rays received by the ionization chamber was sufficiently small for it to be assumed that all these rays passed through the face of the graphite block immediately opposite the chamber in either position of the latter. Taking the direction of the incident beam as "x" axis and the vertical direction as "z" axis, the ratio of the scattered intensities in the horizontal and vertical directions is given by

$$\frac{I_H}{I_V} = \frac{s_H I_0 \int_0^d \int_{y_1}^{y_2} \int_{z_1}^{z_2} e^{-\mu_1 x - \mu_2 y} . (b_1+y)^{-2} dx \, . \, dy \, . \, dz}{s_V I_0 \int_0^d \int_{y_1}^{y_2} \int_{z_1}^{z_2} e^{-\mu_1 x - \mu_2 z} . (b_2+z)^{-2} dx \, . \, dy \, . \, dz}$$

$$= \frac{s_H(z_2-z_1)\{e^{-\mu_2 y_1}(b_1+y_1)^{-1} - e^{-\mu_2 y_2}(b_1+y_2)^{-1} + Ei[-\mu_2(b_1+y_1)] - Ei[-\mu_2(b_1+y_2)]\}}{s_V(y_2-y_1)\{e^{-\mu_2 z_1}(b_1+z_1)^{-1} - e^{-\mu_2 z_2}(b_2+z_2)^{-1} + Ei[-\mu_2(b_2+z_1)] - Ei[-\mu_2(b_2+z_2)]\}},$$

where s_H is the scattering coefficient per unit solid angle, b_1 is the distance from the further edge of the ionization chamber aperture to the nearest face of the graphite block, and y_1, y_2 are the maximum and minimum distances respectively traversed by the scattered rays in the graphite, all relating to measurements in a horizontal plane, and s_V, b_2, z_1 and z_2 are similar quantities for the vertical measurements. As before, μ_1 and μ_2 are the absorption coefficients in the scatterer for the unmodified

TABLE VII.

Polarization Ratios.

Scatterer.	Graphite. $3{\cdot}26 \times 2{\cdot}43 \times 8{\cdot}64$ mm.	
λ	0·31 Å.	0·395 Å.
μ_2	0·430	0·552
b_1	8·136	8·278
b_2	7·778	8·356
y_1	0·164	0·044
y_2	0·274	0·199
z_1	0·306	0·089
z_2	0·956	0·681
$\frac{I_H \cdot s_V}{I_V \cdot s_H}$ 90°	1·19955	1·24177
$\frac{s_H}{s_V}$ 90°	0·946	0·973

and modified rays respectively, it being sufficiently accurate to treat all the scattered rays as modified.

In order to obtain y_1, y_2, z_1, z_2, a strip of photographic plate was mounted inside a cylindrical brass holder so that it almost touched the scatterer on a "yz" face. An exposure was made for the X-ray beam and then a pea lamp placed behind the spectrometer slits was flashed to obtain the outline of the specimen. With a travelling microscope, these distances were then easily measured on the plate to the required accuracy. A steel distance piece, having a screw adjustment, was used to measure b_1 and b_2. Numerical values are given in Table VII.

To obtain the polarization correction factor f_p at any angle we have, since the electric vector of the polarized component is in a horizontal plane,

$$s_H I_0 = s_0 I_u \cdot \frac{(1+\cos^2\phi)}{2} + s_0 I_p \cos^2\phi,$$

$$s_V I_0 = s_0 I_u \cdot \frac{(1+\cos^2\phi)}{2} + s_0 I_p,$$

where I_u and I_p are the unpolarized and polarized parts respectively of the incident beam of intensity I_0. If "r" is the ratio s_V/s_H at $\phi=90^\circ$ then $I_p=I_u \cdot (r-1)/2$ and $s_H=s_0(1+r \cdot \cos^2\phi)/(1+r)$. To calculate absolute values of scattering with partially polarized incident radiation this factor $(1+r \cdot \cos^2\phi)/(1+r)$ must be used instead of the factor $(1+\cos^2\phi)/2$ in the usual expressions for unpolarized radiation, or what is equivalent, the theoretical value for unpolarized rays must be multiplied by a polarization correction factor

$$f_p = 2(1+r \cdot \cos^2\phi)/(1+r)(1+\cos^2\phi).$$

Discussion of Results.

From the series of experiments described above, the following conclusions may be drawn, which, however, are only strictly applicable to the wave-length range investigated, viz., 0·25 to 0·395 Å.

(1) The distribution with angle of total scattered intensity from powdered beryllium at angles greater than 30° may be calculated, within a few per cent., from the theoretical expressions, based on wave-mechanics, giving the intensity of scattering from a gas, *i. e.*, only atomic scattering need be considered.

(2) The angular distribution of scattering, at large angles, is the same for all solids or liquids composed of atoms of low atomic number, and is given by Dirac's equation. The minimum angle, at which this holds good, is less than that for which $(\sin\theta)/\lambda=2$.

(3) For solid elements of any atomic number, at angles large enough for diffraction spectra to be negligible, the ratio of the incoherent and coherent scattering coefficients is given within a few per cent. by the theoretical expressions for scattering by a gas.

(4) The absolute values of the scattering coefficients at such angles are also given within a few per cent. by

the equations for scattering by a gas. This has been shown only for elements of atomic number not greater than aluminium, but in view of (3) it would appear extremely probable that it also holds good for any element.

(5) As a consequence of (3) and (4), the atomic structure factor F may be deduced from measurements of the proportion of modified radiation. This method is free from the complication due to temperature coefficient that exists when F is deduced from examination of crystal spectra, but suffers from the disadvantage that the mathematical process involved is such that any error in the experimental measurements leads to a larger percentage error in F.

It is only possible in a general way to compare the results obtained in the present research with earlier ones. No previous measurements, either relative or absolute, of radiation diffusely scattered by crystalline aggregates appear to have been made using crystal diffracted incident radiation. Conclusion (1) is, however, in agreement with the work of Jauncey and Williams[15], Coven[16], and Harvey[17] on the diffuse scattering from crystals of KCl, NaF, and MgO. They have investigated a range of $(\sin\theta)/\lambda$ from about 0·25 to 1·2 and, by means of formulæ developed by Jauncey and Harvey from equation (4), have added the known intensity going into crystal spectra to that of the diffusely scattered radiation and obtained an average total scattered intensity per electron practically the same as that for a gas of atomic number equal to the average atomic number of the crystal.

Coven has consequently predicted that the total scattering from a metal should be approximately the same as that from the metal in the vapour state, if $(\sin\theta)/\lambda$ is greater than 0·5. At $\phi=30°$, $(\sin\theta)/\lambda$ is 0·835 at 0·31 Å. and 0·655 at 0·395 Å., so that the author's results are in confirmation of this as regards beryllium. It should be mentioned that the most recent work of Harvey[17] was carried out with primary radiation so well filtered by balanced filters that several thousand readings were necessitated.

Measurements of the proportion of radiation modified on scattering have been made by Ross[37], Woo[38], Jauncey and Boyd[39], De Foe[40], and Albrecht[9]. A photographic method was used by Ross. Their results are, in a general way, in agreement with those

described here, but, as either the angles investigated or the effective wave-lengths have been different, a close comparison cannot be made. If, however, it is assumed that the ratio of the modified and unmodified scattering coefficients is given by an expression such as

$$\left(Z-\frac{F^2}{Z}\right)(1+\alpha \,.\, \text{vers}\,\phi)^{-3}/F^2$$

then if, for any element, F may be regarded as a function of $(\sin\theta)/\lambda$ alone, then so may the proportion " P " of modified radiation, except for the factor $(1+\alpha \,.\, \text{vers}\,\phi)^{-3}$.

TABLE VIII.

Percentage of Modified Radiation.

$(\sin\theta)/\lambda$.	2.445		3·116		3·864	
	Albrecht.	Back-hurst.	Albrecht.	Back-hurst.	Albrecht.	Back-hurst.
Li (3) ..	100	....	100	....	100	....
Be (4) ...	....	95·2	....	100	....	100
C (6) ...	95	92·6	97	98·8	99	99
Al (13) ...	63	84·0	72	91·2	84	97·6
S (16) ...	54	80·2	65	85·7	82	95·2
Cu (29) ...	43	63·5	56	74·6	75	88·7

If P_1 is measured at ϕ_1 and P_2 at ϕ_2 with wave-lengths such that $(\sin\theta)/\lambda$ is the same in each case, we should have, in consequence

$$P_2=P_1 r^3/\{1+P_1(r^3-1)\},$$

where

$$r=(1+\alpha_1 \text{ vers } \phi_1)/(1+\alpha_2 \text{ vers } \phi_2).$$

In Table VIII., values available from a graph given by Albrecht (9) are taken for P_1 and the values of P_2 deduced from them are compared with those of the writer, to which, on these assumptions, they should be equal. As will be seen, agreement does not prove to be close for the elements of higher atomic number examined by Albrecht, although

the tungsten radiation used by him was apparently very well filtered.

In conclusion, the author wishes to express his gratitude to Dr. G. W. C. Kaye, O.B.E., the Superintendent of the Physics Department, for his continued interest in this research, and wishes again to acknowledge efficient and frequent help afforded by Mr. P. R. Pallister, B.Sc., in the experimental work. Some of the metals used were prepared in the Metallurgy Department of the Laboratory, and the author was in particular fortunate to have kindly made available a high grade of purity of beryllium prepared by Mr. H. A. Sloman, M.A. The X-ray ionization spectrometer, which was designed expressly for the research, was made by Mr. G. H. Turl in the Instrument Workshop of the Laboratory.

Summary.

Using a homogeneous incident beam obtained by crystal diffraction, measurements have been made of the following :—

(1) The relative angular intensity distribution of radiation scattered from beryllium from 30° to 150° for wavelengths of 0·31 and 0·395 Å.

(2) The relative angular intensity distribution from 60° to 150° of radiation scattered from paraffin wax, water, turpentine, benzene, alcohol, and benzophenone at 0·31 Å.

(3) The relative proportion of modified and unmodified radiation scattered at 150° by Be, C, Al, S, Fe, Cu, Mo, W, Pb at 0·25, 0·31, 0·395 Å.

(4) The absolute value of the angular scattering coefficients at 150° of the modified and unmodified rays scattered from C and Al at 0·31 Å. and from C at 0·395 Å.

The absolute measurements were made by means of direct comparison of the incident and scattered beams, and in all the measurements the X-ray exposures were automatically timed. All measurements were made using an ionization spectrometer, the relative proportion of modified rays being determined by absorption measurements. A full-wave rectification constant potential plant operated the X-ray tube, of special design, which embodied

in itself adequate X-ray shielding and was equipped with forced oil cooling for the anticathode.

Comparison of the results with existing theory shows that, within certain limitations of angle and wave-length the scattering from solids, composed of atoms of any kind and consisting, as in the normal state, of aggregates of small crystals or amorphous material, is given within a few per cent. by the equations based on wave-mechanics for the scattering from gases. This has been found to hold good both for relative angular intensity distribution and also as regards absolute value for both modified and unmodified angular scattering coefficients.

In consequence, measurements of the proportion of modified radiation may be used to determine the atomic structure factor. This method is experimentally difficult, but free from complication due to temperature factor. Tables and graphs are given of results and showing extent of agreement with theory.

References.

(1) Wollan, Phys. Rev. xxxvii. p. 862 (1931).
(2) Herzog, *Zeits. f. Phys.* lxix. p. 207 (1931).
(3) Debye, *Phys. Zeits.* xxxi. p. 419 (1930).
(4) Bewilogua, *Phys. Zeits.* xxxii. pp. 114 and 265 (1931).
(5) Gajewski, *Phys. Zeits.* xxxiii. p. 122 (1932).
(6) Bell, Brit. Journ. of Rad. ii. p. 156 (1929).
(7) Backhurst, Phil. Mag. xiii. p. 28 (1932).
(8) Wellauer, *Arch. für El.* xvi. p. 13 (1926).
(9) Albrecht, *Zeits. f. Phys.* lvii. p. 326 (1929).
(10) Compton, Phil. Mag. viii. p. 961 (1929).
(11) Compton, Phys. Rev. xxi. p. 483 (1923).
(12) Dirac, Proc. Roy. Soc. A, cxi. p. 405 (1926).
(13) Compton, Phys. Rev. xxxv. p. 925 (1930).
(14) Woo, Phys. Rev. xxxviii. p. 6 (1931).
(15) Jauncey & Williams, Phys. Rev. xli. p. 127 (1932).
(16) Coven, Phys. Rev. xli. p. 422 (1932).
(17) Harvey, Phys. Rev. xliii. p. 591 (1933).
(18) Waller, Upsala Dissertation (1925).
(19) Debye, *Ann. der Phys.* xliii. p. 49 (1914).
(20) Simon, *Zeits. f. phys. Chem.* cxxix. p. 321 (1927).
(21) Magnus and Holzmann, *Ann. der Phys.* iii. p. 585 (1929).
(22) Born and Brody, *Zeits. f. Phys.* vi. p. 132 (1921) and viii. p. 205 (1922).
(23) James, Brindley, and Wood, Proc. Roy. Soc. A, cxxv. p. 401 (1929).
(24) James and Brindley, Phil. Mag. xii. p. 81 (1931).
(25) Wentzel, *Zeits. f. Phys.* xliii. pp. 1 and 779 (1927).
(26) Waller, *Zeits. f. Phys.* li. p. 213 (1928).
(27) Waller and Hartree, Proc. Roy. Soc. A, cxxiv. p. 119 (1929).
(28) Woo, Phys. Rev. xli. p. 21 (1932).
(29) Jauncey, Phys. Rev. xxxviii. p. 1 (1931).
(30) Debye, *Phys. Zeit.* xxviii. p. 135 (1927).
(31) Hartree, Proc. Camb. Phil. Soc. xxiv. p. 111 (1928).

(32) Fermi, *Zeits. f. Phys.* xlviii. p. 73 (1928).
(33) Bush and Caldwell, Phys. Rev. xxxviii. p. 1898 (1931).
(34) Heisenberg, *Phys. Zeits.* xxxii. p. 737 (1931).
(35) Bewilogua, *Phys. Zeits.* xxxii. p. 740 (1931).
(36) Du Mond, Phys. Rev. xxxvi. p. 1685 (1930).
(37) Ross, Proc. Nat. Acad. Amer. xi. p. 569 (1925).
(38) Woo, Phys. Rev. xxvii. p. 119 (1926) and xxviii. p. 426 (1926).
(39) Jauncey and Boyd, Phys. Rev. xxviii. p. 620 (1926).
(40) De Foe, Phys. Rev. xxvii. p. 675 (1926).

XXX. *The Magneto-Optical Dispersion of Organic Liquids in the Ultra-Violet Region of the Spectrum.*—Part VII. *The Magneto-Optical Dispersion of Isobutyl Formate, Methyl Butyrate, and Ethyl Malonate. By* R. H. Lavery, *M.Sc., and* Prof. E. J. Evans, *D.Sc., Physics Department, University College, Swansea* *.

THE experimental methods employed in the investigation of the magneto-optical rotations and the refractive indices of the three organic liquids have been fully described in Part I.†. The results have been examined in relation to Larmor's theory ‡ of magnetic rotation. According to this theory, Verdet's constant δ for a wavelength λ is given by the expression

$$\delta = \frac{e}{2mc^2} \cdot \lambda \cdot \frac{dn}{d\lambda}, \quad . \quad . \quad . \quad . \quad . \quad (1)$$

where n is the refractive index, e/m is the ratio of the charge to the mass of the resonators, and c the velocity of light. In the above expression the charge e is measured in electrostatic units and the magnetic field in electromagnetic units.

If the ordinary dispersion of each liquid is represented by an equation of the type

$$n^2-1=b_0+\frac{b_1}{\lambda^2-\lambda_1^2}+\frac{b_2}{\lambda^2-\lambda_2^2}, \quad . \quad . \quad . \quad (2)$$

and the magneto-optical dispersion over the range of

* Communicated by the Authors.
† Stephens and Evans, Phil. Mag. x. p. 759 (1930).
‡ 'Aether and Matter.'—Appendix F, p. 352.

spectrum investigated is controlled by one absorption in the ultra-violet, it can be shown that

$$\phi = n\delta\lambda^2 = K\left(\frac{\lambda^2}{\lambda^2 - \lambda_1^2}\right)^2, \quad . \quad . \quad . \quad . \quad (3)$$

where K is a constant and λ_1 the wave-length of the absorption band. In addition, the value of e/m

Experimental Results.

Ordinary Dispersion.

Table I. (*a*).

Visual Determinations.

Wave-length in microns.	Refractive indices. Isobutyl formate at 10·7° C.	Methyl butyrate at 12·25° C.	Diethyl malonate at 18·5° C.
·6678	$1{\cdot}3876_9$	$1{\cdot}3890_1$	$1{\cdot}4122_4$
·5876	$1{\cdot}3900_6$	$1{\cdot}3913_8$	$1{\cdot}4144_8$
·5016	$1{\cdot}3939_6$	$1{\cdot}3950_3$	$1{\cdot}4181_9$
·4922	$1{\cdot}3944_7$	$1{\cdot}3955_8$	$1{\cdot}4187_5$
·4713	$1{\cdot}3957_5$	$1{\cdot}3969_2$	$1{\cdot}4203_1$
·4472	$1{\cdot}3976_1$	$1{\cdot}3987_0$	$1{\cdot}4221_9$

deduced from the above three equations is given by the expression $-\frac{2Kc^2}{b_1}$.

The refractive indices given in Tables I. (*a*) and I. (*b*) were determined at temperatures in the neighbourhood of 18° C., and were corrected to the temperatures at which the magneto-optical rotations were measured by means of the known values of the temperature coefficients of the three liquids. It was found that the refractive indices of isobutylformate, methyl butyrate, and diethyl malonate diminished by $\cdot 0004_6$, $\cdot 0004_5$, and $\cdot 0004_6$ respectively per degree C. rise of temperature. The refractive indices of the three liquids for various wave-lengths are plotted in figs. 1, 2 and 3.

TABLE I. (*b*).—Photographic Determinations.

Isobutyl formate at 10·7° C.		Methyl butyrate at 12·25° C.		Diethyl malonate at 18·5° C.	
Wave-length in microns.	Refractive index.	Wave-length in microns.	Refractive index.	Wave-length in microns.	Refractive index.
·4794	$1{\cdot}3954_2$	·5700	$1{\cdot}3918_6$	·5218	$1{\cdot}4171_2$
·4651	$1{\cdot}3963_5$	·5218	$1{\cdot}3939_4$	·5153	$1{\cdot}4173_9$
·4508	$1{\cdot}3973_5$	·5106	$1{\cdot}3945_2$	·4768	$1{\cdot}4197_5$
·4378	$1{\cdot}3987_0$	·4866	$1{\cdot}3958_5$	·4675	$1{\cdot}4205_3$
·4275	$1{\cdot}3995_5$	·4675	$1{\cdot}3972_0$	·4536	$1{\cdot}4216_9$
·4178	$1{\cdot}4006_0$	·4508	$1{\cdot}3984_2$	·4415	$1{\cdot}4226_6$
·4123	$1{\cdot}4012_0$	·4275	$1{\cdot}4004_7$	·4378	$1{\cdot}4230_1$
·4023	$1{\cdot}4024_5$	·4023	$1{\cdot}4031_2$	·4185	$1{\cdot}4250_3$
·3923	$1{\cdot}4036_0$	·3861	$1{\cdot}4052_4$	·4063	$1{\cdot}4264_3$
·3862	$1{\cdot}4045_0$	·3800	$1{\cdot}4060_0$	·3950	$1{\cdot}4278_0$
·3817	$1{\cdot}4051_0$	·3745	$1{\cdot}4067_7$	·3895	$1{\cdot}4285_5$
·3722	$1{\cdot}4065_0$	·3688	$1{\cdot}4076_7$	·3823	$1{\cdot}4295_7$
·3602	$1{\cdot}4084_0$	·3654	$1{\cdot}4082_7$	·3712	$1{\cdot}4311_9$
·3569	$1{\cdot}4091_0$	·3582	$1{\cdot}4094_7$	·3600	$1{\cdot}4331_7$
·3455	$1{\cdot}4112_0$	·3455	$1{\cdot}4117_7$	·3545	$1{\cdot}4341_5$
·3381	$1{\cdot}4129_0$	·3381	$1{\cdot}4131_4$	·3449	$1{\cdot}4359_5$
·3280	$1{\cdot}4151_0$	·3308	$1{\cdot}4147_2$	·3416	$1{\cdot}4368_6$
·3208	$1{\cdot}4168_0$	·3247	$1{\cdot}4161_8$	·3378	$1{\cdot}4376_5$
·3176	$1{\cdot}4176_0$	·3194	$1{\cdot}4176_7$	·3338	$1{\cdot}4384_3$
·3147	$1{\cdot}4185_0$				
·3093	$1{\cdot}4200_8$				
·3005	$1{\cdot}4227_0$				
·2961	$1{\cdot}4241_0$				

Fig. 1.

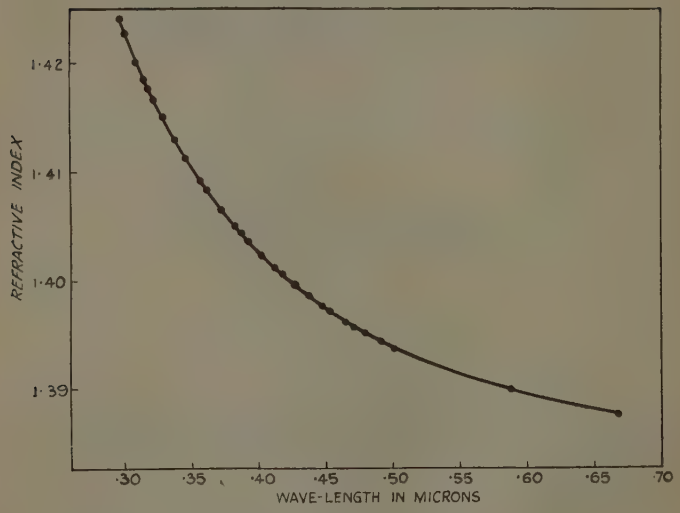

Refractive indices of isobutyl formate at 10·7° C.

Fig. 2.

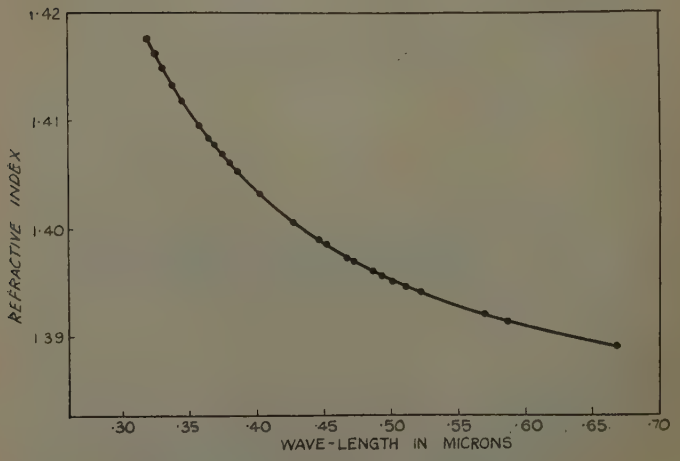

Refractive indices of methyl butyrate at 12·25° C.

Fig. 3.

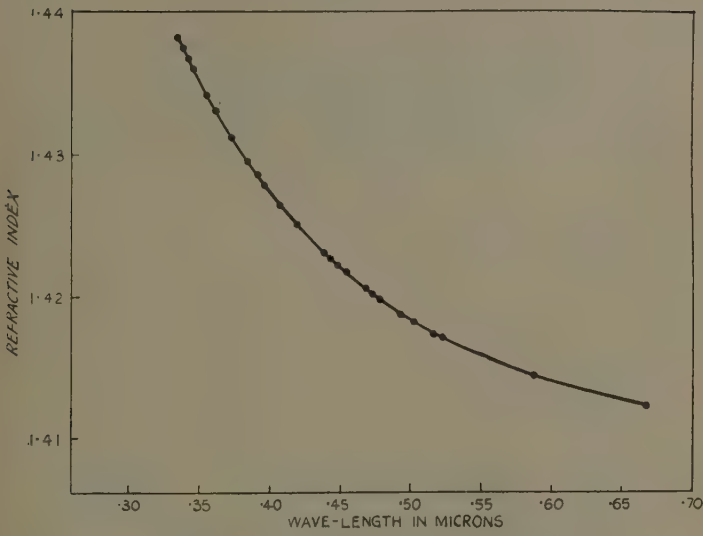

Refractive indices of ethyl malonate at 18·5° C.

TABLE II. (*a*).

Verdet's constant of Isobutyl Formate.

(Temperature =10·7° C.)

Wave-length in microns.	Verdet's constant mins./cm. gauss.	Wave-length in microns.	Verdet's constant mins./cm. gauss.
·4543	$\cdot 0209_8$	·3520	$\cdot 0375_8$
·4488	$\cdot 0215_7$	·3432	$\cdot 0398_0$
·4439	$\cdot 0220_9$	·3360	$\cdot 0420_1$
·4340	$\cdot 0231_9$	·3289	$\cdot 0442_3$
·4249	$\cdot 0243_0$	·3224	$\cdot 0464_5$
·4169	$\cdot 0254_0$	·3163	$\cdot 0486_8$
·4090	$\cdot 0265_1$	·3106	$\cdot 0508_8$
·4022	$\cdot 0276_2$	·3052	$\cdot 0530_9$
·3950	$\cdot 0287_2$	·3005	$\cdot 0553_2$
·3825	$\cdot 0309_4$	·2956	$\cdot 0575_3$
·3712	$\cdot 0331_5$	·2915	$\cdot 0597_5$
·3608	$\cdot 0353_7$	·2872	$\cdot 0619_7$

Isobutyl Formate.

The sample of isobutyl formate employed in the magneto-optical experiments distilled over between 98·4° C. and 98·7° C. at a pressure of 77·015 cm. of mercury, the correct boiling-point* being 98·2° C. at a pressure of 76 cm.

Fig. 4.

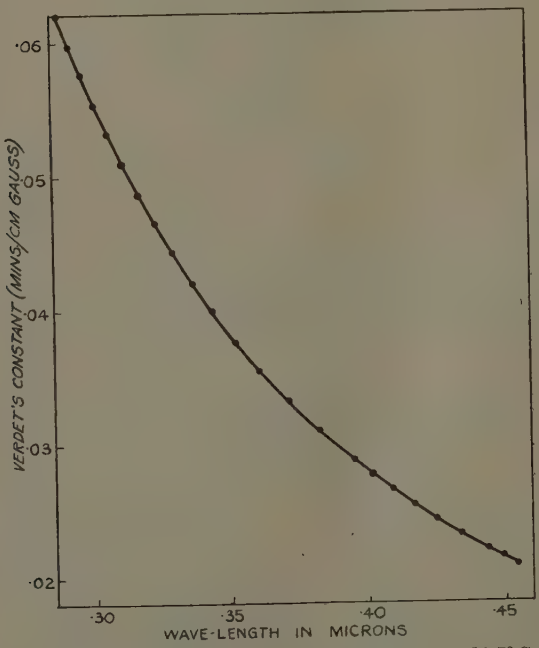

Magneto-optical dispersion of isobutyl formate at 10·7° C.

The experimental results are given in Table II (*a*) and fig. 4.

Table II. (*b*) gives a series of values of the refractive index n and Verdet's constant δ for the given wave-lengths, these values being obtained from fig. 1 and Table II. (*a*) respectively. It was found that the experi-

* 'International Critical Tables,' i. p. 192.

mental results could be represented by a formula of the type

$$\phi = n\delta\lambda^2 = K\left(\frac{\lambda^2}{\lambda^2 - \lambda_1^2}\right)^2 \ldots,$$

and from several pairs of values obtained from Table II. (*b*) the values of λ_1 and K were calculated.

TABLE II. (*b*).

	λ in microns.	δ mins./cm. gauss.	n.
(*a*)	·4488	$\cdot 0215_7$	1·3975
(*b*)	·4169	$\cdot 0254_0$	1·4007
(*c*)	·3520	$\cdot 0375_8$	1·4100
(*d*)	·3224	$\cdot 0464_5$	1·4165

Substitution in the above equation gave the following results :—

From (*a*) and (*c*) $\lambda_1 = \cdot 1079\,\mu$ and $K = 5\cdot 390_1 \times 10^{-3}$

(*b*) and (*d*) $\lambda_1 = \cdot 1088\,\mu$ and $K = 5\cdot 370_2 \times 10^{-3}$

(*a*) and (*d*) $\lambda_1 = \cdot 1081\,\mu$ and $K = 5\cdot 387_6 \times 10^{-3}$

(*b*) and (*c*) $\lambda_1 = \cdot 1086\,\mu$ and $K = 5\cdot 373_0 \times 10^{-3}$

The mean values of λ_1 and K are $\cdot 1083\,\mu$ and $5\cdot 380 \times 10^{-3}$ respectively, and the equation representing the magneto-

TABLE II. (*c*).

λ microns.	∂ (observed).	∂ (calculated).
·4439	$\cdot 0220_9$	$\cdot 0220_8$
·4249	$\cdot 0243_0$	$\cdot 0243_5$
·4090	$\cdot 0265_1$	$\cdot 0265_4$
·3825	$\cdot 0309_4$	$\cdot 0309_3$
·3712	$\cdot 0331_5$	$\cdot 0331_6$
·3608	$\cdot 0353_7$	$\cdot 0354_5$
·3360	$\cdot 0420_1$	$\cdot 0419_8$
·3163	$\cdot 0486_6$	$\cdot 0486_6$
·3005	$\cdot 0553_2$	$\cdot 0553_0$

optical dispersion of isobutyl formate for the range of the spectrum investigated, at a temperature of 10·7° C., is

$$n\delta = 5{\cdot}38_0 \times 10^{-3} \frac{\lambda^2}{\{\lambda^2 - (\cdot 1083)^2\}^2}.$$

The above equation was used to calculate the values of Verdet's constant for wave-lengths at which experimental results had already been obtained. A comparison between the observed and calculated values is given in Table II. (*c*).

TABLE III. (*a*).

Verdet's constant of Methyl Butyrate.

Temperature = 12·25° C.

Wave-length in microns.	Verdet's constant mins./cm. gauss.	Wave-length in microns.	Verdet's constant mins./cm. gauss.
·4540	$\cdot 0198_6$	·3798	$\cdot 0298_1$
·4488	$\cdot 0204_5$	·3741	$\cdot 0309_2$
·4435	$\cdot 0209_7$	·3684	$\cdot 0320_2$
·4380	$\cdot 0215_6$	·3627	$\cdot 0331_4$
·4331	$\cdot 0220_7$	·3531	$\cdot 0353_4$
·4237	$\cdot 0231_8$	·3440	$\cdot 0375_6$
·4155	$\cdot 0242_3$	·3360	$\cdot 0397_7$
·4072	$\cdot 0253_8$	·3287	$\cdot 0419_9$
·4000	$\cdot 0264_9$	·3218	$\cdot 0442_0$
·3927	$\cdot 0276_0$	·3153	$\cdot 0464_2$
·3861	$\cdot 0287_0$	·3094	$\cdot 0486_3$

Methyl Butyrate.

The methyl butyrate employed was distilled over between 102·5° C. and 102·8° C., and at a pressure of 76·9 cm., its true boiling-point * being 102·3° C. at 76 cm.

The experimental results are given in Table III. (*a*) and fig. 5.

In Table III. (*b*), values of Verdet's constants and the refractive indices corresponding to certain wave-lengths

* 'International Critical Tables,' i. p. 192.

are given; these were used to calculate the constants of the dispersion equation for methyl butyrate.

Fig. 5.

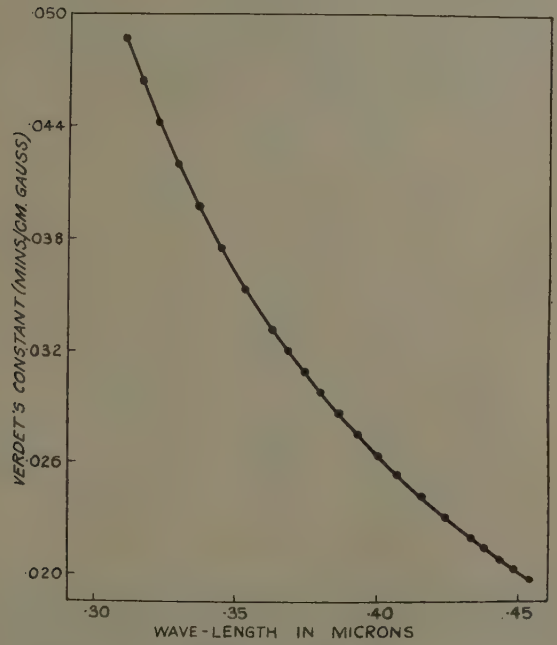

Magneto-optical dispersion of methyl butyrate at 12·25° C.

TABLE III. (*b*).

	λ microns.	δ mins./cm. gauss.	*n*.
(*a*)	·4435	$·0209_7$	$1·3990_3$
(*b*)	·4155	$·0242_8$	$1·4016_4$
(*c*)	·3798	$·0298_1$	$1·4060_6$
(*d*)	·3360	$·0397_7$	$1·4134_8$
(*e*)	·3153	$·0464_2$	$1·4187_5$

From (*a*) and (*c*) $\lambda_1 = \cdot 1083\,\mu$ and $K = 5 \cdot 102_8 \times 10^{-3}$

(*b*) and (*d*) $\lambda_1 = \cdot 1073\,\mu$ and $K = 5 \cdot 117_8 \times 10^{-3}$

(*c*) and (*e*) $\lambda_1 = \cdot 1071\,\mu$ and $K = 5 \cdot 122_7 \times 10^{-3}$

(*a*) and (*e*) $\lambda_1 = \cdot 1076\,\mu$ and $K = 5 \cdot 111_2 \times 10^{-3}$.

The mean values of λ_1 and K are $\cdot 1076\,\mu$ and $5 \cdot 113_6 \times 10^{-3}$ respectively, and the equation representing the magneto-optical dispersion of methyl butyrate over the region of the spectrum investigated is

$$n\delta = 5 \cdot 113_6 \times 10^{-3} \frac{\lambda^2}{\{\lambda^2 - (\cdot 1076)^2\}^2}.$$

TABLE III. (*c*).

λ in microns.	δ (observed).	δ (calculated).
·4488	$\cdot 0204_5$	$\cdot 0204_5$
·4237	$\cdot 0231_8$	$\cdot 0232_3$
·4072	$\cdot 0253_8$	$\cdot 0254_1$
·3927	$\cdot 0276_0$	$\cdot 0276_0$
·3627	$\cdot 0331_4$	$\cdot 0331_8$
·3440	$\cdot 0375_6$	$\cdot 0376_0$
·3287	$\cdot 0419_9$	$\cdot 0419_5$

This equation was used to calculate δ for a few wave-lengths at which experimental determinations had been carried out, the values of n being read off from fig. 2. A comparison of the observed and calculated values is shown in Table III. (*c*).

The equation was also employed to calculate Verdet's constant for sodium light, the value obtained being $\cdot 0113_5$ at 12·25° C. Perkin * found the specific rotation of methyl butyrate for sodium light to be 0·8578 at 16·4° C. Taking $\cdot 0131_0$ to be the value of Verdet's constant of water for sodium light, it is found from Perkin's value of the specific rotation that Verdet's constant of methyl butyrate for sodium light at 16·4° C. is ·01124. The value determined from the above magneto-optical dispersion equation is $\cdot 0113_5$ at 12·25° C.

* Journ. Chem. Soc. xlv. p. 500 (1884).

Ethyl Malonate.

A specimen of pure diethyl malonate was obtained from Dr. Schuchardt, of Görlitz, and the values of Verdet's constant for different wave-lengths are given in Table IV.(*a*) and fig. 6.

TABLE IV. (*a*).

Verdet's constant of Ethyl Malonate.

Temperature = 18·5° C.

Wave-length in microns.	Verdet's constant in mins./cm. gauss.
·4588	$\cdot 0198_6$
·4529	$\cdot 0204_6$
·4481	$\cdot 0209_7$
·4425	$\cdot 0215_6$
·4380	$\cdot 0220_8$
·4327	$\cdot 0226_7$
·4285	$\cdot 0231_8$
·4236	$\cdot 0237_7$
·4198	$\cdot 0242_9$
·4153	$\cdot 0248_8$
·4117	$\cdot 0253_9$
·4040	$\cdot 0265_1$
·3967	$\cdot 0276_1$
·3901	$\cdot 0287_2$

TABLE IV. (*b*).

	λ in microns.	δ mins./cm. gauss.	n.
(*a*)	·4588	$\cdot 0198_6$	$1 \cdot 4212_5$
(*b*)	·3901	$\cdot 0287_2$	$1 \cdot 4284_7$

Since the range of spectrum investigated was so small, only the extreme pair of wave-lengths were employed to solve the magneto-optical dispersion equation; but, as will be seen from Table IV. (*c*), the agreement between

the observed and calculated values of Verdet's constant is good.

From (*a*) and (*b*) $\lambda_1 = \cdot 1124\,\mu$ and $K = 5\cdot 249_7 \times 10^{-3}$.

Thus, the equation representing the magneto-optical

Fig. 6.

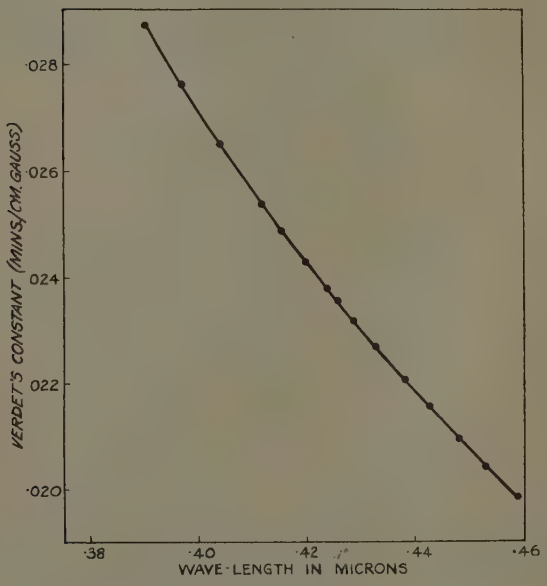

Magneto-optical dispersion of ethyl malonate at 18°5 C.

dispersion of ethyl malonate over the range of wave-lengths investigated is

$$n\delta = 5\cdot 25_0 \times 10^{-3} \frac{\lambda^2}{\{\lambda^2 - (\cdot 1124)^2\}^2}.$$

The accuracy of the representation of the results by this equation is shown in Table IV. (*c*), where a comparison is made of the values of Verdet's constant obtained experimentally and the values calculated from the equation.

Perkin * found the specific rotations of ethyl malonate for sodium light to be ·8823 and ·8775 at 17° C. and 19° C. respectively. The specific rotation at 18·5 is, therefore, ·8787, and taking $\cdot 0131_0$ to be the value of Verdet's constant of water for sodium light, it can be calculated that Verdet's constant of ethyl malonate for sodium light at 18·5° C. is ·01151. The value calculated from the above magneto-optical dispersion equation is $\cdot 0115_2$.

TABLE IV. (*c*).

λ in microns.	δ (observed).	δ (calculated).
·4529	$\cdot 0204_8$	$\cdot 0204_4$
·4481	$\cdot 0209_7$	$\cdot 0209_4$
·4425	$\cdot 0215_6$	$\cdot 0215_4$
·4380	$\cdot 0220_8$	$\cdot 0220_4$
·4327	$\cdot 0226_7$	$\cdot 0226_5$
·4285	$\cdot 0231_8$	$\cdot 0231_5$
·4236	$\cdot 0237_6$	$\cdot 0237_1$
·4198	$\cdot 0242_9$	$\cdot 0242_6$
·4153	$\cdot 0248_8$	$\cdot 0248_6$
·4117	$\cdot 0253_9$	$\cdot 0253_6$
·4040	$\cdot 0265_1$	$\cdot 0264_9$
·3967	$\cdot 0276_1$	$\cdot 0276_2$

The Dispersion Equations.

The experimental results have shown that the magneto-optical dispersion of each of the liquids investigated can be explained by the presence of a single absorption band. If the assumption is now made that the same absorption band is responsible for the ordinary dispersions of the liquids over the same range of wave-length, then the ordinary dispersion of each of the liquids can be represented by the equation

$$n^2-1=b_0+\frac{b_1}{\lambda^2-\lambda_1{}^2}.$$

The constants of the equation can be calculated from two values of the refractive index corresponding to two known wave-lengths.

* Journ. Chem. Soc. *loc. cit.* p. 509.

Isobutyl Formate.

The pairs of values employed in calculating the constants b_0 and b_1 for isobutyl formate are given below :—

λ (microns).	n.	$b_1 \times 10^2$.	b_0.
·6678	$1{\cdot}3876_9$	$\cdot 938_4$	$\cdot 9040_7$
·3602	$1{\cdot}4084_0$		
·5876	$1{\cdot}3900_6$	$\cdot 944_8$	$\cdot 9039_4$
·3280	$1{\cdot}4151_0$		
·5016	$1{\cdot}3939_6$	$\cdot 945_4$	$\cdot 9037_1$
·3093	$1{\cdot}4200_8$		
·4922	$1{\cdot}3944_7$	$\cdot 945_9$	$\cdot 9035_2$
·2961	$1{\cdot}4241_0$		

The mean values of the constants b_1 and b_0 are $\cdot 943_6 \times 10^{-2}$ and $\cdot 9038_1$ respectively ; and the ordinary dispersion equation of isobutyl formate at 10·7° C. is

$$n^2 = 1{\cdot}9038_1 + \frac{\cdot 943_6 \times 10^{-2}}{\lambda^2 - (\cdot 1083)^2}.$$

TABLE V.

λ (microns).	n (observed).	n (calculated).
·4651	$1{\cdot}3963_5$	$1{\cdot}3963_9$
·4275	$1{\cdot}3995_5$	$1{\cdot}3996_3$
·4023	$1{\cdot}4024_5$	$1{\cdot}4023_9$
·3862	$1{\cdot}4045_0$	$1{\cdot}4044_6$
·3602	$1{\cdot}4084_0$	$1{\cdot}4084_9$
·3455	$1{\cdot}4112_0$	$1{\cdot}4112_3$
·3208	$1{\cdot}4168_0$	$1{\cdot}4168_6$
·3005	$1{\cdot}4227_0$	$1{\cdot}4226_4$

The equation was used to calculate n for a few wavelengths at which experimental values had been obtained. Table V. contains a comparison of the calculated and experimental values.

Methyl Butyrate.

The following pairs of values of λ and n were used in calculating the constants of the dispersion equation for methyl butyrate.,

λ (microns).	n.	$b_1 \times 10^2$.	b_0.
·6678	$1{\cdot}3890_1$		
·3621	$1{\cdot}4086_7$	$\cdot 907_1$	$\cdot 9084_6$
·5876	$1{\cdot}3913_6$		
·3455	$1{\cdot}4117_7$	$\cdot 910_9$	$\cdot 9085_8$
·5016	$1{\cdot}3950_3$		
·3308	$1{\cdot}4147_2$	$\cdot 913_9$	$\cdot 9080_3$
·4922	$1{\cdot}3955_8$		
·3194	$1{\cdot}4176_7$	$\cdot 924_5$	$\cdot 9075_7$

The mean values of b_1 and b_0 are $\cdot 914_1 \times 10^{-2}$ and $\cdot 9081_6$ respectively. Thus, the ordinary dispersion equation of methyl butyrate at 12·25° C. is

$$n^2 = 1{\cdot}9081_6 + \frac{\cdot 914_1 \times 10^{-2}}{\lambda^2 - (\cdot 1076)^2}.$$

TABLE VI.

λ (microns).	n (observed).	n (calculated).
·4866	$1{\cdot}3958_5$	$1{\cdot}3959_6$
·4508	$1{\cdot}3984_2$	$1{\cdot}3985_3$
·4275	$1{\cdot}4004_7$	$1{\cdot}4005_7$
·4023	$1{\cdot}4031_2$	$1{\cdot}4032_2$
·3861	$1{\cdot}4052_4$	$1{\cdot}4052_3$
·3688	$1{\cdot}4076_7$	$1{\cdot}4077_1$
·3582	$1{\cdot}4094_7$	$1{\cdot}4094_3$
·3381	$1{\cdot}4131_4$	$1{\cdot}4132_1$
·3247	$1{\cdot}4161_8$	$1{\cdot}4161_9$

From this equation values of n were calculated for several wave-lengths at which experimental values had been found. A comparison of the two is given in Table VI.

Ethyl Malonate.

The constants of the dispersion equation for ethyl malonate were calculated using the following pairs of values for λ and n.

λ (microns).	n.	$b_1 \times 10^2$.	b_0.
·5016	$1{\cdot}4181_9$		
·3545	$1{\cdot}4341_5$	$\cdot 976_5$	$\cdot 9704_0$
·4922	$1{\cdot}4187_5$		
·3416	$1{\cdot}4368_6$	$\cdot 984_0$	$\cdot 9700_0$
·4713	$1{\cdot}4203_1$		
·3378	$1{\cdot}4376_5$	$\cdot 975_5$	$\cdot 9707_1$

The mean values of b_1 and b_0 are $\cdot 978_7 \times 10^{-2}$ and $\cdot 9703_7$ respectively. The ordinary dispersion equation of ethyl malonate at 18·5° C. is, therefore,

$$n^2 = 1{\cdot}9703_7 + \frac{\cdot 978_7 \times 10^{-2}}{\lambda^2 - (\cdot 1124)^2}.$$

TABLE VII.

λ (microns).	n (observed).	n (calculated).
·5218	$1{\cdot}4171_2$	$1{\cdot}4170_6$
·4768	$1{\cdot}4197_5$	$1{\cdot}4198_4$
·4536	$1{\cdot}4216_9$	$1{\cdot}4216_3$
·4378	$1{\cdot}4230_1$	$1{\cdot}4230_4$
·4063	$1{\cdot}4264_3$	$1{\cdot}4263_8$
·3823	$1{\cdot}4295_7$	$1{\cdot}4295_7$
·3600	$1{\cdot}4331_7$	$1{\cdot}4333_0$
·3338	$1{\cdot}4384_3$	$1{\cdot}4385_5$

Table VII. contains a comparison of the experimental results at certain wave-lengths and the values calculated from this equation.

The Calculation of e/m.

The relation between the constant K of the magneto-optical dispersion experiments and the constant b_1 of the ordinary dispersion experiments is

$$K = -\frac{1}{2c^2} \cdot \frac{e}{m} \cdot b_1,$$

and therefore

$$\frac{e}{m} = -\frac{2c^2K}{b_1}.$$

This relation holds when δ is measured in radians per cm. gauss and λ in cm. In the previous calculations, the constants have been evaluated for δ measured in mins/cm. gauss and λ in microns.

The absolute values of K and b_1 for isobutyl formate, methyl butyrate, and ethyl malonate are $1{\cdot}565 \times 10^{-11}$ and $\cdot 944_5 \times 10^{-10}$, $1{\cdot}487_5 \times 10^{-14}$ and $\cdot 914_1 \times 10^{-10}$, and $1{\cdot}527_2 \times 10^{-14}$ and $\cdot 978_7 \times 10^{-10}$ respectively.

Substitution in the above equation gives the following values for e/m :—

Isobutyl formate ..	$e/m = \cdot 99_4 \times 10^7$ e.m.u.
Methyl butyrate	$e/m = \cdot 97_6 \times 10^7$ e.m.u.
Ethyl malonate.....	$e/m = \cdot 93_6 \times 10^7$ e.m.u.

The Experimental Results.

An examination of the observations shows that the magneto-optical dispersion of each liquid over the range of spectrum investigated can be represented by an equation of the type

$$n\delta = K \frac{\lambda^2}{(\lambda^2 - \lambda_1^2)^2},$$

which involves one absorption band of wave-length λ_1, situated in the Schumann-Lyman region of the spectrum. The values of the constants K and λ_1 depend on the nature of the liquid examined.

The refractive indices of the liquids can also be represented within experimental error by an equation of the type

$$n^2 - 1 = b_0 + \frac{b_1}{\lambda^2 - \lambda_1^2},$$

where λ_1 has the same value as that deduced from the magneto-optical experiments. The values of the constants b_0 and b_1 vary from liquid to liquid.

The chief difficulty in the determination of the refractive index is due to variation of temperature, and the experimental results show that an increase of temperature of 1° C. diminishes the refractive index by about 4 in the fourth place of decimals. It is considered that the refractive indices obtained in the present investigation

TABLE VIII.

Liquid.	Molecular weight.	λ_1 (microns).	$K \times 10^3$.	Temp. °C.
A. Ethyl formate * : $(H . CO_2 . C_2H_5)$	74	·1061	4·72	14·8
Propyl formate † : $(H . CO_2 . C_3H_7)$	88	·1077	4·91	20·0
Isobutyl formate : $[(CH_3)_2 . CH . CH_2 . COOH]$..	102	·1083	5·38	10·7
B. Butyric acid ‡ : $(C_3H_7 . COOH)$	88	·1064	$5·28_5$	13·1
Methyl butyrate : $(C_3H_7 . COOCH_3)$	102	·1076	$5·11_4$	12·25
Ethyl butyrate ‡ : $(C_3H_7 . COOC_2H_5)$	116	·1081	$5·25_9$	13·1
C. Ethyl oxalate § : $(C_2H_5OOC . COOC_2H_5)$	146	·1105	$5·39_2$	9·5
Ethyl malonate : $(C_2H_5OOC . CH_2 . COOC_2H_5)$.	160	·1124	5·25	18·5

* Jenkins and Evans, Phil. Mag. xi. p. 377 (February 1931).
† Thomas and Evans, *loc. cit.* xi. p. 1220 (June 1931).
‡ Lewis and Evans, *loc. cit.* xiii. p. 265 (February 1932).
§ Beanland and Evans, *loc. cit.* xv. p. 905 (May 1933).

are accurate to within 1 or 2 in the fourth place of decimals, and the ordinary dispersion equation deduced on the assumption that λ_1 has the same value as that calculated from the magneto-optical experiments, represents the results with the above degree of accuracy.

It is interesting to compare the experimental results with those obtained for other liquids, which have been examined in this laboratory. These results are collected in Tables VIII. and IX.

An examination of Table VIII. shows that the values of λ_1, and K for the formates increase as the molecular weight increases. This statement is true for iso-butyl formate, which differs in structure from the normal ethyl and propyl formates. Also when similar compounds, such as those included in groups B and C, are compared, it is seen that the value of λ_1 increases as the molecular weight becomes higher. The value of K, however, varies irregularly, but when esters of the same acid are compared, it is found that K increases with increase of molecular weight. The value of K depends partly on the specific rotation, which for light of a given wave-length

Table IX.

Liquid.	b_0.	$b_1 \times 10^{10}$.	$\frac{e}{m} \times 10^{-7}$.	Temp. °C.
Ethyl formate	·8323	·830	$·99_6$	12·8
Propyl formate	·8691	·897	·96	20·0
Isobutyl formate	·9038	$·943_6$	$·99_2$	10·7
Butyric acid	·9352	·930	$·99_4$	13·1
Methyl butyrate.....	·9082	·914	$·97_6$	12·25
Ethyl butyrate	·9209	$·910_3$	$1·00_8$	13·1
Ethyl oxalate	·9716	1·034	$·91_0$	9·5
Ethyl malonate.....	$·9703_7$	978_7	$·93_6$	18·5

generally diminishes by a small amount as the temperature rises.

The most interesting result, which follows from an examination of Table IX., is the very low values of e/m. These low values are in agreement with those obtained by other investigators for different substances.

Although the theory employed in the present calculations does not therefore lead to satisfactory values of e/m, it must be remembered that the magneto-optical dispersion equation with one constant K and one absorption band of wave-length λ_1, may not account for the experimental results, if measurements of Verdet's constants were carried out for much lower wave-lengths.

XXXI. *Photographic Photometry based on Scattering.* *By* J. Brentano, *D.Sc., Lecturer in Physics, Manchester University*, A. Baxter, *M.Sc., and* F. W. Cotton, *M.Sc.**

Summary.

A method is developed in which the scattering properties of silver grains are used for measuring photographic actions. As distinct from the ordinary method of photographic absorption photometry, in which a difference effect is observed, a direct effect is introduced by this means.

The relations between exposure and number of silver grains, and of grain-size and scattering, on which this method depends, are discussed, and experiments are described on the scattering and absorbing properties of photographic layers in terms of grain-size, wave-length, and scattering-angle.

A scattering microphotometer is described, and curves are discussed relating scattering to exposure for X-rays. It is found that for small densities proportionality between scattering and exposure is satisfied with great approximation, and that much smaller densities can be evaluated than by absorption. An accuracy of 0·2 per cent. of the limiting value of the range within which proportionality exists can be obtained.

The method is used to investigate the existence of any threshold value for X-rays. Extending the measurements into the range of very small densities which can be evaluated by scattering, it is found that no threshold value can be detected.

The proportionality between scattering and exposure and the shift of photometry into a range of smaller densities make it possible to evaluate an area of varying density in a single process, and to eliminate the " diffusion effect " of the developer, which impairs the evaluation of large densities. The advantages resulting from these two points in the measurement of the intensity of spectral lines are discussed.

Applications are made relating to the evaluation of X-ray reflexions obtained with a crystal-powder camera and of Laue spots.

---

* Communicated by J. Brentano.

1. IN the present paper an account is given of a method for the evaluation of photographic densities based on the scattering of light from the silver particles of the film, which has been briefly described by one of us *. It consists essentially in an arrangement by which a parallel beam of light of constant intensity is directed normally on a photographic film, and in measuring the photographic action by the quantity of light scattered from the silver particles at an oblique angle.

The principal aim in developing this method was to make the photographic measurement of radiation more direct, and in particular to increase accuracy in the region of small densities.

In principle the action of light on a photographic emulsion can be evaluated by any means which measures the quantity of reduced silver. The method generally adopted, on which absorption photometry is based, consists in measuring the decrease in intensity of a parallel beam of light in passing normally through the photographic film, and expressing the photographic action by the density d defined as $d = \log I_0 - \log I$ (Hurter and Driffield), where I_0 is the intensity of the incident beam and I the intensity of the parallel beam after passing through the layer. The reduction of intensity of I_0 in this case is partly due to true absorption and partly to scattering and to deflexion of light out of its original direction. In some designs of photometers part of the scattered light is included in I †, so that the decrease of intensity is more nearly due to true absorption; in all cases absorption plays a predominant part under normal conditions. Limitations of this method are found when evaluating small densities, because the measurement is essentially based on a difference effect, namely, on comparing the intensity I_0 of the beam entering and of the beam I emerging from the layer, and is therefore liable to comparatively large relative errors when the quantities I_0 and I are both large compared with their variation. A further limitation is experienced when evaluating areas of uneven density—for instance, the intensity of spectral lines, in so far as the absorption of the beam of light used in the process of photometry is not a linear

* J. Brentano, *Zeitschr. f. Physik*, lxx. p. 74 (1931).

† These conditions have been investigated by R. Jürgens, Diss., Hamburg (1928).

function of the exposure of the photographic emulsion. Although the relation between d and exposure, "the blackening curve," may in certain cases approximate very closely to a linear relation, the change of the recorded I values with exposure is in general far from linear. Thus photometry of an unevenly exposed area cannot be done by determining the absorption for this area in a single process, but must be carried out by determining the absorption point by point in sections sufficiently small to make the variation of density over each section negligible. These point by point values must be translated into exposures by means of a "blackening curve."

Both the estimate of the mass of silver and of the number of silver grains involve direct effects, and overcome therefore the disadvantage associated with the measurement of a difference effect. The first measurement is difficult owing to the smallness of the quantities, the total quantity of silver being of the order of 1 to 3 mg. per sq. cm. The counting of the number of grains is inconvenient in practical application. By measuring the scattering properties of the film, comparatively simple conditions arise, in so far as for small exposures the number of grains is held to be proportional to the exposure, while the size of the grains, which mainly depends on development and not on exposure, has less effect on their scattering than on their absorbing properties. Thus we are estimating the photographic action by a phenomenon which is mainly connected with the number of grains and little influenced by their size.

It seems justifiable to discuss these conditions more in detail, because, on the one hand, they determine the experimental work required to establish the most suitable conditions for scattering photometry, and on the other hand indicate the direction in which further improvement could be achieved.

2. As to the relation between the number of grains and exposure, Scheffers * counted the number of silver grains per sq. cm. over a wide range of exposures, and found it approximately proportional to the density as defined above up to density values of about 1·8. The same relation was found for the mass of silver.

* Scheffers, *Zeitsch. f. Phys.* xx. p. 109 (1923).

His exposures were taken with visible light. It is difficult to state definite general relations when referring to the visible part of the spectrum, owing to the fact that the action of light is not represented by the Bunsen Roscoe reciprocity law, but in terms of densities by Schwarzschild's expression $d=it^p$, where i is the intensity of radiation, t is the time of exposure, and p is a function of the density d, having values between 0·4 and 1·8 *. For the more usual range of exposures with average type emulsions p values are between 0·8 and 1·3.

Owing to the departure of p from unity and to its variation through the range of exposures, any measurement depends on both time and radiation intensity. For X-rays, however, the value of p is found to be unity within the limits of experimental error, and, further, the threshold value of exposure below which no photographic action takes place is negligible or small; exposures can thus be expressed by the product of intensity by time †. For this reason, and also because we were particularly interested in the application to the measurement of X-ray reflexions, the method has in the first place been developed with X-rays.

J. Eggert and W. Noddack have determined the number of silver atoms of the latent image and also the number of atoms in terms of the quanta of absorbed radiation, and have extended these measurements to X-rays and to α-rays ‡. They found that in the visible range one atom of silver corresponds approximately to the absorption of one quantum, and one silver nucleus corresponds to the absorption of approximately 300 quanta. For X-rays about 1000 silver atoms correspond to one quantum of energy absorbed. The general validity of these results has been questioned §, and the

* J. Eggert, *Zeitsch. f. Techn. Physik* (1933); for general data on the photographic action of light see E. v. Angerer, 'Wissenschaftliche Photographie' (1931).

† H. Krönckе, *Ann. d. Phys.* xliii. p. 687 (1914); Friedrich and Koch, *Ann. d. Phys.* xlv. p. 399 (1914); Glocker and Traub, *Phys. Zeits.* xxii. p. 351 (1921); Bouwers, 'Over het meten der intensiteit van Röntgenstralen' (1924).

‡ J. Eggert and W. Noddack, *Sitzungber. d. preuss. Akad. d. Wiss.* p. 631; *Naturwiss.* xv. p. 57 (1927). Similar measurements in the visible were also made by H. Kieser, *Zeits. f. Wiss. Photog.* cccxxi. p. 26 (1929); A. Smakula, *Zeits. f. Phys.* lxiii. p. 762 (1930).

§ G. B. Kistiakowsky, 'The Chemical Catalogue,' pp. 41–51 (1928); J. Eggert and W. Noddack, *Zeits. f. Phys.* lviii. p. 861 (1929).

interpretation given does not cover the whole aspect of photographic action.

Considering in a more general way the production of the latent image, its close relation to the liberation of silver from haloids and to photoelectric and photoconduction phenomena, is indicated by a large number of recent investigations *. The experiments of R. Hilsch and R. W. Pohl † on the appearance of induced absorption bands in haloid crystals after exposure to light, and the interpretation of the Herschell effect, *i. e.*, the disappearance of the latent image after exposure to long wave radiation or heating as a "bleaching effect" of photoconduction, confirm this view ‡. The assumption is that the action of light involves essentially a photoelectric process, which leads to the liberation of neutral silver atoms within the silver bromide crystals, and thus produces local deformations of the electrical fields of the lattice, and establishes suitable conditions for the chemical action of the developer §. The process may be direct or indirect, and is certainly indirect in the case of X-rays. We can expect, however, that for X-rays, where one quantum of incident radiation represents more energy than is required for the formation of one developable centre or nucleus, the production of these nuclei is the result of locally strong absorption of the intermediate stages of X-rays or photoelectrons.

In this view the number of nuclei should be proportional to the exposure and the number of silver grains too, except where several nuclei formed within the same silver bromide crystal or within adjacent crystals may lead to the production of only one grain. This will be relatively more frequent for large exposures. We should thus expect that the number of grains is proportional to the exposure at first, with a relative decrease for large

* Fajans, *Zeits. f. Elektrochem.* xxviii. p. 499 (1922); S. E. Shepherd and E. P. Wightman, Eastman Kodak Co. Res. Lab. i. Comm. p. 85 (1923); F. C. Toy, H. A. Egerton, and J. D. C. Vick, Phil. Mag. iii. p. 482 (1927). For a general survey see A. L. Hughes and L. E. Dubridge, 'Photoelectric Phenomena,' p. 339 (1932).

† R. Hilsch and R. W. Pohl, *Nachr. d. Ges. d. Wiss. zu Göttingen Math-Phys. Klasse*, p. 176 (1930): *Zeits. f. Phys.* lvii. p. 145 (1929), lix. p. 812 (1930), lxiv. p. 606 (1930).

‡ A. L. Hughes and L. E. Dubridge, 'Photoelectric Phenomena,' p. 339 (1932): R. W. Gurney, Proc. Roy. Soc. cxli. p. 209 (1933).

§ This does not consider the action of silver sulphide and other sensitisers which enhance the photographic action of light but not of X-rays.

exposures. Proportionality may be better satisfied by choosing conditions of development which will prevent the merging of the reduced silver into large units, a point which we shall discuss later.

3. Apart from proportionality between the number of grains and exposure, the question arises of whether scattering is an adequate means for measuring the number of grains. The average size of silver particles in a photographic film extends from about $5 \cdot 10^{-5}$ cm. to $5 \cdot 10^{-4}$ cm., and the particles are therefore too large to satisfy the Rayleigh conditions of scattering from extremely small particles. Work on the scattering from particles of a size comparable with the wave-length of light has been done by Mie, Shoulejkin, and Blumer *, but mostly with regard to the scattering from perfect dielectrics. Jobst † calculates the total scattering from a spherical gold particle in water for various wave-lengths, considering conditions which correspond to those of colloidal suspensions. For particle diameters somewhat smaller than the wave-length of the visible range he finds conditions of preferential scattering, which are determined by the optical constants of the particles, of the surrounding medium, and by the wave-length; for instance, for particles of 100 $\mu\mu$ diameter this takes place for a wave-length of 600 $\mu\mu$. Jobst also compares the energy scattered with the energy absorbed for different particle sizes and wave-lengths. It is difficult to draw a close analogy between the spherical particles considered by Jobst and the irregular particles of silver in the gelatine layer. It should be noted, however, that Jobst's calculations agree with the predominant scattering of certain wave-lengths, which was, for instance, observed by Ehrenhaft ‡ in experiments with small silver particles in a Millikan condenser, when pronounced scattering through larger angles was observed for certain ranges of wave-lengths depending on the size of the particles. We may expect the silver particles used by Ehrenhaft to be similarly irregular in shape to the silver particles in the gelatine, and we may thus

* G. Mie, *Ann. d. Phys.* xxv. p. 377 (1908); W. Shoulejkin, Phil. Mag. xlviii. p. 317 (1924); H. Blumer, *Zeits. f. Phys.* xxxviii. p. 304 (1926).

† Jobst, *Ann. d. Phys.* lxxvi. p. 863 (1925).

‡ F. Ehrenhaft, *Phys. Zeits.* xviii. p. 352 (1917). See also R. Feick, *Ann. d. Phys.* lxxvii. p. 573 (1925).

be justified in applying Jobst's results to such particles. It would then follow that for particles larger than those giving preferential scattering the scattered intensity increases more with wave-length than does absorption, while the scattering in terms of cross-section changes less with particle size than does absorption. For very large particles Sauer * has shown that scattering should be independent of the wave-length. For very small particles it would appear that these conditions of selective scattering might be approximated by a suitable choice of emulsion or wave-length.

Fig. 1.

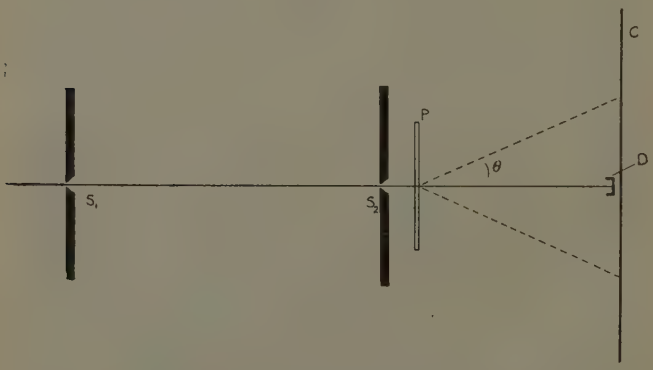

Arrangement for observing scattering.

4. To establish the most suitable conditions for scattering photometry, experiments were carried out on the angular distribution of scattered radiation for different emulsions and for different incident wave-lengths. The arrangement used (fig. 1) consists of two diaphragms S_1 and S_2, defining a narrow parallel beam of light, which falls normally on the photographic film in P. The transmitted beam is absorbed in D, while the light scattered at any angle θ with respect to the direct beam can be observed in the plane C. The scattering of radiations from different parts of the spectrum was obtained by interposing filters. Each of the filters comprises about 1/10th of the wave-length range of the visible

* E. Sauer, *Zeits. f. Inst.* li. (1921).

spectrum, and the middle of the transmitted bands have wave-lengths :

for red.....	640 $\mu\mu$,
green ...	530 $\mu\mu$,
blue	450 $\mu\mu$.

The curves (figs. 2 (*a*) to 3 (*b*)) give the quantity of scattered light per unit area on C in terms of the angle θ

Fig. 2 (*a*).

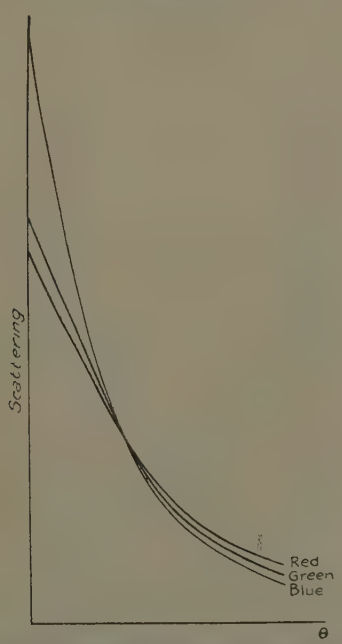

Angular distribution of the scattered intensity for a coarse-grain emulsion of light density.

in relative values. They are plotted on such a scale as to make one point coincide for each of the three wave-lengths used. The curves are typical for coarse and fine-grain emulsions, and represent the range of variability of different commercial types examined.

Figs. 2 (*a*) and 2 (*b*) refer to Ilford panchromatic emulsion, for which the average grain-size as measured with an oil-immersion microscope was 4.10^{-4} cm. As will be seen

the scattering falls off most rapidly for the blue and least rapidly for the red, and this was especially so for long exposures. Figs. 3 (*a*) and 3 (*b*) refer to a Paget slow lantern plate, with an average grain-size of $5{\cdot}5.10^{-5}$ cm. Here, with a fine-grain emulsion the scattering decreases again most rapidly in the blue, but it extends through the largest angular range for the green. The size is too large to account for this effect by preferential scattering,

Fig. 2 (*b*).

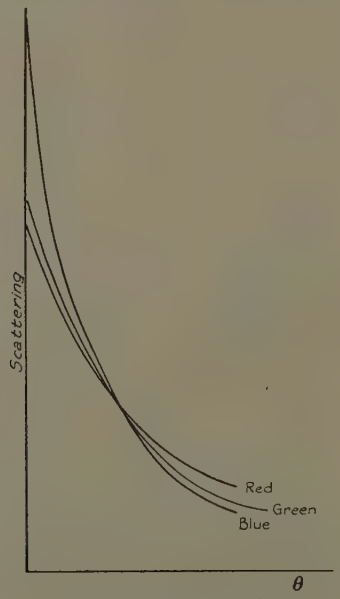

Angular distribution of the scattered intensity for a medium-grain emulsion of medium density.

as calculated by Jobst, when considering the whole grain as one scattering unit ; it could, however, arise if we may consider the irregularly distributed fragments of the grain as separate scattering units. It would be of particular advantage to use such a selective scattering effect, and give prominence to the scattering from the silver particles. Experiments in this direction by varying the wave-length were not successful, and it is probable that with the

commercial emulsions examined, the range of variability of the silver grains is too large to give prominence to any selective effect.

Experiments were made with clear gelatine films containing no silver, and it was found that the scattering from the gelatine surface lies mainly within a range of 5°. It varies considerably for various emulsions, being a minimum for thinly coated lantern slides, but it is largely affected by handling of the film, owing to scratching of the

Fig. 3 (*a*).

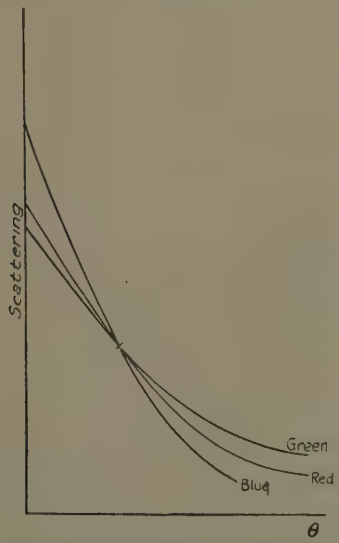

Angular distribution of scattered intensity for a fine-grain emulsion of light density.

surface. For the scattering from a glass surface experiments have been made by Pokrowski *, and it was found to be inversely proportional to the angle θ, and to be much less than for gelatine. The surface scattering is therefore greatly reduced by covering the gelatine with glass, making optical contact by means of Canada balsam. The technique adopted was to place a drop of Canada balsam solution in xylol on the gelatine surface, and to press a microscope slide against it, sealing the borders by passing over them

* G. I. Pokrowski, *Zeits. f. Phys.* lxv. p. 1 (1930).

with a hot soldering-iron. In the case of films on celluloid support both sides were covered in this way, the film being sandwiched between two microscope slides. Suitable slides free from scratches were provided by Messrs. Chance Bros. Ltd., to whom we are indebted for the care in selecting and packing them. In all subsequent work we made use of this technique to reduce the surface scattering. When examining light densities it

Fig. 3 (*b*).

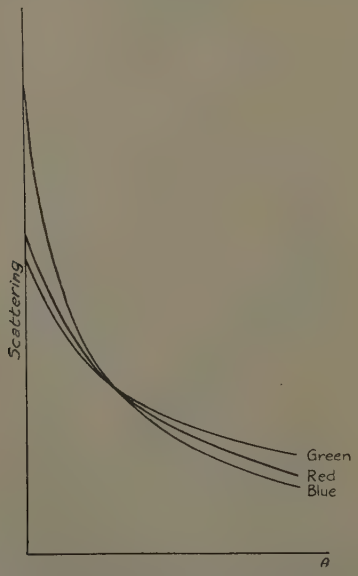

Angular distribution of scattered intensity for a medium-grain emulsion of medium density.

was found that some irregular scattering remains which could be attributed to the presence of small foreign particles within the gelatine or firmly fixed on its surface *. This is scarcely perceptible when exploring large areas, but becomes noticeable in the use of a microphotometer for very small densities, and will be referred to again.

* Much of this can be removed by careful wiping of the film with a pad of cotton-wool moistened with alcohol; but the greatest care must be used in all handling of the film.

5. The intensity of the scattered light is affected by absorption in the film. The absorption due to the silver particles depends on their distribution, and so far as it refers to the scattered light it will depend on the angle of scattering and increase rapidly with increasing angle. Experiments on absorption were therefore undertaken under conditions comprising an average inclination of the beam similar to that in the experiments on scattering. The results for the two emulsions referred to above are given in fig. 4 in relative measure.

Fig. 4.

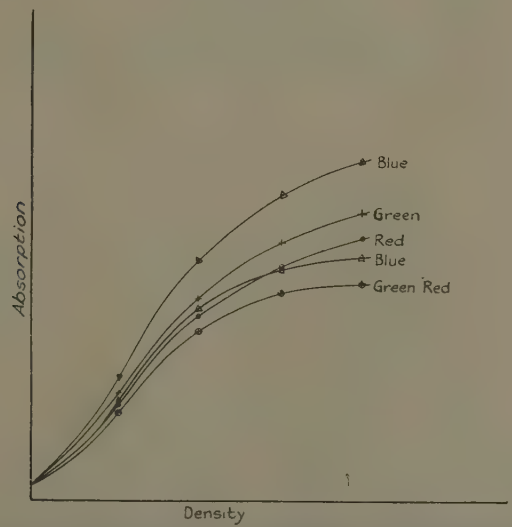

Relative absorption for various wave-lengths in a coarse-grain silver emulsion (higher curves) and in fine-grain emulsion (lower curves).

For both films, the Ilford panchromatic and the Paget slow lantern plate, the absorption is greatest for blue and least for red.

6. For the purpose of establishing the best conditions for photometry the angular range of scattering should be chosen so as to make the effect of scattering from the gelatine or from the glass covering the film small, and to avoid on the other hand angles so large as to increase unduly the absorption of the scattered beam in the film. It will appear from the experiments that the best

conditions are obtained for a range for θ from 6° to 15°. In selecting the wave-length for scattering preference might be given to green for fine-grain emulsions. The gain, however, for the commercial emulsions examined is not very pronounced, while absorption is considerably less for long wave radiation. Illumination with a wave-length in the region of 600 μ is best. This long-wave illumination has the further advantage that the emission from a metal filament is much steadier

Fig. 5.

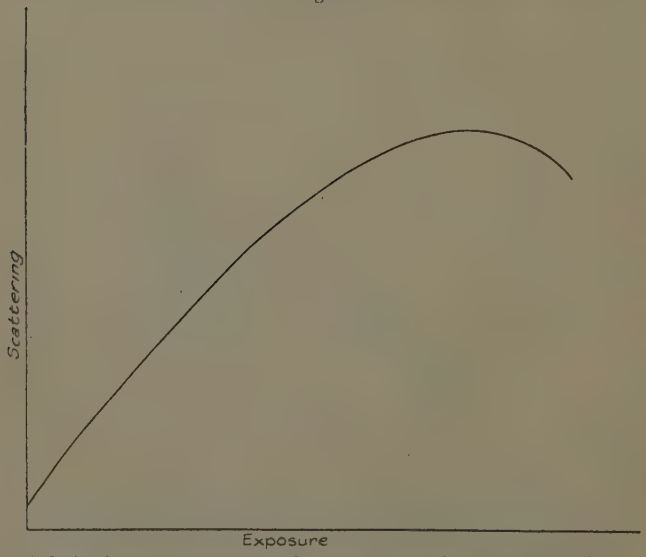

Relation between scattering and exposure extending to high densities.

in the red and less affected by voltage fluctuation than in the short wave range. Fine-grain types of emulsion seem preferable, giving considerably greater scattering in the range of larger angles. The effect of wave-length and of grain-size will be discussed further in connexion with the shape of the blackening curves obtained.

Experiments relating scattering to exposure were done with an arrangement similar to the one described previously, they indicate a linear relation for small exposures with a gradual falling off of scattering for larger

exposures. For very large exposures actually a falling off of scattering occurs due to increasing absorption of the scattered light, giving an effect similar in appearance to solarization, although taking place in a different range of densities and being due to a different cause. A typical curve of this type is shown in fig. 5. The interesting part of the curve for the practical purposes of photometry is the initial approximately straight section.

These results may not be discussed in detail, as the practical requirements of photometry are better met with a type of instrument using a converging beam, which could be used for microphotometry. The detailed discussion of the scattering properties may therefore be referred to the observations taken with this instrument.

Fig. 6.

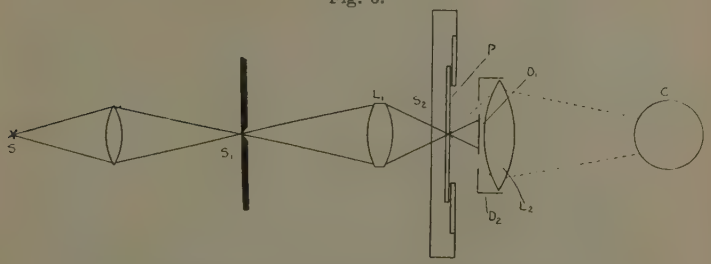

Diagram of optical part of microphotometer.

7. For evaluating the total intensity of spectral lines a linear relation between exposure and scattered light would actually dispense with the necessity of a close point-to-point microphotographic measurement. To locate the exact distance of peaks and to determine the distribution of intensities it was desired however to design an instrument which could also be used for a detailed evaluation.

Fig. 6 gives a diagrammatic view of the optical part of the instrument. S is a source of light illuminating slit S_1, an image S_2 of which is projected on the photographic film in P by means of a lens system L_1. This lens consists of a Cooke-Hobson cinema anastigmat of F/1·8 aperture and 1 in. focal length. It is held in a helical focussing mount. The distances between the lens L_1

and S_1 and S_2 respectively are chosen so as to give a reduction of the size of the original slit in the ratio of 1 to 3. The width and height of slit S_1 could be adjusted by means of micrometer screws. The direct beam passing through the photographic film falls on a small diaphragm D_1 of such size as to collect the beam diverging from S_2, and in addition the light scattered within an angular range of 5° beyond the aperture of the direct beam. The scattered light which passes the diaphragm D_1 is collected by an optical condenser system L_2 on to a photoelectric cell in C. An iris diaphragm D_2 situated in the same plane with D_1 limits the maximum angular range of the scattered radiation received by the photoelectric cell. An iris diaphragm is also provided in the lens system L, and stops of various size can be placed in D_1, so that various conditions of illumination can be obtained. The film in P can be rotated in its own plane and displaced in this plane in two directions at right angles; spectral lines could thus be set parallel to the slit and records taken at various heights. For the purpose of recording X-ray lines the the slit image S_2 was generally ·025 mm. wide and 2 mm. high, so that the area simultaneously exposed was ·05 mm.^{2}. When using films mounted between glass plates the focussing of S_1 on to the gelatine required making an allowance for the interposition of the glass. The illumination of the slit S_1 was provided by a 6 volt 12 watt filament, and the short-wave side of the spectrum was cut off by a red Ilford tricolour process filter. In the early experiments different kinds of filters were used; it was found that the tricolour process filter was practically equivalent to a more strictly monochromatic filter for the long-wave range. The transmission of this filter extends from 5,800 to 7,100 Å.U. For greater sensitivity the intensity of illumination could be increased by using an Ilford blue minus filter, ranging from 5,000 to 7,000 Å.U., without appreciable increase in flattening of the blackening curve.

The photoelectric cell was a B.T.H. gas-filled cæsium cell, with a voltage of 6 volts applied between the electrodes, so that ionization by collision was negligible and the action conformed to that of a vacuum cell. This cell was exceptionally stable and proved to be superior to a number of other cells of various types tried.

The light scattered from the photographic film is always a small fraction only of the incident beam, so that very weak illuminations were received by the cell. The photoelectric currents were of the order of 10^{-12} amp., and were recorded on a Gambrell galvanometer having an internal resistance of 7000 ohms and a sensitivity of $5 \cdot 10^{-9}$ amps/sec. div.

The required magnification of the photoelectric current was obtained by means of a balanced bridge circuit giving the required stability with respect to external disturbances and fluctuations of the anode voltage, described by one of us in previous publications *.

The actual recording was done by moving the photographic film on a carrier in a direction normal to the illuminating slit image S_2 and recording the galvanometer deflexions on a drum, the rotation of which was linked with the displacements of the photographic film. Marks on the drum indicate the zero position of the galvanometer and check the correct working of the mechanical linkage between the photographic film and the recording drum. Under normal conditions the spot of light on the drum is steady, and no appreciable variation of the intensity of the light source S occurs after the circuits have been switched on for one hour. The time lag of the photoelectric cell used is negligible and the speed of recording mainly determined by the inertia of the galvanometer. With the galvanometer used the photographic film in P can be displaced by 1·8 mm. per minute.

8. Blackening curves of scattering in terms of exposure were obtained by the use of exposure marks, prepared with a rotating disk, giving eleven stepped bands each 2·5 mm. wide, with exposure times increasing in the constant ratio of 1·5. These exposure marks were taken at a distance of 2 feet from the X-ray bulb, so that the intensity of the beam should be fairly uniform. To secure greater equality the film and the rotating sector were actually displaced and rotated in their own plane during the course of the exposure. For some exposures a stepped disk was used, giving a linear progression of exposures 1, 2, 3, 4, 5, 6. The steps in this case were 4 mm. wide, and this disk, covering a less

* J. Brentano, 'Nature,' cxxviii. p. 532 (1921); Phil. Mag. vii. p. 685 (1929); *Zeits. f. Phys.* liv. p. 571 (1929).

wide range of exposures and giving a greater area for each step, was particularly suited for accurate measurements in the range of small densities. A further disk used was cut to an equiangular spiral, giving an increment of 1 mm. radius for 6·25°. Disks of this spiral type are often used for obtaining areas of variable density ; they are, however, exposed to large systematic errors. Exposure marks were also obtained by means of a "pin-hole" camera, consisting of nine tubular lead chambers, at the bottom of which the film was placed. The other ends were closed by a disk with apertures of uniform size, increasing in number from 1 to 9. Exposures were taken by placing this camera against a copper plate from which secondary X-rays were scattered, in a similar way as in the experiments of Friedrich and Koch *, and by placing it in the direct beam at a large distance from the bulb, providing independent rocking motions in two directions in such a way as to give uniform exposures. Exposure marks obtained with the various disks and with the pin-hole camera were compared on many occasions, so as to secure the accuracy of the relative exposure values. A copper anticathode was used in conjunction with a nickel filter and 18 kv. applied to the bulb, so as to obtain mainly X-radiation of a wave-length in the neighbourhood of 1·5 Å.U.

The scattering curves obtained determine the relation between exposure and scattered light as measured by the photoelectric current or the galvanometer deflexions. The photometer was set according to the conditions established by our scattering experiments, and these were compared with different settings, varying the extent of the angular projection of the stop D_1 and varying the wave-length of the scattered light. In a general way the conditions established by our previous experiments were proved to be correct. Fig. 7 illustrates, as an example, the effect of changing the light from red to blue for a series of steps on a Kodak dental C film. The curve obtained for red approximates a straight line up to considerably larger densities than for blue. As to the effect of changing the angle of incidence of the illuminating beam and the range of scattering, the diameter of the disk D_1 actually defines only the minimum

* Friedrich and Koch, *Ann. d. Phys.* xlv. p. 399 (1913).

angle of deflexion of scattered light collected on the photoelectric cell. For this reason the arrangement is not very sensitive to variation of the diaphragms D_1 and D_2. It was confirmed, however, that with a fine-grain emulsion the optimum conditions are reached for a setting of the diaphragm D_1 so as to exclude the light scattered at angles less than 7°, and D_2 so as to comprise a range of 10° to 13° between D_1 and D_2.

Scattering curves were obtained for a number of emulsions and estimates of the grain-size made. We are indebted to Messrs. Kodak, Ltd., for providing us with

Fig. 7.

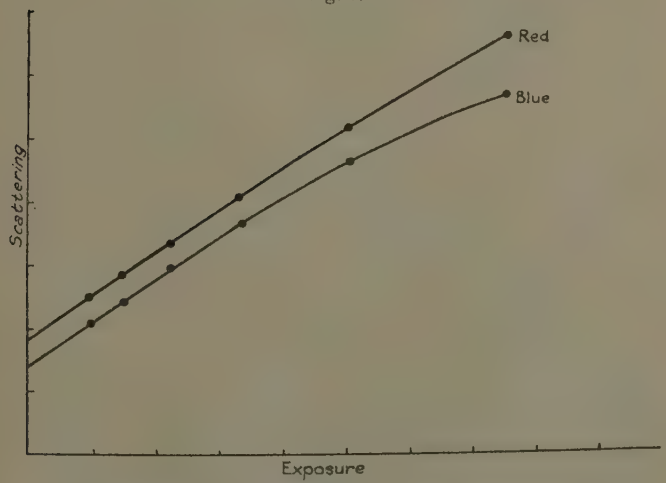

Scattering curves recorded with different wave-lengths from the same film.

a variety of emulsions, some of which were received from Rochester, U.S.A., in special packing to avoid surface abrasions. Fig. 8 shows scattering curves for some typical emulsions, for which the average silver grain-sizes are tabulated below :—

	Grain-size.
Cine negative	$4{\cdot}0.10^{-4}$ cm.
„ duplicating	1·4 „
Dental C	1·3 „
Cine positive	0·9 „

It will be seen that all curves cut the ordinate for zero exposure at a certain height which represents the scattering from the unexposed film and is mainly due to the silver particles forming the chemical fog of the negative. The difference in steepness indicates different X-ray sensitivities as measured by scattering. For large exposures the curves decrease in steepness, this occurs for smaller scattering values with the coarser emulsions. In general this is essentially accounted for by the absorption of the incident and scattered light by the

Fig. 8.

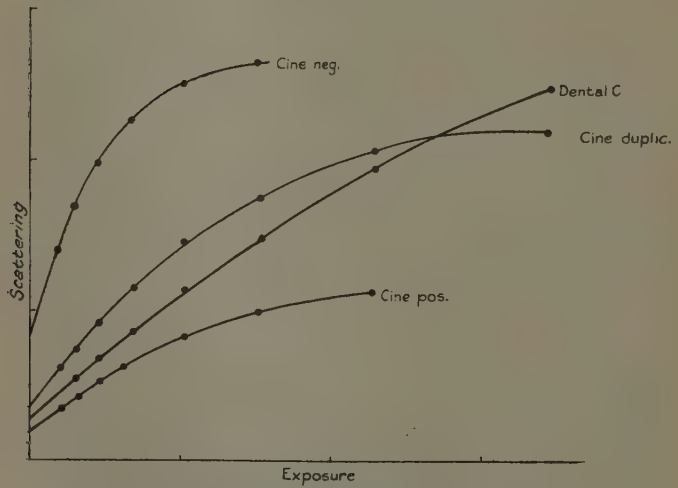

Scattering curves for various emulsions for the same range of exposures.

silver particles, an effect which becomes predominant over scattering with increasing densities, in particular with large grains.

It must, however, also be considered that another reason for the flattening of the scattering curve is that with increasing exposure the chance that any nucleus produced by the absorption of radiation may lead to the formation of an additional silver-grain decreases, as we have already discussed. Assuming the formation of nuclei of the latent image to be proportional to exposure, the number of silver grains will only be proportional

so long as each nucleus is a separate centre for the development of a new grain. With increasing density of the nuclei in terms of the silver bromide particles the number of grains developed will fall off. This deficiency will be particularly marked in an emulsion containing little silver bromide, where a certain scattering value is only reached when a greater proportion of the silver bromide particles has been affected. Comparing dental C and cine positive, the latter emulsion contains much less silver bromide, and we find that the flattening of the scattering curve actually occurs at smaller scattering values, although the silver particles are less large. With cine positive an increase of the exposure did not give the accentuated drop observed with heavily loaded emulsions. This is to be expected if the flattening of the curve is due to the reason given above.

9. A number of experiments were made to determine how the scattering properties of the silver particles could be affected by different conditions of development. Various commercial fine-grain developers were tried, but gave no marked change. In varying the conditions of development two lines were followed : on the one hand, it was tried to reduce the quantity of fog, and thus lower the density for zero exposure. The developer best satisfying this condition was a solution of 1 : 20 of Rodinal with 0·25 per cent. of potassium bromide, developing the films for 4 minutes for thin emulsions and for 5 minutes for thick emulsions at a temperature of 16° C. This method of development gave not the minimum fog, but the minimum fog without appreciable suppression of the small densities. Rodinal was preferred owing to its easy standardization, although other developers gave slightly more favourable results. The other line was to obtain a fine-grain emulsion by the short action of a concentrated developer, so as to prevent the formation of large silver grains and produce the greatest possible number of nuclei. During development each nucleus becomes the centre of formation of a silver grain, the size of this grain depending on the particular conditions of development. According to the discussion in § 8 the number of fresh nuclei formed during any additional exposure, which can produce new independent silver grains, is proportional to the amount of silver

bromide left outside the range of formation of the nuclei already in existence. A process of development which prevents the merging of the nuclei will enhance proportionality between the number of silver grains and exposure in the range of larger nuclear densities. Using Rodinal in a concentration of 1 : 5, without any addition of potassium bromide, and developing for one minute at 16° C., films were obtained having a fog density about equal to the density obtained with the development described before, but with considerably greater uniformity of grain-size. The difference in the scattering curves is shown by fig. 9 for two dental C films exposed under identical conditions and developed according to the two methods described.

Fig. 9.

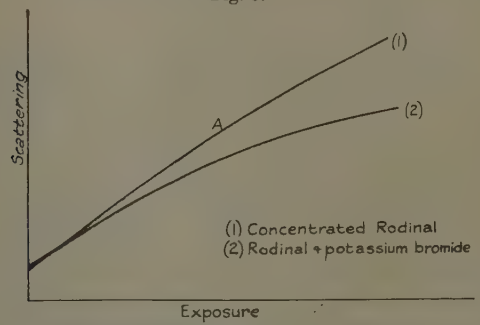

Scattering curves for different conditions of development.

Referring to fig. 9, curve 1, it will be seen that for the practical purpose of photometry a nearly linear relation exists between scattering and exposure up to the point marked A, which corresponds to a density of 0·23 in terms of the Hurter and Driffield scale. This range of approximate proportionality extends to densities about 1/10th of those used in absorption photometry. On the other hand, the high accuracy for small densities offsets the limitation of the range. The average error of measurement is found to be 0·2 per cent. of the exposure value up to which proportionality can be assumed.

The shift of photometry into the range of smaller densities has one particular advantage, in so far as it reduces errors due to the varying rate of diffusion of

the developer. This affects high density values, where the rate of development is largely controlled by the renewal of the developer and the removal of soluble bromides from the gelatine during development *. For a narrow line of great density surrounded by a field where the density is small this diffusion effect is not the same as for an extended area, so that the application of a blackening curve derived from steps of greater area to the evaluation of a sharp spectral line is not justified. With the small densities used in scattering photometry these effects become negligible, particularly when the development is carried out in a concentrated developer during a very short time, as described above.

10. It was of particular interest to examine the initial part of the scattering curve more closely, as with the scattering method the existence of any threshold value for X-rays might be detected. The earliest measurements on the photographic action of X-rays by Kröncke and by Friedrich and Koch † showed no threshold. Some of the later measurements gave indication of an irregularity of the blackening curve for very low densities which could be interpreted as a threshold value ‡.

Density marks were obtained with reduced exposures and accurate records taken with the microphotometer by observing the minima of the scattering values for each field. For these light densities small irregularities due to dust particles or scratches, which add to the scattering, become prominent when operating the microphotometer with a narrow beam, but the finding of a constant minimum value for each step gives a definite measurement for the scattering from the silver grains. Fig. 10 shows the result of such measurements with dental C film developed for one minute in 1 : 5 Rodinal. The crossing of the curves corresponds to the fact that,

* Eberhard, *Phot. Korr.* lix. p. 15 (1922), indicates a special development with oxalate of iron to counteract this effect. It can, however, not be avoided entirely by this means.

† H. Kröncke, *loc. cit.*; Friedrich and Koch, *loc. cit.*

‡ E. Jönsson, *Ark. f. Mat. Astron. och Fysik*, xviii. p. 18 (1924); W. Busse, *Zeits. f. Phys.* xxxiv. p. 11 (1925). For a summary of the work done on this subject see J. Eggert and W. Rahts, 'Handbuch d. Physik,' xix. p. 602 (1928); F. Kirchner, 'Handbuch d. Physik,' xxiv. part 1 (1930).

according to the varying range of densities, the photometer was adjusted to different sensitivities. Curves 1 and 2 were obtained with a copper anticathode and a nickel filter, curves 3 and 4 with a molybdenum anticathode and a zirconium filter, so that in one case the prevalent wave-length is about 1·5 Å.U., in the other case about 0·7 Å.U. The two ranges of radiation differ in so far as with molybdenum radiation the K-radiation of bromine is excited, and may therefore lead to a different energy distribution of the photoelectrons excited by the

Fig. 10.

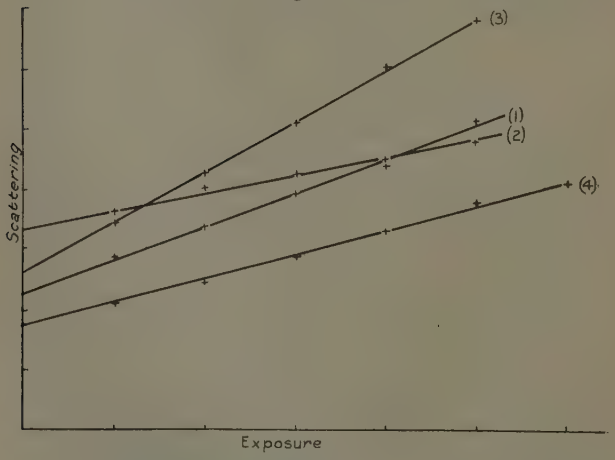

Scattering curves for very small X-ray exposures.

primary X-rays. It will be seen that the curves obtained for the two ranges of radiation are essentially of the same type. Densities for the first marks could not be established by absorption photometry, but for the largest densities the Hurter and Driffield values are :

Curve.	Density.
1.....	0·023
2.....	0·011
3.....	0·012
4.....	0·0075

The exposures corresponding to the first marks of smallest density are one-fifth, one-sixth resp. of those for which the densities are given above. All the points fall closely on straight lines indicating the accuracy and consistency of the scattering photometry for these small densities. The linear character of the relation by which they can be represented shows that for X-ray exposures, even with the extension of measurement into the range of extremely small densities, no threshold value can be detected. It is interesting to note that in the earlier part

Fig. 11.

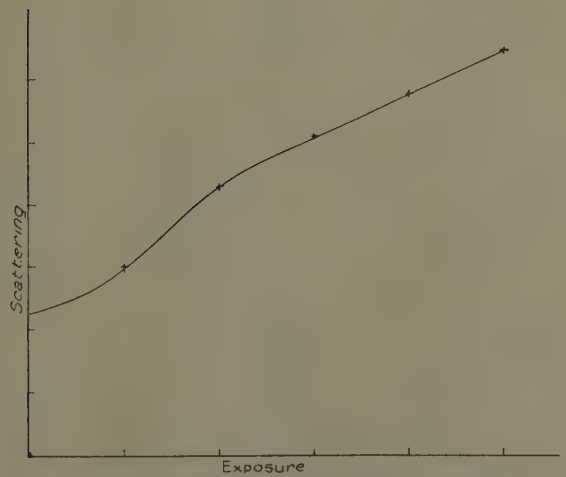

Scattering curve modified by the addition of potassium bromide to the developer.

of this work, when using a developer containing a large amount of potassium bromide, curves were obtained giving no definite threshold value, but an irregular rise for small densities, as illustrated by fig. 11.

11. One application of scattering photometry for which it seems particularly suited is the quantitative measurement of X-ray crystal reflexions.

The X-ray reflexions evaluated by us were obtained from crystal powders using a flat layer, so as to satisfy definite conditions of absorption—a method which has

been described by one of us *. This method conforms with focussing conditions, and produces sharp lines when applied to a powder consisting of crystal units, with a sufficient number of regularly spaced planes to give good resolution. With small crystal units broadening occurs which is symmetrical and which is an expression for the limited number of reflecting planes and the limited resolving power of the crystal units. When the powder consists of crystal elements of varying size the resultant intensity distribution of the lines is due to the superposition

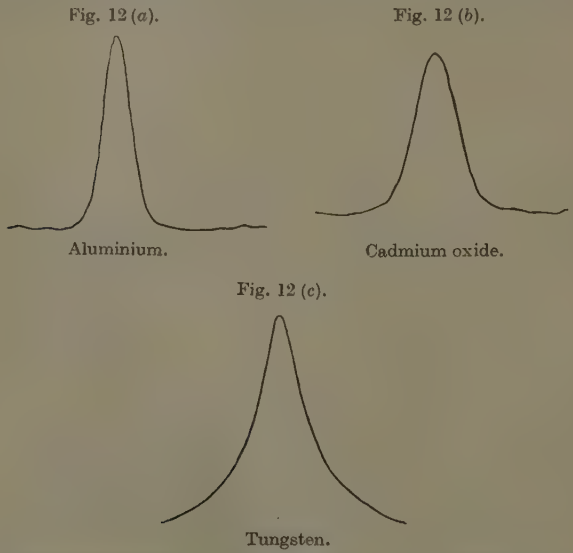

Photometer records of (200) reflexions of copper Kα radiation from powders of aluminium (12 *a*), cadmium oxide (12 *b*), tungsten (12 *c*).

of images of varying width. This is illustrated by figs. 12 (*a*) to 12 (*c*), which show the intensity distribution of reflexions of copper Kα-radiation from aluminium powder, mechanically ground tungsten, and precipitated cadmium oxide. The cadmium oxide and the tungsten give broadened lines and the tungsten reflexion shows the intensity distribution characteristic of a mixture of particles of

* J. Brentano, Proc. Phys. Soc. London, xxxvii. p. 184 (1925) ; Phil. Mag. vi. p. 178 (1928).

heterogeneous size. A certain number of comparatively large particles accounts for the sharp central peak, while the gradual falling off is due to small or deformed crystals. In such cases the intensity measurement of the reflexions depends considerably on the correct recording of the outer sloping parts of the line; these could not be determined with sufficient accuracy by absorption photometry, owing to its uncertainty in the region of small densities, Such conditions are found in those cases where the powder is very fine, and the presence of a certain proportion of comparatively larger crystals giving a sharp and high peak

Fig. 13.

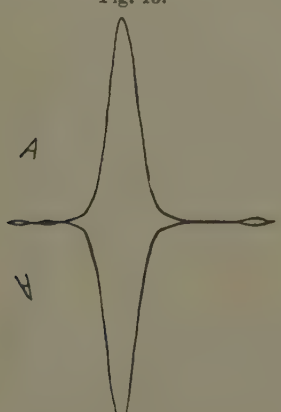

Evaluation of the photometer record.

is liable to obliterate the broad reflexion bands from the small particles.

The technique adopted in evaluating the intensities which depends on the original symmetry of the lines produced by the X-ray goniometer * involves the use of a duplicate of the photometer record. Superposing this on the original, reversing it from right to left, any lack of symmetry which may be due to the irregularities of the film or of the recording can be detected and the film be rejected if this is found. From the reversal and from

* In the case of neighbouring lines of unequal intensity, for instance of the Kα doublet, the slit system of the X-ray goniometer is adjusted so as to separate the lines definitely, or not to resolve them at all, making the entrance slit large compared with the distance of the lines.

reference marks on the record indicating definite scattering values any change of background is determined. The actual evaluation of the intensity consists then in reversing the photographic record with respect to the duplicate from top to bottom and finding the position of best adjustment, as indicated by fig. 13. By this procedure the position of the background with respect to the line is well defined Provided the limiting value of densities is not exceeded the area represents the intensity and is evaluated by planimetry. In the case of very strong lines, where the density in the centre of the line exceeds the range of proportionality between scattering and exposure, a blackening curve is applied to correct for lack of proportionality. In extreme cases, where very high densities are reached in the central part of a sharp line, this is recorded by absorption photometry, while the outer parts of the line are recorded by scattering, both records being taken on the microphotometer with the same ratio of displacement between film and recording drum. By working on the same scale the records can easily be combined. Removing the diaphragm D_1 and altering the stop D_2 it is easy to pass from one system of recording to the other.

In general the exposures are adjusted so as not to exceed the range of proportionality between scattering and exposure. When only the total intensity and not the exact intensity distribution is required it is of advantage to use a wide slit, recording the intensity from a wider area simultaneously, In this way accidental variations and, in particular, the inequalities of grain distribution are eliminated and very smooth records obtained. Comparisons have shown that the results obtained with fine and with broader illuminating slits S_2 agree within 2 per cent., which is the accuracy of the individual evaluation.

12. Experiments were made to apply the scattering method to the evaluation of Laue spots or to spots obtained with the rotating single crystal. The intensity of these spots falls off from a centre in all directions, so that they present considerable difficulties to absorption photometry, as various parts of an extended exploring slit comprise different densities.

Spots were prepared with a radial fall of intensity from a central peak value representing definite ratios

of exposures extending from 1 to 4. These spots were evaluated with the scattering microphotometer by recording them with a narrow slit in a series of bands, so as to cover the whole area of the spots in succession, and, secondly, by illuminating the whole spot at once with a uniform parallel beam of light and measuring the total scattered radiation. In this latter case the scattering due to an equally large area of unexposed film is subtracted. It was found that both methods gave identical results within a limit of error of 1·0 per cent. Comparing the recorded values with the actual intensity ratios, the maximum error was 1·5 per cent.

We wish to thank Professor W. L. Bragg, F.R.S., for various facilities in carrying out this work.

We are obliged to Messrs. Kodak, Ltd., for providing us with a number of emulsions used in the present investigation.

One of us (A. B.) is indebted to the Department for Scientific and Industrial Research for a grant enabling him to devote himself to this research.

August 16th, 1933.

XXXII. *An Experimental Determination of the Thermal Conductivity of Air between 0° and 100° C.** *By* S. W. Milverton, *A.R.C.S., D.I.C., Ph.D., Imperial College of Science and Technology* †.

Introduction.

FEW records exist of attempts to obtain accurate thermal conduction measurements for gases over a continuous temperature range from 0° to 100° C. During the development of a method for investigating the conduction of heat through vapours, an account of which work is shortly to be published, it became necessary to design a system for use in this range. The present paper includes an account of the development of such a system, and the determination of fresh values of the

* Portion of Thesis approved for the degree of Doctor of Philosophy in the University of London.

† Communicated by H. S. Gregory, D.I.C., Ph.D., A.R.C.S.

conductivity of air by data obtained from the necessary test for the absence of convection, together with an investigation of the radiation corrections to be applied for various temperature conditions.

Part I.

Conduction Measurements.

Method.

For the conductivity measurements a hot-wire system was employed. The gas under investigation was contained in a glass tube, along the axis of which a fine electrically heated platinum wire was stretched. From a knowledge of the rate of energy loss from the wire and the temperature difference across the gas the thermal conductivity of the latter could be calculated.

The wire was included in the main arm of a Callendar-Griffiths bridge, by means of which its resistance was determined. For elimination of heat loss along the thicker leading wires the method of compensation was employed, *i. e.*, a second shorter wire under the same conditions as the first was included in the opposite arm of the bridge. Such an arrangement was used by Gregory and Archer * in their determinations of the conductivities of air and hydrogen, and they have given the theory of the method and shown that, under the conditions they employed, the difference of resistance of the two wires when the same current passed through both was the same as the resistance of a similar wire, of length equal to the difference of lengths of the wires, and at a temperature equal to that of the central parts of the latter. Thus, since this resistance was that measured by the bridge, compensation was secured. A development of their analysis was applied to the conditions used in the present work, and indicated that in all the conductivity measurements the compensation was efficient.

It can also be shown that, provided the conductivity of the gas is linear with temperature, the heat conducted radially from the wire to the wall is the same as would be conducted if the space between them were filled with

* Proc. Roy. Soc. A, vol. cx. p. 91 (1926).

a substance of uniform conductivity equal to that of the gas at the mean temperature of the wire and the wall.

The relations used for calculation of the conductivity are

$$\frac{2\pi K_g'(\theta_1-\theta_2)(l-l')}{\log_e'(r_2/r_1)} = \frac{C^2R}{J} \quad . \quad . \quad . \quad . \quad (1)$$

and

$$\theta_1 = \frac{R-R_0}{R_{100}-R_0} \times 100. \quad . \quad . \quad . \quad . \quad . \quad (2)$$

In (1) and (2) l and l' are the respective lengths of the wires and r_1 and r_2 the radii of the wires and tubes respectively; C is the current through the wires, and R the resistance indicated by the bridge, J being Joule's equivalent; θ_1 is the temperature of the central parts of the wires (referred to as the "temperature of the wire"), θ_2 the temperature of the tubes, and K_g the conductivity of the gas at the temperature $(\theta_1+\theta_2)/2$; R_0 and R_{100} are the respective resistances indicated by the bridge when the wires are at 0° and 100° C.

Relation (2) is the ordinary platinum thermometer equation, and from it, when R, R_0, and R_{100} are known, θ_1 can be obtained and substituted in (1) for calculation of K_g, θ_2 being determined as described later.

In practice terms must be included to represent the energy transfer by convection and radiation, and these are discussed below.

Convective Losses.

The elimination of convection constitutes one of the chief problems in work on conduction through gases and vapours. When a hot-wire system is employed the method adopted is, in general, either that of performing experiments under widely different conditions, *e. g.*, with tubes of various diameters or with the apparatus in different positions, or that of designing the apparatus so as to reduce convection to a negligible value. Since the former method usually implies the assumption of Maxwell's Law that the conductivity of the substance is independent of pressure—a law which, while having been verified for permanent gases, may not be assumed to apply to vapours—it could not be used in the present case, and the latter was therefore adopted.

The form of tube employed was similar to that used by Gregory and Archer * for verification of Maxwell's Law for air, viz., a narrow tube arranged vertically with the inlet-tube at the lower end, the thin wire being stretched coaxially by means of a thicker platinum spring at the lower end, and continued as far as possible into the closed upper end of the tube. The efficiency of such a system in reducing convective losses may be appreciated on examination of their results. Since convection in a gas varies considerably with pressure, the effect is assumed to have been eliminated if the energy loss from the wire to the wall—under constant temperature conditions—is independent of the pressure of a gas between them. The system employed was tested by measuring the current required to maintain a constant temperature gradient for different pressures of air in the tubes. The method and results are discussed later; it is sufficient to note that there is ample evidence that convection had been eliminated in the case of air.

Correction for Radiation.

It was considered desirable to obtain fresh results for radiation loss from the wire under various temperature conditions, rather than to rely on previous determinations for similar wires or on theoretical formulæ. A complete investigation was therefore made, and is included in the present paper. By means of the results radiation corrections could be made to the total rate of energy loss in conductivity experiments.

Other Corrections.

(a) *Correction of Temperatures to Absolute Scale.*—It was necessary to convert the temperature θ_1, determined from relation (2); and θ_2 from the platinum scale to the absolute scale before substituting in (1). Callendar's formula, connecting a platinum scale temperature *pt* with its corresponding absolute scale temperature *t*, was used, viz.,

$$t - pt = 1{\cdot}50(t-100)t \times 10^{-4}.$$

(b) *Determination of Temperature at External Boundary of Gas.*—In equation (1) θ_2 is the temperature of the

* Phil. Mag., March 1926, p. 593.

inside surface of the tube containing the gas. In practice it was the external temperature θ_3 that was known. On applying (1) to the tube, we have

$$\theta_2 - \theta_3 = \frac{C^2 R . \log_e (r_3/r_2)}{2\pi K_p J(l-l')},$$

where r_3 and K_p are the external radius and thermal conductivity respectively of the material of the tube. From this θ_2 could be determined. The tube system employed was of pyrex, the thermal conductivity of which has been determined at various temperatures by Stephens*. The results were used in the present investigation, in which, therefore,

$$K_p = 0{\cdot}00245 . \log_{10}(\theta_3 + 273) - 0{\cdot}00352.$$

The temperature difference across the wall was never more than one-ninth per cent. of the total difference.

(c) *Temperature Drop and Accommodation.*—The effect of temperature drop and of accommodation was eliminated in the case of air by the method recently developed by Dr. Gregory †. A series of values for the energy loss from the wire for constant temperature conditions at various pressures having been obtained, the reciprocal of the rate of energy loss was plotted against that of pressure, for the lowest pressures used. The intercept of the resulting straight line on the axis of the former gave the value of the rate of energy loss to be used for calculation of the conductivity of the gas. Typical lines are shown in fig. 1, in which the reciprocal of the square of the current is plotted against that of pressure. Near the upper end of each line in the figure is indicated the corresponding temperature difference across the gas, while the quantity by which the ordinate of each point on that line has been reduced—for convenience in plotting—is shown near the middle of the line. Since this method utilizes comparatively low pressures, it also eliminates the effect of any slight convection, which, however, in the present case had already been eliminated, even at much higher pressures, by careful design of the apparatus.

* Phil. Mag., November 1932, p. 897.
† Phil. Mag., February 1933, p. 301.

Construction of Apparatus.

(a) *Tubes and Bath.*—The tubes were constructed from a piece of uniform bore pyrex-tube, the thin wire being stretched coaxially between thicker platinum leads fused into the ends. Each tube had a gas inlet near its lower end, and the system was mounted vertically.

Fig. 1.

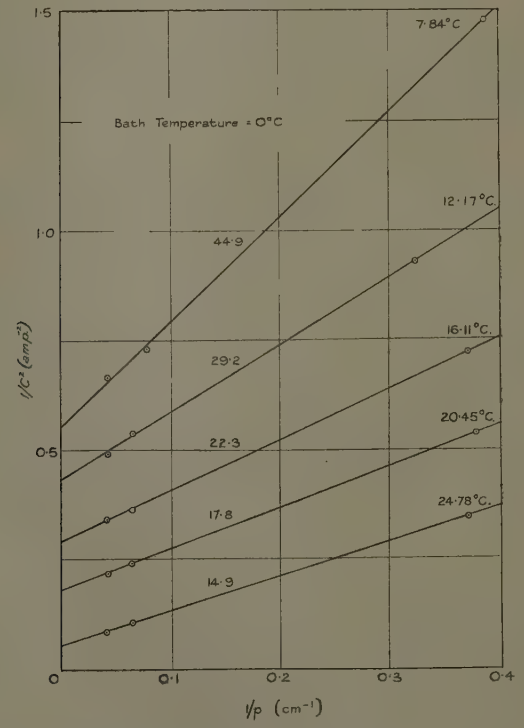

The dimensions of the tube system were :—

Radius of wire (r_1)	0·005065 cm.
Internal radius of tubes (r_2)	0·3963 cm.
External radius of tubes (r_3)	0·470 cm.
Length of main wire (l)	24·715 cm.
Length of compensating wire (l') .	4·821 cm.

All values have been reduced to 0° C. For the lengths of the wires at higher temperatures the coefficient of linear expansion of platinum is taken as ·000009 per degree C. The variation of the radii with temperature does not appreciably affect the results.

The bath used for the maintenance of the tubes at a known temperature was of the usual form, viz., a twelve-gallon galvanized iron tank, the water in which was drawn down by means of a propeller through the sides of a gauze cylinder into a wide vertical tube, from the lower end of which it passed to the surface through two similar tubes, the conduction system being contained in one of these. It was well lagged with cotton wool. For measurements at temperatures not much above 0° C. the bath was filled with crushed ice and water. Its modification for higher temperatures is described later.

(b) *Electrical Apparatus.*—The usual circuit was employed, the platinum wires being respectively connected in series with a Hartmann-Braun standard ohm and a manganin coil of approximately the same resistance. The current through the system was determined by measurement of the potential difference across the standard ohm, using a Crompton potentiometer—in conjunction with a Weston cadmium cell—which was calibrated by the makers during the course of the experiments. The bridge used was very accurately calibrated. The current was supplied by accumulators, and the rheostats used for its adjustment were as follows:—First, a series of manganin coils, each of which could be shorted by means of a mercury-cup system, as in a bridge; secondly, a screw contact on manganin wires, and, for final adjustment, a continuous-current mercury rheostat as described by Mann *.

Four thick copper rods were soldered to the cables from the platinum wires at such distances from the thick leads that the total length of cable included between each pair of rods was the same and under the same temperature conditions. Then, by placing each pair in a mercury cup, the wires could be shorted and the zero-point of the system found.

* Journ. Scient. Inst. vol. viii. p. 362 (1931).

Ice and Steam Points.

The resistances of the wire at ice and steam temperatures respectively were determined by immersion of the tubes in the appropriate bath and observation of the current necessary to maintain a fixed temperature gradient for four or five different values of the latter, all less than half a degree. Then the required fixed point was obtained by extrapolation on the straight line given by plotting the square of the current against the bridge setting.

Since it was found that there was a gradual –though small decrease of these resistances, but not of the temperature coefficient of resistance, with time, the ice-point was determined on every occasion when measurements were taken using an ice-bath. This was clearly not so necessary when a higher temperature bath was employed, the bath-point itself being then found, but in these cases the ice-point was determined within one or two days.

Convection Test and Conductivity of Air.

The tube-system was connected through a tap to a Hyvac pump, and through another to a supply of dry, dust-free, carbon-dioxide-free air. The pressure in the system was determined by a U-tube mercury manometer, one side of which was open to the atmosphere. An ice-bath was used, and, after several preliminary evacuations and fillings, the tubes were filled with air to a pressure of about 60 or 70 cm.

The bridge-settings corresponding to the required series of wire-to-wall temperature differences having been determined, the bridge was set for the lowest. Then the heating current was varied until the bridge galvanometer indicated that the system was balanced, when the value of the current was obtained by the potentiometer. The adjustment and measurement of the current were performed at intervals until constancy of conditions was obtained. Keeping the bridge-setting fixed, the pressure was reduced by steps to a few centimetres, the current being adjusted and measured at each pressure. These operations were repeated for each of the other bridge-settings.

When a bridge is being balanced the current should,

for greatest accuracy, be reversed. In the conductivity experiments this procedure would retard observations excessively, on account of the disturbance of conditions in the tubes on the momentary interruption of the current during reversal. Tests were therefore made to ascertain the inaccuracy introduced by assuming the bridge to be balanced if the galvanometer spot remained at its free zero when connexion to the bridge-system was made, the current being continuous. The results showed that, for the comparatively large currents used in the conductivity experiments, the error introduced was negligible, and the quicker method was therefore adopted. The much smaller currents used in the determination of ice- and steam-points, however, were liable to large errors if the current were not reversed, and consequently this was done in finding ice-, steam-, and, later, bath-points.

Results.

The results are given in the tables below. In these R is given in ohms, θ_1 and $\theta_1 \quad \theta_2$ in degrees C., C in ampères, and K_g in calories per centimetre per second per degree C. θ_g is the mean temperature of the gas in degrees C., p is its pressure in centimetres of mercury, C_0 is the value of the current, in ampères, after correction

TABLE I.

R = 2·52983. $\theta_1 = 7{\cdot}852$.

$\theta_1 - \theta_2 = 7{\cdot}845$.

p.	C.	C_0.
64·43	0·14829	..
54·61	0·14829	..
44·55	0·14824	..
33·73	0·14819	..
23·37	0·14814	..
12·56	0·14804	..
2·59	0·14684	0·14832

$E_r = 4{\cdot}45 \times 10^{-6}$. $E = 664{\cdot}40 \times 10^{-6}$.

$K_g = 587{\cdot}6 \times 10^{-7}$. $\theta_g = 3{\cdot}93$.

TABLE II.

$R=2{\cdot}57139$. $\theta_1=12{\cdot}180$.

$\theta_1-\theta_2=12{\cdot}169$.

p.	C.	C_0.
64·48	0·18368	..
54·21	0·18368	..
44·10	0·18363	..
33·04	0·18363	..
23·32	0·18353	..
15·25	0·18338	..
3·09	0·18218	0·18369

$E_r=7{\cdot}10\times10^{-6}$. $E=1035{\cdot}65\times10^{-6}$.

$K_g=590{\cdot}5\times10^{-7}$. $\theta_g=6{\cdot}10$.

TABLE III.

$R=2{\cdot}60924$. $\theta_1=16{\cdot}125$.

$\theta_1-\theta_2=16{\cdot}110$.

p.	C.	C_0.
70·51	0·21041	..
64·38	0·21041	..
53·02	0·21036	..
44·00	0·21031	..
33·63	0·21026	..
24·02	0·21016	..
15·25	0·21006	..
2·69	0·20841	0·21039

$E_r=9{\cdot}50\times10^{-6}$. $E=1378{\cdot}50\times10^{-6}$.

$K_g=593{\cdot}7\times10^{-7}$. $\theta_g=8{\cdot}07$.

TABLE IV.

$R = 2{\cdot}65085$. $\theta_1 = 20{\cdot}469$.

$\theta_1 - \theta_2 = 20{\cdot}450$.

p.	C.	C_0.
70·76	0·23583	..
61·04	0·23583	..
52·82	0·23578	..
43·45	0·23573	..
34·48	0·23568	..
23·47	0·23558	..
15·50	0·23543	..
2·64	0·23353	0·23580

$E_p = 12{\cdot}30 \times 10^{-6}$. $E = 1759{\cdot}05 \times 10^{-6}$.

$K_g = 596{\cdot}8 \times 10^{-7}$. $\theta_g = 10{\cdot}24$.

TABLE V.

$R = 2{\cdot}69235$. $\theta_1 = 24{\cdot}808$.

$\theta_1 - \theta_2 = 24{\cdot}784$.

p.	C.	C_w
69·86	0·25860	..
62·43	0·25860	..
52·57	0·25855	..
43·65	0·25850	..
33·93	0·25840	..
24·27	0·25830	..
15·30	0·25815	..
2·69	0·25610	0·25859

$E_p = 15{\cdot}10 \times 10^{-6}$. $E = 2148{\cdot}55 \times 10^{-6}$.

$K_g = 601{\cdot}5 \times 10^{-7}$. $\theta_g = 12{\cdot}42$.

for temperature drop and accommodation, E_r is the rate of heat loss by radiation from unit length of the wire, in calories per second per centimetre, obtained from the investigation described later, and E is the rate of heat loss by conduction from unit length of the wire, in the same units.

The value of J is taken as 4·182 joules per calorie.

Modification of Bath for use at Higher Temperatures.

It was necessary to design a bath for use at temperatures between 0° and 100° C. After consideration of the respective merits of various types of bath it was decided to attempt the adaptation of the existing bath to the new conditions, as it was known to be extremely efficient.

This was thermally insulated as far as possible by asbestos, cotton-wool, and felt, and a lid provided. Heating was effected by means of four electric fire-bars arranged vertically in a 3½-inch copper tube, which stood in the bath. When the maximum heating power of 2 kilowatts was employed the bath could be heated to 80° C. in about two hours. By means of a time-switch the current could be switched on at any time before the day's work was due to begin.

In conjunction with the main heater was employed a 250-watt immersion-heater controlled by toluene bulb and relay in the usual way. Although the bulb was useful for keeping the bath temperature constant over long periods, while actually taking measurements it was eliminated, and the system hand-controlled, much speedier working being thereby effected. For this purpose a three-pole switch was included in the circuit. The resistance which was put in series with the auxiliary heater on operation of the relay was variable, and by this means delicate adjustment of the rate of heat supply to the bath was possible.

The conduction system indicated slight but rapid fluctuations of bath temperature. This effect was found to be due to the circulation of the water from near the surface, which had been slightly cooled; this was prevented by closing the holes within 3 inches of the top of the gauze cylinder by copper-strip, when a very steady bath temperature could be obtained. Greatest

steadiness was obtained with the water in the bath at a definite level, which was automatically maintained by a siphon arrangement. The propeller was run at such a speed that any sudden increase in this while the bridge was balanced produced no change in temperature of the wire, indicating that the outside surfaces of the tubes were at the same temperature as the bath.

Measurement of Bath Temperature.

Accurate measurement of bath temperature was required. A form of platinum thermometer was employed, with the advantage over the usual type of having its coil in much closer thermal connexion with the water, so that heating by the current through the former was negligible. The device is due to Dr. Gregory, and consisted of a length of fine platinum wire coated with a thin layer of glass, and afterwards wound on a glass tube, the ends being welded to thicker platinum leads and the joints coated with glass. A few centimetres of the wire were similarly wound on the same tube for compensation, and cable leads taken to a bridge system in the usual way. The thermometer was placed vertically in the bath between the conduction-tubes. It was possible to measure the temperature of the bath directly with the thermometer, but, with improved methods of reproducing bath conditions, the method adopted was to use the thermometer merely as an indicator of equality of temperature throughout the day, at the end of which the bath-point could be found, using the conduction system in a similar manner to that for finding the ice-point.

Experimental Procedure.

The procedure for obtaining readings was as follows :— The main heater current was adjusted so that, with the control-switch closed, the bath cooled about one-hundredth of a degree in four minutes, and the bridges were set for the desired temperatures. Then, with the switch open, the bath was heated to about one-twohundredth of a degree above its final temperature, and the current through the conduction system adjusted so that both bridge galvanometer spots passed their zero positions at the same time, a few seconds sufficing to reheat the bath for the next reading. A similar process

was employed in finding the bath-point, but was complicated and lengthened by the necessity of continually reversing the current through the main bridge. However, it was sometimes possible to adjust the variable resistance controlled by the relay, so that the bath temperature kept constant at the required point during the period

Results.

TABLE VI.

R=3·32964. θ_1=92·101.

$\theta_1-\theta_2$=11·387.

p.	C.	C_0.
61·24	0·17400	..
51·57	0·17395	..
41·46	0·17395	..
32·99	0·17390	..
22·87	0·17385	..
13·85	0·17375	0·17401

$E_r=13{\cdot}00\times10^{-6}$. $E=1197{\cdot}75\times10^{-6}$.

$K_g=729{\cdot}8\times10^{-7}$. $\theta_g=86{\cdot}41$.

TABLE VII.

R=3·36734. θ_1=96·125.

$\theta_1-\theta_2$=15·407.

p.	C.	C_0.
61·69	0·20207	..
51·67	0·20207	..
42·30	0·20202	..
32·29	0·20202	..
22·72	0·20192	..
14·10	0·20182	0·20206

$E_r=17{\cdot}90\times10^{-6}$. $E=1633{\cdot}15\times10^{-6}$.

$K_g=735{\cdot}4\times10^{-7}$. $\theta_g=88{\cdot}42$.

TABLE VIII.

$R=3\cdot40889$. $\theta_1=100\cdot570$.

$\theta_1-\theta_2=19\cdot847$.

p.	C.	C_0.
61·34	0·22855	..
51·37	0·22855	..
42·35	0·22855	..
32·79	0·22850	..
23·17	0·22840	..
13·85	0·22825	0·22862

$E_r=23\cdot35\times10^{-6}$. $E=2116\cdot35\times10^{-6}$.
$K_g=739\cdot8\times10^{-7}$. $\theta_g=90\cdot65$.

TABLE IX.

$R=3\cdot45049$. $\theta_1=105\cdot024$.

$\theta_1-\theta_2=24\cdot296$.

p.	C.	C_0.
61·89	0·25189	..
51·92	0·25189	..
42·10	0·25184	..
32·79	0·25179	..
22·77	0·25169	..
13·70	0·25154	0·25195

$E_r=29\cdot20\times10^{-6}$. $E=2601\cdot20\times10^{-6}$.
$K_g=742\cdot8\times10^{-7}$. $\theta_g=92\cdot88$.

required for the system to regain equilibrium after reversal of current; then the bath-point determination was considerably simplified.

Using a bath temperature of 80·702° C., measurements were obtained for air. The methods of taking measurements and calculating results were as previously described.

Discussion of Results.

(a) *Convection Test.*—It is seen, from Tables I.–IX., that the current required to maintain a constant temperature gradient across the air in the tubes is almost independent of pressure over a range of 30 or 40 cm. There is, however, a slight but definite downward trend as the pressure is reduced from the neighbourhood of that of the atmosphere, the variation being of the order, on the average, of less than 3 in 20,000 per 10 cm. pressure change. If this variation were due entirely to convective losses the order of its magnitude would suggest that these losses were negligible in comparison with the energy transfer by conduction. Further, the values of C_0, obtained by a method which eliminates the effect of convection, of temperature drop, and of imperfect accommodation, are in close agreement with the values of C for pressures of about 60 or 70 cm.; this is an additional indication that even at these high pressures convective losses were quite negligible, and that the variation in the values of C was due almost entirely to the temperature drop and accommodation effects. It is thus apparent that the design and construction of the tube system had been entirely successful in eliminating convective losses in the case of air.

(b) *Conductivity of Air.*—The lines given by plotting the conductivity K_g against the mean temperature θ_g of the air are seen in fig. 2. In both cases no definite departure from the linear law is indicated over the separate temperature ranges.

By extrapolation the following values of the conductivity are obtained:—

$581{\cdot}0 \times 10^{-7}$ cal. cm.$^{-1}$ sec.$^{-1}$ deg. C.$^{-1}$ at 0°C., and

$718{\cdot}0 \times 10^{-7}$ cal. cm.$^{-1}$ sec.$^{-1}$ deg. C.$^{-1}$ at 80° C.

Also the lower temperature line gives a temperature coefficient, referred to the conductivity at 0°, of ·00281 per degree C. between 4° and 13° C.

The range of the experiments is not wide enough to give a complete verification of Sutherland's Law. If, however, this law is assumed to be true for air, the constants can easily be determined, as follows:—

If the law holds,

$$K_g = \frac{AT_g^{1.2}}{1+B/T_g},$$

where A and B are constants, and $T_g = \theta_g + 273$. Plotting $T_g^{3/2}/K_g$ against T_g should give a straight line, from the slope of which A is obtained, while the intercept on the T_g-axis gives B. Actually the points indicate a slight curvature of this line, suggesting that the law is not

Fig. 2.

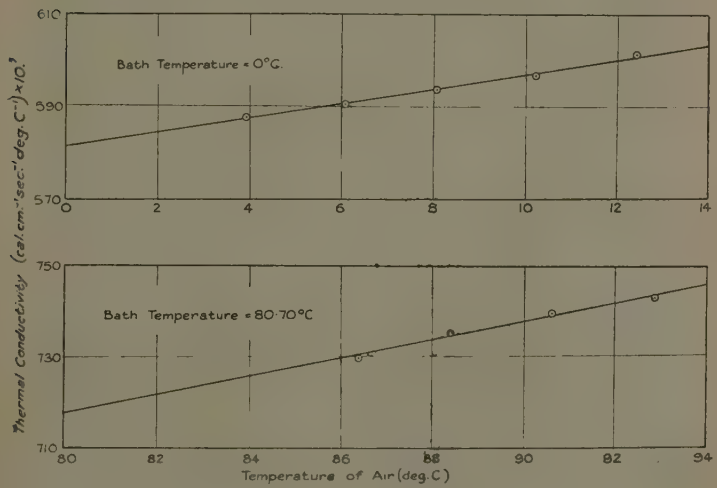

absolutely true for the range considered. On drawing the best straight line through the points the constants are obtained.

The expression becomes

$$K_g = \frac{5{\cdot}626\ T_g^{1\,2}}{1+165/T_g} \times 10^{-6},$$

and represents all the experimental results within one-third per cent.

Part II.

Determination of Radiation Corrections.

Principle of Investigation.

The experiments described below were undertaken with a view to the determination of the rate of energy transfer by radiation in the tube system for various temperature gradients and for bath temperatures between 0° and 100° C. In the past investigators of radiation loss have often adopted the method of obtaining as high a vacuum as possible, and assuming the heat transfer across this to be entirely due to radiation. In the present case, however, the procedure was to measure the energy loss for fixed bath temperature and temperature difference at several small, but measurable, pressures and to obtain the radiation by extrapolation to zero pressure.

The gas employed was atmospheric air, and results were obtained for pressures from ·000005 cm. to about ·0012 cm. of mercury, in which range the rate of energy transfer was found to be linear with pressure.

Note.—As the rate of heat transfer from the wire in the experiments at low pressure was less than in normal conductivity determinations, the conditions for compensation were not so perfectly fulfilled in the former as in the latter case. The purpose of the investigation, however, was to obtain values for radiation corrections to conductivity results, these corrections amounting, in the case of air, to little more than 1 per cent. Thus extreme accuracy in the low-pressure measurements was not demanded, and for the purpose of the radiation corrections we can assume the compensation to have been perfect.

Arrangement of Apparatus.

The pressure of gas in the tubes was measured by a McLeod gauge, and evacuation was effected through a wide-bore tap by an electrically heated mercury-vapour pump, backed by the Hyvac. A trap was included next to the tube system, and was immersed in liquid air, its purpose being to keep the tubes free of mercury vapour and of any other vapour which might be liberated from the glass or taps. Another tap served for the admission of dry, dust-free, carbon-dioxide-free air.

Experimental Procedure.

The system was first freed of occluded gases and vapours by prolonged evacuation while heating as far as possible. After this treatment it was found possible to obtain by the pumps alone a pressure as low as that stated above, and to maintain this when the system was isolated. The method adopted involved the admission of air, with subsequent production of low pressure and isolation from the pump, after which there was found to be a very gradual increase of pressure with time. This was obviously due only to air, on which the experiments were being performed; it was too slow to affect individual results, and could therefore be ignored provided the pressure was determined after each reading.

The method of taking readings was exactly similar to that for high-pressure conduction results. In this case the electrical system was much more sluggish in responding to current changes and in attaining equilibrium afterwards; this necessitated very fine adjustment of auxiliary bath-heating current to ensure constancy of temperature during the period of variation.

The bath temperature having been fixed, results were obtained for the required series of temperature gradients at the lowest pressure attainable. Then air was admitted to give the highest pressure required, the series again taken, the pressure lowered, and the process repeated until results had been obtained for all temperature gradients at four pressures. In each case the pressure was taken immediately after balancing the bridge.

The following method for quickly attaining any desired pressure was adopted:—A preliminary evacuation was performed, and when the pressure was below about half a millimetre was continued by opening the pump-tap for two-second intervals, alternately with which the pressure was taken. Thus a pressure-time curve was obtained. For the production of a definite low pressure air was admitted to a pressure of a few millimetres and the pump-tap opened until the pressure had been lowered to within the range of the curve, when the further period of evacuation required could be read off.

Results were obtained for bath temperatures of 0° and of about 27°, 54°, 81°, and 99° respectively.

Determination of Pressure.

The pressure p' indicated by the gauge—at 20° C.—was not exactly equal to the pressure of gas p in the tube system at θ_3, the connecting tube being narrow in comparison with the mean free path of the gas molecules.

According to Knudsen * the variation of pressure along a tube of diameter $2r$, along which the absolute temperature T varies, is given by

$$\frac{dp}{p} = \frac{1}{2(1+2r/\lambda)} \cdot \frac{d\mathrm{T}}{\mathrm{T}},$$

where λ is the mean free path of the gas molecules. On integration we obtain the form

$$\frac{p}{p'} = \left(\frac{\mathrm{T}}{\mathrm{T}'}\right)^{\alpha},$$

in which

$$\alpha = \frac{1}{2(1+2r/\lambda)},$$

where λ is taken as the mean of the values of the mean free path at the ends of the connecting tube.

The radius of the tube connecting the gauge to the tube system was ·25 cm. The actual pressure p of the gas in the tubes was determined by means of the relations above, and is tabulated with the results, together with p'. The greatest divergence of p from p' is just over 10 per cent.

It should be noted that the results obtained for the radiation are unaffected by this correction.

Results.

In the tables below θ_1 and $\theta_1 - \theta_2$ ($= \theta_1 - \theta_3$, since the temperature difference across the glass wall is, for these low energy transfers, negligible) are given in degrees C., p' and p in centimetres of mercury, and C in ampères; E_t is the total rate of energy loss in calories per second per centimetre of wire, while E_r is the rate of energy loss by radiation in the same units.

* *Ann. der Phys.* vol. xxxiv. p. 593 (1911).

TABLE X.

Temperature of bath = 0° C.

θ_1.	$\theta_1-\theta_2$.	$p'.10^3$.	$p.10^3$.	C.	$E_t.10^6$.	$E_r.10^6$.
7·797	7·797	0·005	0·005	0·01210	4·45	
		0·410	0·400	0·01405	6·00	
		0·830	0·810	0·01570	7·49	
		1·180	1·155	0·01695	8·74	4·45
12·123	12·123	0·010	0·010	0·01515	7·09	
		0·420	0·410	0·01750	9·46	
		0·835	0·815	0·01950	11·75	
		1·175	1·150	0·02105	13·69	7·05
16·069	16·069	0·005	0·005	0·01745	9·55	
		0·435	0·425	0·02010	12·67	
		0·835	0·815	0·02235	15·66	
		1·180	1·155	0·02410	18·21	9·50
20·411	20·411	0·005	0·005	0·01965	12·30	
		0·440	0·430	0·02265	16·34	
		0·840	0·820	0·02525	20·31	
		1·185	1·160	0·02715	23·48	12·30
24·749	23·749	0·005	0·005	0·02165	15·17	
		0·445	0·435	0·02500	20·22	
		0·850	0·830	0·02775	24·92	
		1·195	1·170	0·02990	28·93	15·10
28·654	28·654	0·005	0·005	0·02330	17·81	
		0·450	0·440	0·02690	23·74	
		0·855	0·835	0·02990	29·33	
		1·200	1·175	0·03205	33·70	17·80

TABLE XI.

Temperature of bath = 27·123° C.

θ_1.	$\theta_1-\theta_2$.	$p'.10^3$.	$p.10^3$.	C.	$E_t.10^6$.	$E_r.10^6$.
35·895	8·772	0·005	0·005	0·01390	6·50	
		0·440	0·445	0·01560	8·18	
		0·785	0·790	0·01725	10·01	
		1·150	1·160	0·01815	11·08	6·50
40·255	13·132	0·005	0·005	0·01700	9·86	
		0·440	0·445	0·01905	12·38	
		0·790	0·795	0·02105	15·12	
		1·170	1·180	0·02220	16·82	9·80

TABLE XI. (*cont.*).

Temperature of bath = 27·123° C.

θ_1.	$\theta_1-\theta_2$.	$p'.10^3$.	$p.10^3$.	C.	$E_t.10^6$.	$E_r.10^6$.
44·197	17·074	0·005	0·005	0·01930	12·88	
		0·445	0·450	0·02175	16·36	
		0·790	0·795	0·02375	19·50	
		1·195	1·205	0·02525	22·04	12·85
48·550	21·427	0·005	0·005	0·02175	16·59	
		0·455	0·460	0·02435	20·80	
		0·800	0·805	0·02655	24·72	
		1·200	1·210	0·02825	27·99	16·55
52·935	25·812	0·005	0·005	0·02385	20·24	
		0·455	0·460	0·02675	25·45	
		0·815	0·820	0·02910	30·12	
		1·205	1·215	0·03105	34·30	20·20

Table XII.

Temperature of bath = 54·106° C.

θ_1.	$\theta_1-\theta_2$.	$p'.10^3$.	$p.10^3$.	C.	$E_t.10^6$.	$E_r.10^6$.
62·418	8·312	0·010	0·010	0·01445	7·65	
		0·375	0·390	0·01555	8·86	
		0·840	0·870	0·01700	10·59	
		1·220	1·260	0·01810	12·00	7·60
66·381	12·275	0·010	0·010	0·01755	11·43	
		0·380	0·395	0·01900	13·39	
		0·840	0·870	0·02065	15·82	
		1·225	1·265	0·02190	17·79	11·40
70·766	16·660	0·010	0·010	0·02040	15·64	
		0·390	0·405	0·02215	18·44	
		0·840	0·870	0·02400	21·65	
		1·225	1·265	0·02550	24·44	15·60
74·801	20·695	0·005	0·005	0·02270	19·61	
		0·390	0·405	0·02465	23·12	
		0·840	0·870	0·02680	27·33	
		1·225	1·265	0·02830	30·47	19·55
79·215	25·109	0·005	0·005	0·02505	24·19	
		0·395	0·410	0·02715	28·41	
		0·845	0·875	0·02955	33·66	
		1·225	1·265	0·03125	37·64	24·15

TABLE XIII.

Temperature of bath = 80·788° C.

θ_1.	$\theta_1-\theta_2$.	$p'.10^3$.	$p.10^3$.	C.	$E_l.10^6$.	$E_r.10^6$.
92·043	11·255	0·005	0·005	0·01810	13·10	
		0·380	0·410	0·01915	14·66	
		0·775	0·830	0·02040	16·64	
		1·210	1·280	0·02170	18·83	12·90
96·085	15·297	0·005	0·005	0·02105	17·91	
		0·410	0·445	0·02235	20·20	
		0·790	0·845	0·02385	23·00	
		1·255	1·325	0·02535	25·99	17·80
100·527	19·739	0·005	0·005	0·02395	23·48	
		0·420	0·455	0·02555	26·72	
		0·820	0·875	0·02715	30·18	
		1·305	1·380	0·02900	34·43	23·30
104·979	24·191	0·005	0·005	0·02655	29·21	
		0·445	0·480	0·02835	33·30	
		0·840	0·895	0·03020	37·79	
		1·355	1·435	0·03215	42·83	29·10
109·430	28·642	0·005	0·005	0·02900	35·27	
		0·455	0·490	0·03110	40·56	
		0·865	0·925	0·03300	45·67	
		1·360	1·440	0·03505	51·52	35·20

TABLE XIV.

Temperature of bath = 98·776° C.

θ_1.	$\theta_1-\theta_2$.	$p'.10^3$.	$p.10^3$.	C.	$E_l.10^6$.	$E_r.10^6$.
108·308	9·532	0·005	0·005	0·01770	13·10	
		0·425	0·470	0·01840	14·15	
		0·820	0·890	0·01950	15·90	
		1·150	1·235	0·02035	17·31	13·00
112·322	13·546	0·005	0·005	0·02105	18·72	
		0·430	0·475	0·02200	20·45	
		0·825	0·895	0·02325	22·84	
		1·150	1·235	0·02415	24·64	18·60
116·792	18·016	0·005	0·005	0·02425	25·14	
		0·435	0·480	0·02535	27·47	
		0·830	0·905	0·02685	30·82	
		1·150	1·235	0·02790	33·28	25·05

TABLE XIV. (*cont.*).

Temperature of bath = 98·776° C.

θ_1.	$\theta_1-\theta_2$.	$p'.10^3$.	$p.10^3$.	C.	$E_t.10^6$.	$E_r.10^6$.
120·865	22·089	0·005	0·005	0·02680	31·03	
		0·440	0·485	0·02810	34·12	
		0·840	0·915	0·02970	38·11	
		1·150	1·235	0·03090	41·25	30·90
125·338	26·562	0·005	0·005	0·02945	37·91	
		0·450	0·495	0·03095	41·86	
		0·845	0·920	0·03260	46·44	
		1·150	1·235	0·03390	50·23	37·80

Application to Conductivity Measurements.

The values of E_t were plotted against those of p for each temperature difference, a straight line being obtained in every case. A typical set of lines is shown in fig. 3, in which the temperature differences are indicated. From the intercept of each line on the heat-loss axis was obtained the value of the radiation loss E_r corresponding to the particular temperature conditions. These values are given in the tables, and were plotted against the corresponding values of $\theta_1-\theta_2$. For each bath temperature a curve was obtained, as shown in fig. 4.

From these curves can be obtained radiation corrections to conduction results, when the temperature of the bath used for the latter is the same, or very nearly the same, as one of those used for the radiation results. For other bath temperatures interpolation can be effected by other curves derived from those in fig. 4 or by means of the formula given below.

The theoretical investigation of the radiation from a bright platinum wire under the conditions used in the present investigation is a matter of some difficulty. It has been found possible, however, in the present case to represent the radiation results by an empirical relation, viz.,

$$E_r = 1{\cdot}87\ (T_1^{3{\cdot}82} - T_2^{3{\cdot}82}) \times 10^{-14},$$

in which E_r is the rate of heat transfer, in calories per second, by radiation from the wire to the wall, at absolute

temperatures T_1 and T_2 respectively, per centimetre of wire. This represents all the results within just over 2 per cent.

Fig. 3.

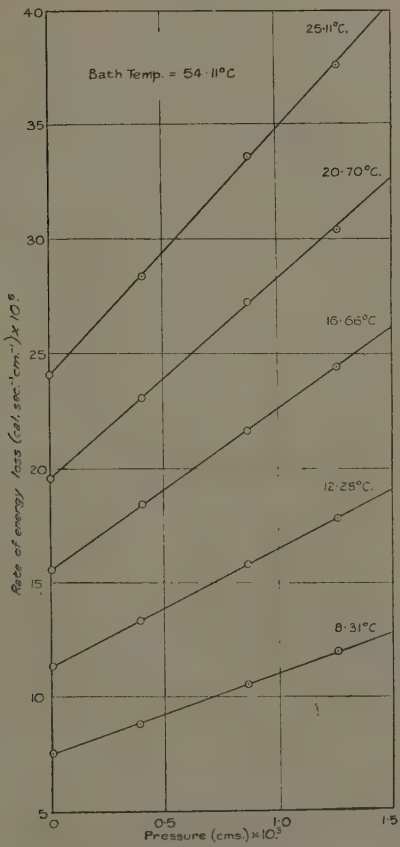

If E_R is the rate of radiation loss in calories per second, per square centimetre of wire surface,

$$E_R = 5{\cdot}88\,(T_1^{3{\cdot}82} - T_2^{3{\cdot}82}) \times 10^{-13}.$$

These relations can be used in future conductivity work, as the accuracy with which they represent the

experimental results is well within that demanded for radiation corrections in such work.

Fig. 4.

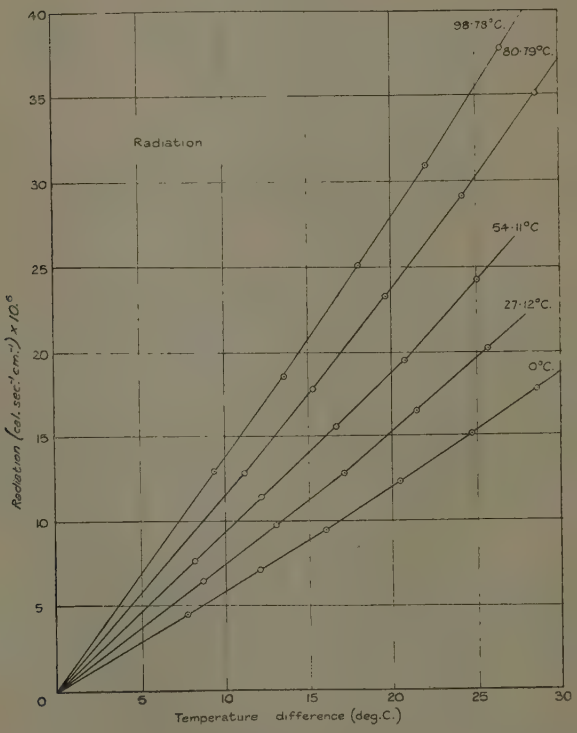

In conclusion, the author wishes to record his thanks to Professor G. P. Thomson for the facilities afforded for the work, and to Dr. H. S. Gregory for his keen interest and helpful advice.

XXXIII. *Use of Oseen's Approximation in Problems of Heat Transfer.* *By* N. A. V. Piercy, *D.Sc.*, *and* R. J. Schmidt, *Ph.D.**

1. *Introduction.*

Analysis of the convection of heat from a short body in a viscous stream is very complex and several assumptions and approximations are necessary. It is usual to neglect variation, due to unequal temperature distribution, of the thermal conductivity k, the heat capacity per unit volume c, the density ρ, and the kinematic viscosity ν of the fluid. If steadiness and two-dimensional flow are then assumed, the equation for the temperature θ at any point in the fluid is

$$u\frac{\partial\theta}{\partial x}+v\frac{\partial\theta}{\partial y}=\frac{k}{c}\nabla^2\theta, \quad . \quad . \quad . \quad . \quad . \quad (1)$$

where θ is required to satisfy given thermal boundary conditions, while u and v are determined by the equations of motion of a viscous incompressible fluid and the hydrodynamical boundary condition of no slip. In the present paper we shall assume that equation (1) sufficiently represents the problem.

The calculation of u and v calls for an approximation to the equations of motion. Of the two well-known modern approximations, that due to Prandtl must be expected to give results in fair agreement with measurements of flow at considerable Reynolds numbers provided the motion remains steady. On the other hand, experience suggests that Prandtl's approximation is appreciably less tractable than that proposed by Oseen, viz.,

$$\nu\nabla^4\psi=\mathrm{U}\nabla^2(\partial\psi/\partial x), \quad . \quad . \quad : \quad . \quad . \quad (2)$$

where ψ is the stream function and U the undisturbed velocity.

Unfortunately, Oseen's equation is valid only for small Reynolds numbers, such as those which are characteristic of hot-wire anemometry. It has been widely anticipated that at larger Reynolds numbers (2) would lead to a calculated flow bearing no relation to reality. But recent

* Communicated by the Authors.

work * does not confirm this view in the case of flat plates, for which the flow obtained from (2) is similar to that found from Prandtl's approximation, except that the friction is 70 per cent. greater and the boundary layer of viscous effects one-third thinner. A somewhat similar result may perhaps be anticipated for fins of narrow section, such as are frequently used in engineering for cooling.

It is almost obvious that estimations of heat transfer in such cases are much less influenced by errors in u and v than are calculations of friction. This will be proved, and the work will suggest means of correcting approximations to heat transfer from measurements of friction. Thus there is a prospect that Oseen's equation may prove of service in certain problems of convection which are of practical importance.

This question is investigated in the present paper for the case of tangential flat plates. Considerable Reynolds numbers will be assumed, and the velocity appropriate to (2) is then known at all points in terms of the probability integral. Denoting the downstream length of the plate, whose span is assumed infinite, by l, and taking its trace on the xy-plane to lie on the x-axis from $x=0$ to $x=l$, the expression for u is

$$u=\frac{2U}{\sqrt{\pi}}\int_0^{\left(\frac{Ry^2}{4xl}\right)^{\frac{1}{2}}} e^{-z^2}dz, \qquad . \quad . \quad . \quad . \quad (3)$$

where $R=Ul/\nu$, and v readily follows. This convenient expression permits a fairly general solution of (1) consistent with Oseen's approximation.

Blasius's well-known solution gives, on the other hand, the flow that accords with Prandtl's approximation, and Fage and Falkner † have recently worked out the corresponding convection, according to (1). These authors have also carried out special experiments for comparison. Thus it will be possible to scrutinise closely the results obtained in the present paper.

2. *Simplification of the Equation for Temperature.*

Before substituting the special expressions for u and v derived from Oseen's approximation, (1) will be trans-

* Piercy and Winny, Proc. Roy. Soc. A, cxl. (1933).

† Fage and Falkner, Aer. Res. Com., R. & M. no. 1408 (1931).

formed to a more convenient form. In this we follow the work of Fage and Falkner, except that it is desirable to introduce slightly different coordinates.

It is usually true that $\partial^2\theta/\partial x^2$ may clearly be neglected in comparison with $\partial^2\theta/\partial y^2$. Making this assumption reduces (1) to

$$u\frac{\partial\theta}{\partial x}+v\frac{\partial\theta}{\partial y}=\frac{k}{c}\cdot\frac{\partial^2\theta}{\partial y^2}. \quad . \quad . \quad . \quad . \quad . \quad (4)$$

Denote by θ_0 the temperature elevation of the plate above the distant fluid, and define θ, a temperature difference ratio, as

$$\theta\equiv(\theta_0-\theta)/\theta_0. \quad . \quad . \quad . \quad . \quad . \quad (5)$$

Then (4) becomes

$$u(\theta-1)\frac{\partial\theta_0}{\partial x}+\theta_0\left(u\frac{\partial\theta}{\partial x}+v\frac{\partial\theta}{\partial y}\right)=\frac{k}{c}\cdot\theta_0\cdot\frac{\partial^2\theta}{\partial y^2}. \quad . \quad (6)$$

No difference of temperature exists between any point of the surface of the plate and the adjacent fluid, but θ_0 is not restricted to be uniform. Attention will be confined, however, to thermal boundary conditions which can be expressed in the form

$$\theta_0=\mathrm{B}x^p, \quad . \quad . \quad . \quad . \quad . \quad . \quad . \quad (7)$$

so that (6) reduces to

$$u\frac{p}{x}(\theta-1)+u\frac{\partial\theta}{\partial x}+v\frac{\partial\theta}{\partial y}=\frac{k}{c}\cdot\frac{\partial^2\theta}{\partial y^2}. \quad . \quad . \quad . \quad (8)$$

Convenient coordinates suggested by (3) are

$$\xi=\left(\frac{\mathrm{R}y^2}{4xl}\right)^{\frac{1}{4}}, \quad \eta=\frac{x}{l}, \quad . \quad . \quad . \quad . \quad . \quad (9)$$

and these transform (8) to

$$u\left\{\frac{p}{\eta}(\theta-1)-\frac{\xi}{2\eta}\cdot\frac{\partial\theta}{\partial\xi}+\frac{\partial\theta}{\partial\eta}\right\}+v\left(\frac{\mathrm{R}}{4\eta}\right)\cdot\frac{\partial\theta}{\partial\xi}=\frac{k}{c}\left(\frac{\mathrm{R}}{4\eta l}\right)\frac{\partial^2\theta}{\partial\xi^2}.$$
$$. \quad . \quad . \quad (10)$$

It will be found that the assumption $\partial\theta/\partial\eta=0$ gives a solution of (10) which satisfies the thermal boundary

conditions at the plate and at infinity. With this assumption the equation finally reduces to

$$u\left\{p(\theta-1)-\frac{\xi}{2}\cdot\frac{d\theta}{d\xi}\right\}+v\left(\frac{\mathrm{R}\eta}{4}\right)^{\frac{1}{2}}\cdot\frac{d\theta}{d\xi}=\frac{k\mathrm{R}}{4cl}\cdot\frac{d^2\theta}{d\xi^2}. \quad (11)$$

It will be noted that, although a suggestion has been adopted from (3), this expression is quite general in regard to u and v and is in no wise restricted to Oseen's approximation.

3. *Solution to Oseen's Approximation with Uniform Temperature along the Plate.*

In the nomenclature of (9), (3) becomes

$$u=(2\mathrm{U}/\sqrt{\pi})\int_0^{\xi}e^{-z^2}dz, \quad . \quad . \quad . \quad . \quad (12)$$

from which the equation of continuity and the hydrodynamical boundary condition at the plate give

$$v=\frac{\mathrm{U}}{\sqrt{(\pi\mathrm{R}\eta)}}(1-e^{-\xi^2}). \quad . \quad . \quad . \quad . \quad (13)$$

In this section we consider only a plate of uniform temperature, so that $p=0$. Making the substitutions, (11) becomes

$$\frac{\mathrm{U}}{\sqrt{\pi}}\left\{\frac{1-e^{-\xi^2}}{2}-\xi\int_0^{\xi}e^{-z^2}dz\right\}\frac{d\theta}{d\xi}=\frac{k\mathrm{R}}{4cl}\cdot\frac{d^2\theta}{d\xi^2}. \quad (14)$$

Writing

$$f(\xi)\equiv 1-e^{-\xi^2}-2\xi\int_0^{\xi}e^{-z^2}dz, \quad . \quad . \quad . \quad (15)$$

$$\lambda\equiv\frac{2}{\sqrt{\pi}}\cdot\frac{c\nu}{k}, \quad . \quad . \quad . \quad . \quad . \quad . \quad . \quad . \quad (16)$$

the equation takes the form

$$\frac{d^2\theta}{d\xi^2}=\lambda f(\xi)\frac{d\theta}{d\xi}. \quad . \quad . \quad . \quad . \quad . \quad (17)$$

On dividing through by $d\theta/d\xi$ and integrating twice, we find from this equation

$$\theta=\mathrm{A}\int_0^{\xi}e^{\lambda\int_0^{\xi}f(\xi)\,d\xi}.d\xi+\mathrm{C}. \quad . \quad . \quad . \quad (18)$$

Now, θ vanishes when $\xi=0$, and is equal to unity when $\xi\to\infty$. Hence C=0 and

$$1=A\int_0^{\infty} e^{\lambda\int_0^{\xi} f(\xi)\,d\xi}\,.d\xi. \quad . \quad . \quad . \quad . \quad . \quad (19)$$

It follows that

$$\frac{\theta}{\theta_0}=\frac{\displaystyle\int_{\xi}^{\infty} e^{\lambda\int_0^{\xi} f(\xi)\,d\xi}\,.d\xi}{\displaystyle\int_0^{\infty} e^{\lambda\int_0^{\xi} f(\xi)\,d\xi}\,.d\xi} \quad . \quad . \quad . \quad . \quad . \quad (20)$$

The heat-loss, H, from unit span of the plate in unit time is given by

$$H=-2k\int_0^{l}\left(\frac{\partial\theta}{\partial y}\right)_{y=0}.dx. \quad . \quad . \quad . \quad (21)$$

Substituting from (5) and (9),

$$H=2k\int_0^{l}\theta_0\left(\frac{R}{4xl}\right)^{\frac{1}{3}}\left(\frac{\partial\theta}{\partial\xi}\right)_{\xi=0}.dx. \quad . \quad . \quad (22)$$

Hence from (18) and (19) we obtain finally

$$\frac{H}{k\theta_0}=\frac{2R^{\frac{1}{3}}}{\displaystyle\int_0^{\infty} e^{\lambda\int_0^{\xi} f(\xi)\,d\xi}\,.d\xi}. \quad . \quad . \quad . \quad . \quad (23)$$

The definite integral in (23) is readily evaluated by graphical means, and this process is required if the fluid is heated to a greater depth than it is affected by viscosity. But for fluids of poor conductivity, such as air and water, the thermal boundary layer is thin, and a good approximation can readily be obtained. Retaining first terms only in the expansions, we have

$$\int_0^{\infty} e^{\lambda\int_0^{\xi} f(\xi)\,d\xi}\,.d\xi=\int_0^{\infty} e^{-\lambda\xi^3/3}\,.d\xi$$

$$=\left(\frac{3}{\lambda}\right)^{\frac{1}{3}}\int_0^{\infty} e^{-w^3}\,.dw$$

$$=\left(\frac{3}{\lambda}\right)^{\frac{1}{3}}\Gamma\left(\tfrac{4}{3}\right). \quad . \quad . \quad . \quad (24)$$

Hence we have approximately for a flat plate of uniform temperature in a stream of poorly conducting fluid

$$\frac{H}{k\theta_0} = \frac{2R^{\frac{1}{2}}}{\left(\frac{3\sqrt{\pi}}{2}\cdot\frac{k}{c\nu}\right)^{\frac{1}{3}}\Gamma(\frac{4}{3})}$$

$$= 1{\cdot}616\left(\frac{k}{c\nu}\right)^{-\frac{1}{3}}R^{\frac{1}{2}}, \quad . \quad . \quad . \quad . \quad (25)$$

according to (1) and Oseen's approximation.

For air the mean experimental value of $k/c\nu$ is 1·3, giving from (25)

$$H/k\theta_0 = 1{\cdot}48R^{\frac{1}{2}}. \quad . \quad . \quad . \quad . \quad . \quad (26)$$

We have evaluated (23) graphically for this value of $k/c\nu$ and find for the coefficient on the right-hand side of (26) the value 1·46. Thus the error involved in taking account of the first terms only in the expansions of the expressions for the velocities is less than 2 per cent. for gases.

4. *Relation between Approximations to Heat Transfer and to Friction.*

The heat-loss can, of course, be evaluated directly for different distributions of temperature along the plate. Labour is saved, however, by the following theorem, which is also of service in comparing the theoretical results with experiment.

Let ψ be the stream function found from any particular approximation to the equations of motion, the only restriction being that it can be expanded in the form

$$\psi = Uy(\alpha\xi + \alpha_2\xi^2 + \alpha_3\xi^3 \ldots .) \quad . \quad . \quad . \quad (27)$$

The requirement is of a fairly general nature ; from (12) it will be seen to be satisfied at considerable Reynolds numbers by the solution to Oseen's approximation, and it is also satisfied by Blasius's * solution to Prandtl's approximation. For heat transfer to fluids of low conductivity, as has been verified for air, terms of higher order than the first may be neglected. In these circumstances we have

* Blasius, *Zeits. f. Math. u. Phys.* (1908).

$$\psi = \mathrm{U}y\alpha\xi,$$

$$u = -\frac{\partial\psi}{\partial y} = -2\mathrm{U}\alpha\xi,$$

$$v = \frac{\partial\psi}{\partial x} = -\mathrm{U}\alpha\xi^2(\nu/\mathrm{U}x)^{\frac{1}{2}}, \quad . \quad . \quad . \quad (28)$$

and equation (11) for $d\bar{\theta}/d\xi$ becomes

$$\frac{d^2\bar{\theta}}{d\xi^2} = \frac{2c\nu\alpha}{k}\left\{\xi^2\frac{d\theta}{d\xi} - 4\xi p(\theta - 1)\right\}. \quad . \quad . \quad (29)$$

Now let ψ' be the stream function determined from some other approximation to the equations of motion, still subject to the restriction that has been imposed, so that

$$\psi' = \mathrm{U}y(\alpha'\xi + \alpha_2'\xi^2 + \alpha_3'\xi^3 \ldots .) \quad . \quad (30)$$

The temperature at a given point will not be the same as in the first case. Denote it at any point in the second case by θ', and define

$$\theta' = (\theta_0 - \theta')/\theta_0. \quad . \quad . \quad . \quad . \quad . \quad (31)$$

It is clear that an equation exactly similar to (29) will result for θ' except that θ', α' will replace θ, α. Introduce

$$\epsilon = \left(\frac{\alpha'}{\alpha}\right)^{\frac{1}{2}}\xi \quad . \quad . \quad . \quad . \quad . \quad . \quad (32)$$

and substitute for ξ and α' in the equation for θ'. It becomes

$$\frac{d^2\theta'}{d\epsilon^2} = \frac{2c\nu\alpha}{k}\left\{\epsilon^2\frac{d\theta'}{d\epsilon} - 4\epsilon p(\theta' - 1)\right\}. \quad . \quad . \quad (33)$$

Equations (29) and (33) are the same and satisfy the same boundary conditions. Hence

$$\left(\frac{d\bar{\theta}}{d\epsilon}\right)_{\epsilon=0} = \left(\frac{d\bar{\theta}}{d\xi}_{\xi=0}\right) \quad . \quad . \quad . \quad . \quad . \quad (34)$$

or

$$\left(\frac{d\bar{\theta}'}{d\xi}\right)_{\xi=0} \cdot \left(\frac{\alpha}{\alpha'}\right)^{\frac{1}{2}} = \left(\frac{d\bar{\theta}}{d\xi}\right)_{\xi=0} \quad . \quad . \quad . \quad . \quad (35)$$

Thus if h is the intensity of heat transfer at a given point in the first case and h' that at the same point in the second,

$$\frac{h'}{h} = \left(\frac{\alpha'}{\alpha}\right)^{\frac{1}{2}} \quad . \quad . \quad . \quad . \quad . \quad . \quad . \quad (36)$$

But if f is the local intensity of skin friction in the first case and f' that in the second, $f'/f=\alpha'/\alpha$. Hence

$$\frac{h^3}{f}=\frac{h'^3}{f'}, \quad . \quad . \quad . \quad . \quad . \quad . \quad . \quad (37)$$

for any particular fluid, Reynolds number, and thermal boundary specification. If F is the whole friction, it follows that H^3/F is independent of the approximation employed provided it is of the type considered *.

5. Extension of Results with Oseen's Approximation and Comparison with other Theories and with Experiment.

The heat transfer to fluids of poor conductivity that accords with Blasius's solution of the flow to Prandtl's approximation has been worked out by Fage and Falkner (*loc. cit.*) for various values of p. The mean intensity of skin friction with this flow is given by $1{\cdot}327\rho U^2/2R^{\frac{1}{2}}$, while with flow to Oseen's approximation it is given asymptotically by $2{\cdot}257\rho U^2/2R^{\frac{1}{2}}$. Hence by the relation (37) we can immediately deduce heat-losses calculable with Oseen's approximation for fluids of poor conductivity from Fage and Falkner's results. The latter are to be increased in the ratio $(2{\cdot}257/1{\cdot}327)^{\frac{1}{3}}=1{\cdot}194$. For instance, Fage and Falkner find for the case of uniform temperature in air a value for $H/(k\theta_0 R^{\frac{1}{2}})$ equal to 1·240. When increased in the above ratio this agrees with (26). Different methods are used for obtaining the two results and the comparison is of value as a check.

The heat-loss for inviscid flow past plates of uniform temperature is given † by

$$H/k\theta_0=2{\cdot}257\left(\frac{Ulc}{k}\right)^{\frac{1}{2}}. \quad . \quad . \quad . \quad . \quad . \quad (38)$$

For air, using the mean experimental value 1·3 for $k/c\nu$, this result may be expressed in the form

$$H/k\theta_0=1{\cdot}98R^{\frac{1}{2}}. \quad . \quad . \quad . \quad . \quad . \quad (39)$$

Comparison of the coefficient on the right-hand side with 1·48 from (26) and with 1·24, given by Fage and Falkner,

* The formula (37) will not, of course, be compared with Reynolds's well-known relationship between heat transfer and friction. Section 4 is not concerned with physical relationships, but only with errors involved in analytical approximations.

† Piercy and Winny, Phil. Mag. xvi. p. 396 (1933).

shows that Oseen's approximation is capable of accounting for a large proportion of the reduction of heat-loss due to viscosity.

A case of particular interest is when $p=0{\cdot}4$. For this value of p, Fage and Falkner have measured the convection from thin platinum foils heated to 150° C. temperature elevation in a stream of air. The Reynolds number ranged from 10^3 to 10^4 approximately. Writing θ_M for the mean temperature elevation of the plate, and ascribing values to the physical constants appropriate to the mean * of the temperatures of the plate and of the distant fluid, we have for the value of $H/(k\theta_M R^{\frac{1}{2}})$:—

From Fage and Falkner's experiments.....	1·50
From Fage and Falkner's theory	1·325
From the present theory.....	1·58

The remarkable degree of success achieved in predicting the experimental results by the present theory is surprising and calls for discussion. With the postulate that the true stream function can be expanded closely in the form (27), we might apply the theorem of Section 4 to estimate the friction from the measured heat-loss, although the relationship is unsuitable for this reverse process, experimental errors being trebled. The value obtained would be much too great for real steady flow. At the smaller Reynolds numbers concerned Blasius's formula may be expected to under-estimate the friction, but, according to (37) and such friction measurements that exist, the correction required to be applied on this score to Fage and Falkner's prediction of heat transfer would be small. It would appear either that(1) fails to represent the physical problem with sufficient completeness or that the mean experimental value for the conductivity is in considerable error.

For small temperature elevations (1) would appear to be suitable since, in the absence of convection, steadiness may persist in flow past flat plates for Reynolds numbers as great as 5×10^5. It would be of interest to observe whether the temperature elevation employed in the experiments, where the plates were horizontal, would

* This choice is not important. If the mean temperature of the plate were chosen instead, the experimental coefficient would be increased by only 2 per cent.

cause turbulence to arise at moderate Reynolds numbers in the upper boundary layer owing to its being heated from below. The convection from a vertical plate might then be less, in some circumstances, than that from a horizontal one.

The value of the thermal conductivity of air is regarded as uncertain within ± 10 per cent. To bring the observations into the closer agreement we should expect with Fage and Falkner's prediction from Prandtl's approximation, it would be necessary to ascribe a 10 per cent. error to the mean experimental value of the conductivity.

While such uncertainties remain in the problem, we can only conclude from the foregoing evidence that Oseen's approximation leads to a prediction of heat transfer which is in fair agreement with experiment.

6. *Note on Range of Present Theory.*

Use of the formula (3) assumes that a boundary layer of viscous effects may be said to exist, but the restriction implied as to the lower limit of Reynolds number remains vague. It is probably permissible to view the question in the light of the known error incurred in estimating friction from the asymptotic instead of from the complete solution of Oseen's equation. Particulars of this error and of the thickness, Δ, of the boundary layer at the back edge of the plate are given below through a wide range.

R.	Error in asymptotic approximation to friction.	Δ/l.
10,000	$-0{\cdot}7$ per cent.	0·0364
1000	$-2{\cdot}0$,, ,,	0·115
100	$-6{\cdot}2$,, ,,	0·364

On this basis the use of (3) appears justifible for Reynolds numbers which exceed a comparatively small value, although they must be well removed from those of hot-wire anemometry, for instance.

The authors acknowledge with pleasure suggestions made by Prof. L. Bairstow, C.B.E., F.R.S. The work has also been aided by a grant from the Department of Scientific and Industrial Research.

XXXIV. *X-ray Study of Aluminium-Zinc Alloys.* By Prof. E. A. Owen, *M.A., D.Sc., and* John Iball, *Ph.D., University College of North Wales, Bangor* *.

[Plates XII.–XIV.]

THE aluminium-zinc alloys have received considerable attention from metallurgists† and the system presents some interesting features. Several equilibrium diagrams of the system have been suggested, the one at present accepted being that put forward by Hanson and Gayler, although later workers have cast some doubt concerning certain regions of the diagram, in particular, the pure β-region which some claim not to be a solid solution of definite extent, but an "intermetallic compound" having the formula Al_2Zn_3 such as was suggested by Rosenhain and Archbutt in earlier work. Much difficulty has been experienced in examining some of the alloys by metallurgical methods, as the alloys spontaneously decompose in a short time after quenching with the production of an alloy exhibiting a structure quite different from that which it had immediately after quenching.

We have not been able to trace more than one X-ray examination conducted on the system. This was carried out by Phebus and Blake ‡; it was found that the region between 0 and 20 per cent. zinc is a solid solution of zinc in aluminium, the aluminium lattice decreasing from 4·0435 to 4·0345 A. From 20 to 95 per cent. zinc, both the aluminium and the zinc structures were present, but no compounds were observed.

The first part of the present paper deals with alloys quenched from different temperatures, but photographed in the main with a precision camera at ordinary room temperatures. This procedure yielded useful data, but it was found that in order to obtain information concerning the β-region, and, in fact, other regions above the

* Communicated by the Authors.

† Shepherd, J. Phys. Chem. ix. p. 504 (1905); Rosenhain and Archbutt, Roy. Soc. Trans. ccxi. p. 316 (1912); Bauer and Vogel, *Intern. Z. Metallographie*, viii. p. 101 (1916); Hanson and Gayler, J. Inst. Met. xxvii. p. 267 (1922); Sander and Meissner, *Z. f. Metallkunde*, xiv. p. 385 (1922); Tanabe, J. Inst. Met. xxxii. p. 415 (1924); Isihara, J. Inst. Met. xxxiii. p. 73 (1925).

‡ Phebus and Blake, Phys. Rev. xxv. p. 107 (1925).

transformation temperature, it was necessary to take the X-ray photographs at the actual temperature of annealing. A technique had therefore to be developed to cope with this difficulty. The second part of the paper is devoted to the results obtained when the alloys were maintained at high temperature during the X-ray exposure.

It should be emphasized here that the present paper contains an account of what we consider to be a preliminary and incomplete survey of the system.

1. *Photographs taken at Room Temperature.*

A preliminary general survey of alloys annealed at 250° C. and quenched into iced water was carried out

Fig. 2.

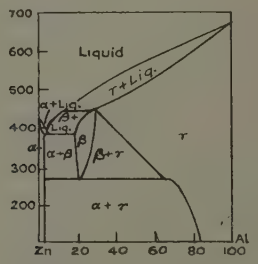

Aluminium–zinc equilibrium diagram (Hanson and Gayler).

with the powder spectrum camera to find the types of structure present in alloys at this temperature. The photographs of alloys containing 90, 70, 50, 30, and 10 per cent. aluminium are shown in fig. 1 (Pl. XII.), from which it will be observed that the 90 per cent. alloy is in the pure γ-region, which has a face-centred cubic structure, and that the other alloys are all in the mixed $(\alpha+\gamma)$ region, the photographs showing a mixture of face-centred cubic and close-packed hexagonal structures. From these photographs it was deduced that the phase fields for alloys annealed at 250° C. were similar to those recorded by Hanson and Gayler in their equilibrium diagram of this system (fig. 2).

It was necessary before proceeding further to investigate the effect of various heat treatments on the alloys.

Effect of lump annealing.—Photographs were taken with the precision camera of alloys after various heat treatments in lump form and the results compared with those obtained with "as cast" ingots. For this purpose alloys in the pure γ-region were examined. Using copper radiation, two Kα doublets were recorded on the film, but measurements were made only on the doublet from the (333) plane, since it was in the best position for accurate estimation of the parameter.

Filings were taken from "as cast" ingots of alloys having compositions 90 and 70 per cent. aluminium by weight. These were annealed for 6 hours at 410° C., quenched in iced water, and an X-ray photograph

TABLE I.

Crystal Parameters of Filings annealed for Six Hours at 410° C. and quenched in Iced Water.

Composition (per cent. Al by weight).	Condition of ingot.		
	As cast.	Lump annealed at 400° C.	
		for 14 hrs.	for 600 hrs.
90	$4{\cdot}036_6$ Å.	$4{\cdot}036_3$	$4{\cdot}036_1$
70	$4{\cdot}024_6$	$4{\cdot}024_8$	$4{\cdot}024_7$
60	—	$4{\cdot}022_3$	$4{\cdot}022_2$

taken on the precision camera. The ingots were then annealed at 400° C. for 14 hours. Further filings were taken and treated in the same way as the first batch. The ingots were replaced in the furnace and annealed for 586 hours (600 hours in all) at 400° C. The results are shown in Table I., from which it will be observed that the parameters measured after each annealing treatment are almost identical with those obtained with the "as cast" specimen, thus showing that lump annealing is unnecessary with these alloys.

Effect of different times of anncaling alloy in powder form.—Filings from an alloy containing 85 per cent. aluminium by weight were annealed at 250° C. for 6 hours and 24 hours respectively. Identical parameter values

were obtained with the two specimens, from which it may be inferred that 6 hours annealing in powder form is sufficient at 250° C., and therefore also at any higher temperature, to remove the effects of cold work.

Further measurements were made on this alloy after annealing the powder at various temperatures. According to the equilibrium diagram of Hanson and Gayler this alloy is in the γ-region from room temperature to nearly 600° C. The parameters remained constant for all temperatures up to 410° C., but beyond this temperature, at 550° C., a definite decrease in parameter occurred (Table II.). At this stage of the work this decrease could not be explained. It was found from photographs

TABLE II.

Annealing temperature.	Time of annealing.	Parameter (Å.).
110° C.	12 hours.	$4{\cdot}036_2$
110° C.	60 ,,	$4{\cdot}036_1$
250° C.	6 ,,	$4{\cdot}036_7$
250° C.	24 ,,	$4{\cdot}036_7$
410° C.	7½ ,,	$4{\cdot}036_1$
550° C.	2 ,,	$4{\cdot}035_4$

taken later at the actual annealing temperature, that the γ-region does not extend at high temperatures as far as was previously supposed; the effect now observed may possibly be due to this cause.

γ-phase parameters at 250° C.—Measurements were now made of the parameters of the γ-phase in alloys extending over a wide range of composition when the powder was annealed at 250° C. and quenched. The composition was determined by chemical analysis for some, but not all, the alloys investigated. It is only necessary to know the composition accurately in the pure region. The powder was annealed in each instance for 6 hours, this time being sufficient, according to the preliminary investigation, to produce equilibrium. The results obtained are summarized in Table III.

TABLE III.

γ-Phase Parameter of Alloys annealed at 250° C.

Composition.		γ-phase parameter (Å.).	Mean atomic volume (Å.^{3}).
Weight per cent. Al.	Atomic per cent. Al.		
100	100·0	$4·040_0$	$16·49_6$
95·5	97·8	$4·039_7$	$16·48_1$
90·0	95·6	$4·037_8$	$16·45_5$
85·0	92·8	$4·036_7$	$16·44_4$
81·0	90·7	$4·034_5$	$16·41_7$
70·0	85·0	$4·034_6$	$16·41_9$
61·2	79·1	$4·034_0$	$16·41_2$
48·0	69·0	$4·034_0$	$16·41_2$
40·0	61·8	$4·034_9$	$16·42_2$
25·0	44·7	$4·034_0$	$16·42_2$

The relation between composition and mean atomic volume based on these results is shown in fig. 3. The parameter decreases linearly with increasing zinc content

Fig. 3.

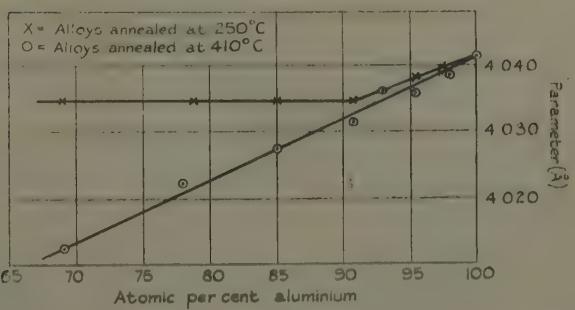

in the pure region and remains constant in the mixed region. The limit of solubility of zinc in aluminium at 250° C. is approximately 9·3 atomic per cent., or 20 per cent. by weight. This is nearer to the position of the

boundary at this temperature given by Bauer and Vogel. than to that given by Hanson and Gayler.

γ-phase parameters at 410° *C.*—In an attempt to fix the limit of the pure γ-region at 410° C. the procedure adopted was to anneal the alloys in lump form at 400° C. for about 14 hours. These were quenched in iced water and filings taken from them at a depth of at least 1 mm. below the surface. The filings were sealed in evacuated silica tubes and annealed at 410° C. for 6 hours—sometimes the time of annealing was increased to 14 hours—and then quenched. It was realized that to retain the alloys in the equilibrium state existing at 410° C. very efficient quenching would be necessary. The samples in powder form were therefore enclosed in evacuated silica tubes at one end of which small bulbs with wall thickness of about 0·15 mm. were blown. Each tube during the annealing process was held in a vertical tube furnace, with the bulb lowermost, by a stout nichrome wire passing through a small hole in the top cover of the furnace, the bottom end being fitted with a plug of asbestos cloth. During the quenching operation, the plug was removed and the wire carrying the tube pushed quickly into the quenching medium just below the furnace. Very rapid quenching was effected in this manner. The powder was immediately removed from the tube, mounted on the camera, and photographed in the shortest possible time. About $2\frac{1}{2}$ to 3 hours elapsed between the quenching operation and the completion of the exposure.

Alloys containing not less than 50 per cent. aluminium by weight gave sharp reflexion lines, but alloys containing 40 and 35 per cent. aluminium gave no lines on the precision camera when treated as above described. No lines other than those belonging to the γ-phase could be detected on the films. The parameters obtained are included in Table IV.

The mean atomic volume decreases approximately linearly with the composition indicating the existence of a pure phase at 410° C. over the range of composition investigated. This is in accordance with the equilibrium diagram of Hanson and Gayler. We were unable to determine the limit of the phase at this temperature because of the difficulty of obtaining photographs with alloys of composition lower than about 70 atomic per

cent. aluminium. When the values of the parameters given in Table IV. are plotted against composition on the same graph as the alloys annealed at 250° C., it will be observed (fig. 3) that the slopes of the initial parts of the two curves are slightly different, an effect which is probably due to the fact that the surface of the powder grains, owing to the high annealing temperatures, is richer in zinc than the chemical analysis of the powder would indicate *.

Since no reflexion lines could be obtained with alloys in the region of 50 per cent. aluminium by weight when

TABLE IV.

γ-Phase Parameters of Alloys annealed at 410° C.

Composition.		γ-phase parameter (Å.).	Mean atomic volume (Å.^{3}).
Weight per cent. Al.	Atomic per cent. Al.		
100	100·0	$4{\cdot}040_9$	$16{\cdot}49_6$
95·5	97·8	$4{\cdot}039_4$	$16{\cdot}47_8$
90·0	95·6	$4{\cdot}036_1$	$16{\cdot}43_7$
81·0	90·7	$4{\cdot}031_6$	$16{\cdot}42_0$
70·0	85·0	$4{\cdot}027_2$	$16{\cdot}32_9$
60·0	78·4	$4{\cdot}022_2$	$16{\cdot}26_8$
48·0	69·0	$4{\cdot}012_5$	$16{\cdot}03_9$

quenched from 410° C., the investigation was continued from the α-end of the diagram. As in the case of pure zinc, nickel radiation was used. The α-phase is restricted to such a narrow range that it is difficult to find the rate of change of atomic volume with composition. The range of solubility is about 1 to 2 per cent. aluminium by weight, but although the range is narrow, a definite increase in atomic volume was found. The α-phase parameters of alloys annealed at 250° C. are given in Table V.

Up to this stage the alloys were annealed at a given temperature, quenched, and the parameters of the phases present obtained from photographs taken at room temperature with the precision camera. But for slight

* See Owen and Pickup, Proc. Roy. Soc. A, cxxxix. p. 526 (1933).

changes in the positions of the γ-boundary the results so far recorded corroborate the findings of Hanson and Gayler. It was impossible to obtain any information concerning alloys quenched from temperatures higher than about 260° C. in the neighbourhood of the β-region, as this phase is unstable at room temperature and decomposes spontaneously into $(\alpha+\gamma)$. Information concerning alloys above the eutectoid line could therefore be obtained only by photographing these alloys at the annealing temperatures. The only line of attack seemed to be to take spectrum photographs of these alloys while they were being heated at the required temperatures.

TABLE V.

α-Phase Parameters of Alloys annealed at 250° C.

Composition.		Axial ratio.	Base side (Å.).	Mean atomic volume (Å.^{3}).
Weight per cent. Al.	Atomic per cent. Al.			
0·0	0·0	1·856	$2·659_0$	$15·10_9$
2·0	5·0	1·869	$2·655_7$	$15·15_8$
4·8	11·2	1·869	$2·656_1$	$15·16_5$
25·0	44·7	1·869	$2·656_3$	$15·16_8$

II. *Photographs taken at High Temperatures.*

The development of the high temperature technique employed in the present investigation has already been described in a previous paper *. Copper radiation was used and the samples during exposure were surrounded by an atmosphere of nitrogen.

The first alloy examined was one containing 25 per cent. aluminium by weight. Powdered samples of the alloy were subjected to various heat treatments. One sample was annealed for 6 hours at 250° C. and quenched in iced water; it gave a photograph at room temperature showing the α and γ structures. Another sample was annealed in a silica tube at 375° C. where it should consist wholly of the β-phase. A spectrum photograph started

* Owen and Iball, Phil. Mag. xvi. p. 479 (1933).

immediately after quenching contained lines which were identical with those obtained with the sample quenched from 250° C. When the samples were heated during exposure at 310° C. or 375° C. a definite change in structure was noticeable (see fig. 4 (Pl. XII.)). It was clear from these photographs that the structure of the alloy existing above the transformation line was unstable at room temperature and that severe quenching did not prevent the samples from returning, after a very short interval, to the structure existing at 250° C. Also the structure

TABLE VI.

Spectrum Photograph at 375° C. of Alloy containing 25 per cent. Aluminium by Weight.

Sin θ from calibration curve.	Reflecting planes.	λ.	Parameter (Å.).
0·2987	(111)	β	4·028
0·3308	(111)	α	4·025
0·3449	(200)	β	4·028
0·3817	(200)	α	4·028
0·5399	(220)	α	4·027
0·5722	(311)	β	4·026
0·6342	(311)	α	4·025
0·6617	(222)	α	4·029
0·7645	(400)	α	4·025
0·8327	(331)	α	4·028
0·8547	(420)	α	4·026
0·9351	(422)	α	4·027
		Mean parameter....	4·027 Å.

of the alloy above was different from that below the transformation temperature.

Structure of the β-phase.—According to the equilibrium diagram of Hanson and Gayler, an alloy containing 25 per cent. aluminium by weight should, at 375° C., be well within the pure β-region. The photograph taken at this temperature showed well-defined lines, all of which belonged to a face-centred cubic structure. The result of the measurement of the lines is shown in Table VI.

The β-phase possesses, therefore, a face-centred cubic structure, the parameter of the alloy containing 25 per cent. aluminium by weight, being 4·027 Å. at 375° C. The structure is similar to that of the γ-phase.

TABLE VII.

Spectrum Photograph at 375° C. of Alloy containing 15 per cent. Aluminium by Weight.

Sin θ.	Reflecting planes.	λ.	Parameter Å.	
			Face-centred cubic.	Close-packed hexagonal (c= 1·900).
0·4513	$(10\bar{1}2)$	α	..	2·662
0·4894	(220)	β	4·015	
0·5419	(220)	α	4·012	
0·5648	$(10\bar{1}3)$	α	..	2·661
0·5740	(311)	β	4·014	
0·5771	$(11\bar{2}0)$	α	..	2·664
0·6357	(311)	α	4·011	
0·6520	$(11\bar{2}2)$	α	..	2·665
0·6630	(222)	α	4·016	
0·6826	$(20\bar{2}1)$	α	..	2·668
0·6925	$(10\bar{1}4)$	α	..	2·665
0·7530	(331)	β	4·021	
0·7657	(400)	α	4·016	
0·8061	$(20\bar{2}3)$	α	..	2·668
0·8340	(331)	α	4·018	
0·8558	(420)	α	4·017	
0·8930	$(21\bar{3}1)$	α	..	2·669
0·9366	(422)	α	4·021	
	Mean values.....		4·016 Å.	2·666 Å.

To find if this structure extended towards the α-phase an alloy containing 15 per cent. aluminium by weight was photographed at 375° C. Twenty-four lines appeared on the film, the result of the measurement of which is shown in Table VII.

All the lines in the photograph are accounted for by a face-centred cubic structure of parameter 4·016 Å., and a close-packed hexagonal structure of base side 2·666 Å. and axial ratio 1·900. The value of the parameter of the cubic constituent is lower than that of alloy 25. The fact that the second constituent has a close-packed hexagonal structure shows that this alloy is in the $(\alpha+\beta)$ region. Whether the β-phase existed as a separate phase distinct from the γ-phase was not clear at this stage of the investigation. It seemed quite

TABLE VIII.

Face-centred Cubic Parameters in Alloys photographed at 350° C.

Composition (per cent. Al by weight).	Parameter (Å.).	Composition (per cent. Al by weight).	Parameter. (A.).
100	4·077	48	4·058
95	4·072	44	4·059
90	4·069	41	4·050
84	4·064	37	4·038
80	4·070	33	4·030
70	4·065	25	4·023
61	4·072	15	4·022
54	4·059		

definite, however, that the cubic reflexions on the photograph represented the structure hitherto known as beta (β).

At this stage it was decided to examine a number of alloys at short intervals of composition across the diagram. According to the accepted equilibrium diagram, it is possible at 350° C. to examine alloys of all compositions without going above the solidus. Alloys varying in composition from pure aluminium to 15 per cent. aluminium were accordingly prepared. The results obtained with the fourteen alloys examined are collected together in Table VIII.

The relation between the compositions of the alloys and the parameters of the cubic lattices existing at 350° C. is shown in fig. 5. Only two types of structures exist across

the diagram at this temperature, the face-centred cubic and the close-packed hexagonal, the latter extending as a pure phase for about 1 to 2 per cent. aluminium; between this and 30 per cent. aluminium a mixture of the two structures appears. The pure β-phase extends from about 31·5 to 44 per cent. aluminium at this temperature.

The parameter of the aluminium-saturated β-solution remains constant and has the value 4·059 Å. at this temperature. Mixed with the β-phase in this region is the zinc-saturated γ-phase, having the same structure as the β-phase, but a parameter of 4·068 Å. This parameter is slightly lower than that of pure aluminium at this temperature, viz., 4·077 Å.

Fig. 5.

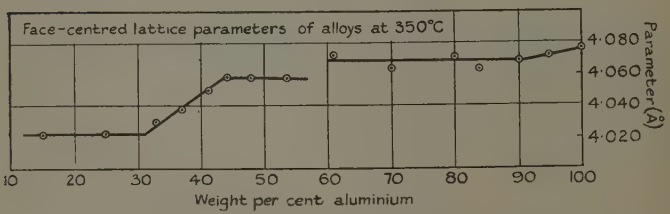

To obtain further information concerning the $(\beta+\gamma)$ region the structures of alloys 80 and 70 per cent. aluminium were examined at a higher temperature. If these alloys were still in the mixed region their parameters should be identical, but if they were in the pure γ-region, the parameter of alloy 70 should be lower than that of alloy 80. Photographs were accordingly taken at 450° C. The definition of the spectral lines was almost as good as that in photographs of alloys taken at room temperature. Both alloys gave the same parameter (4·082 Å), thus confirming the result obtained at 350° C., that this region consisted of a mixture of two phases. Lines from one phase only were recorded on the photograph, those belonging to the other phase being too faint and too close to the other lines to show up separately. At other compositions and temperatures of annealing the two structures are distinctly recorded on the same film. These results will be discussed later.

These measurements lead to the following conclusions :—

The β-phase is a solid solution with a face-centred cubic structure. It extends at 350° C. over a range of composition from 31·5 to 44·0 per cent. aluminium, which is different from that shown in previously published equilibrium diagrams. Between 44 per cent. and 90 per cent. aluminium approximately at this temperature, two face-centred cubic lattices of slightly different dimensions exist together in a mixed ($\beta+\gamma$) region. The difference between the two parameters at this temperature is not large enough for the two sets of lines to be distinctly separated. The boundary of the γ-phase occurs at about 90 per cent. aluminium. These results do not agree with those recorded earlier in this paper and obtained at room temperature with alloys quenched from 410° C. The γ-phase under those conditions extended over a long range of compositions in accordance with the diagrams of Tanabe, and Hanson and Gayler, whereas now it is much more limited in extent.

We thus find by X-ray analysis a corroboration of the results of micrographic analysis when alloys are annealed at temperatures above the transformation temperature and quenched, but when the alloys are examined at the temperature of annealing, the results are different, a mixed region appearing in place of the pure phase found previously. To explain these results further investigation of the system in this region by more refined methods is necessary.

Determination of the transformation temperature.—A series of alloys were prepared to cover a range of composition from about 90 to 15 per cent. aluminium. These were photographed at temperatures ranging up to 310° C. with a view to fixing the transformation temperature. According to Hanson and Gayler the transformation takes place at 256° C., but there seems to be no definite agreement in the thermal diagrams on this point. Isihara puts the line at 280° C. and Tanabe at 270° C.

Photographs of alloys at 290° C.—Photographs of seven different alloys were taken at 290° C. The lines which appeared on the film indicated the same type of crystal structure as that obtained with alloys quenched from 250° C. Alloys 80 and 90 showed the face-centred cubic

structure of the γ-phase. At 70 per cent. aluminium extra lines began to appear, and these become progressively

TABLE IX.

Spectrum Photograph at 290° C. of Alloy containing 25 per cent. Aluminium by Weight.

Sin θ.	Reflecting planes.	λ.	Parameters Å.	
			Close-packed hexagonal (c= 1·89).	Face-centred cubic.
0·4085	$(10\bar{1}2)$	β	2·665	
0·4520	$(10\bar{1}2)$	α	2·664	
0·4845	(220)	β	..	4·055
0·5113	$(10\bar{1}3)$	β	2·667	
0·5210	$(11\bar{2}0)$	β	2·667	
0·5364	(220)	α	..	4·053
0·5666	$(10\bar{1}3)$	α	2·663	
0·5775	$(11\bar{2}0)$	α	2·662	
0·5898	$(11\bar{2}2)$	β	2·665	
0·6108	(0004)	α	2·664	
0·6187	$(20\bar{2}1)$	β	2·660	
0·6290	(311)	α	..	4·053
0·6530	$(11\bar{2}2)$	α	2·664	
0·6663	$(20\bar{2}0)$	α	2·664	
0·6835	$(20\bar{2}1)$	α	2·665	
0·6966	$(10\bar{1}4)$	α	2·661	
0·7342	$(20\bar{2}2)$	α	2·660	
0·8088	$(20\bar{2}3)$	α	2·663	
0·8263	(331)	α	..	4·055
0·8320	$(10\bar{1}5)$	α	2·667	
0·8400	$(11\bar{2}4)$	α	2·665	
0·8484	(420)	α	..	4·052
0·8944	$(21\bar{3}1)$	α_1	2·664	
0·8967	$(21\bar{3}1)$	α_2	2·664	
0·9279	(422)	α	..	4·059
		Mean values	2·664 Å.	4·054 Å.

stronger as the aluminium content decreases. The parameter of the cubic structure becomes approximately constant for alloys below about 82 per cent. aluminium.

The other set of lines appearing on these photographs belongs to the close-packed hexagonal structure of the α-phase.

Details of the measurements of one photograph taken at this temperature (290° C.) with alloy 25 are included in Table IX. to show the degree of agreement obtained. The lines in these photographs were as well defined as those recorded at room temperature. Eight lines occurring at small angles of reflexion have been omitted.

It was evident from these results that the transformation takes place at a temperature higher than 270°C. The γ-phase parameters for the alloys examined are given in Table X., and the photographs obtained at this temperature are shown in fig. 6 (Pl. XIII.). By comparing these photographs with those of alloys quenched from

TABLE X.

Composition (per cent. Al by weight).	γ-phase parameter at 290° C.	Composition (per cent. Al by weight).	γ-phase parameter at 290° C.
100	4·071 Å.	41	4·054 Å.
90	4·061	33	4·052
70	4·054	25	4·054

250° C. (fig. 1), it will be seen that the arrangement of the lines is identical in the two cases.

Photographs of alloys at 310° *C.*—Seven alloys in the region from 15 to 70 per cent. aluminium were investigated at 310° C. The results of the measurement of the photograph taken with alloy 15 are shown in Table XI., which includes the lines reflected at the larger glancing angles only.

After increasing the aluminium content sufficiently, two distinct sets of lines, each belonging to a face-centred cubic structure make their appearance on the film. The results obtained with one alloy containing 41 per cent. aluminium are given in Table XII. The two sets of lines measured were distinctly resolved in the photographs ; these are reproduced in fig. 7 (Pl. XIII.).

As the aluminium content of the alloy increases the intensity of the lines giving the smaller parameter decreases until at 61 per cent. aluminium only one line of this set is measurable. Alloy 70 gave only the γ-phase lines. As the aluminium content decreases, the second set of lines can be measured. Decreasing the aluminium content

TABLE XI.

Spectrum Photograph at 310° C. of Alloy containing 15 per cent. Aluminium by Weight.

Sin θ.	Reflecting planes.	λ.	Parameter (Å.). Close-packed hexagonal (c= 1·89).	Parameter (Å.). Face-centred cube.
0·5656	$(10\bar{1}3)$	α	2·668	
0·5770	$(11\bar{2}0)$	α	2·665	
0·6357	(311)	α	..	4·011
0·6528	$(11\bar{2}2)$	α	2·664	
0·6631	(222)	α	..	4·016
0·6831	$(20\bar{2}1)$	α	2·666	
0·7668	(400)	α	..	4·010
0·8090	$(20\bar{2}3)$	α	2·663	
0·8343	(331)	α	..	4·016
0·8561	(420)	α	..	4·016
0·8945	$(21\bar{3}1)$	α	2·665	
0·9372	(422)	α	..	4·018
		Mean values....	2·655 Å.	4·015 Å.

still further causes the close-packed hexagonal structure of the α-phase to appear on the photographs.

Thus at 310° C. two face-centred cubic lattices of slightly different parameters co-exist and each lattice reflects separately. The mean values of the parameters of the two cubic lattices are given in Table XIII.

The photographs taken at 310° C. show structures which are different from those at 290° C., so the transformation temperature must be between these limits of temperature. In an attempt to fix this temperature more definitely

TABLE XII.

Spectrum Photograph at 310° C. of Alloy containing 41 per cent. Aluminium by Weight.

Sin θ.	Reflecting planes.	λ.	Parameter Å.	
			β-phase.	γ-phase.
0·5359	(220)	α	..	4·057
0·5419	(220)	α	4·012	
0·5681	(311)	β	..	4·056
0·5728	(311)	β	4·022	
0·6288	(311)	α	..	4·055
0·6349	(311)	α	4·016	
0·6563	(222)	α	..	4·058
0·6620	(222)	α	4·022	
0·7583	(400)	α	..	4·055
0·7651	(400)	α	4·019	
0·8261	(331)	α	..	4·056
0·8331	(331)	α	4·022	
0·8475	(420)	α	..	4·056
0·8550	(420)	α	4·021	
0·9281	(422)	α	..	4·058
0·9361	(422)	α	4·023	
		Mean values....	4·019 Å.	4·056 Å.

TABLE XIII.

Composition (per cent. Al by weight(.	Parameter at 310°.	
	β-phase.	γ-phase.
70	..	4·055
61	..	4·052
48	4·018	4·056
41	4·019	4·056
33	4·015	4·051
25	4·014	
15	4·015	

another photograph was taken at 300° C. The lines in the photograph (Table XIV.) showed that the alloy was

TABLE XIV.

Spectrum Photograph at 300° C. of Alloy containing 37 per cent. Aluminium by Weight.

Sin θ.	Reflecting planes.	λ.	Parameter Å.	
			Close-packed hexagonal.	Face-centred cubic.
0·4083	$(10\bar{1}2)$	β	2·665	
0·4517	$(10\bar{1}2)$	α	2·665	
0·4845	(220)	β	..	4·055
0·5118	$(10\bar{1}3)$	β	2·664	
0·5210	$(11\bar{2}0)$	β	2·667	
0·5362	(220)	α	..	4·055
0·5670	$(10\bar{1}3)$	α	2·661	
0·5777	$(11\bar{2}0)$	α	2·661	
0·5915	$(11\bar{2}2)$	β	2·658	
0·6293	(311)	α	..	4·051
0·6536	$(11\bar{2}2)$	α	2·661	
0·6560	(222)	α	..	4·059
0·6676	$(20\bar{2}0)$	α	2·659	
0·6839	$(20\bar{2}1)$	α	2·663	
0·7355	$(20\bar{2}2)$	α	2·665	
0·8092	$(20\bar{2}3)$	α	2·662	
0·8268	(331)	α	..	4·053
0·8340	$(10\bar{1}5)$	α	2·661	
0·8410	$(11\bar{2}4)$	α	2·662	
0·8481	(420)	α	..	4·054
0·8822	$(21\bar{3}0)$	α	2·662	
0·8948	$(21\bar{3}1)$	α	2·664	
0·9281	(422)	α	..	4·058
0·9330	$(21\bar{3}2)$	α	2·664	
		Mean values....	2·662 Å.	4·055 Å.

in the same condition of equilibrium as alloys quenched from 250° C. Hence the transformation temperature lies between 300° C. and 310° C., each of these temperatures being considered correct to within $\pm 5°$ C. The higher

temperature of transformation now obtained may be due to the fact that the specimen was maintained at a constant temperature for a considerable period of time during observation. Under these conditions it was more likely to be in a state of true equilibrium than if the temperature were slowly changing as is sometimes the case when the transformation temperature is determined. Another factor which may have a bearing on the result is that in place of a single sample of appreciable size, fine filings were used.

There are three sources of error in estimating the temperature of the specimen. One is due to the fact that the thermo-couple junction may not coincide precisely with the position where the X-ray beam strikes the fibre. If the junction is higher or lower than the correct position, then, owing to convection currents, the registered temperature will also be higher or lower than that of the desired spot on the fibre. By moving the junction along the axis of the coil it was found that the temperature variation from 5 mm. below to 5 mm. above the spot where the beam fell on the fibre did not exceed 8° C. The second source of error is in the calibration of the pyrometer. The calibration was repeated periodically and sometimes a slight displacement of the calibration curve was necessary, this change being due to the fatigue of the galvanometer suspension. The third source of error arises from any unsteadiness of the current passing through the heating coil. The current was supplied by a battery of cells of large capacity, and several series of observations showed that it remained constant over long intervals. For example, when the pyrometer was left in position for four hours and the galvanometer deflexion was watched carefully, the temperature variation did not exceed 5° C.

A number of photographs were now taken at various temperatures above the transformation temperature.

Photographs of alloys at 325° *C.*—The photographs taken at this temperature are reproduced in fig. 8 (Pl. XIV.), and the results of the measurements are shown in Table XV. The lines from the two components of the alloys are sharply defined and well separated in these photographs.

Photographs of alloys at 375° C.—Photographs were taken at this temperature of thirteen alloys, ranging

in composition from 98 to 10 per cent. aluminium. Some of the photographs are reproduced in fig. 9 (Pl. XIV.), and a summary of the results is given in Table XVI.

From a graphical representation of the results (fig. 10) it will be seen that at 375° C. the extent of the β-phase

TABLE XV.

Composition (per cent. Al by weight).	Parameter at 325° C.	
	β-phase.	γ-phase.
48	4·015 Å.	4·055 Å.
37	4·016	4·056
33	4·016	4·055
25	4·017	—

TABLE XVI.

Face-centred Cubic Parameters in Alloys photographed at 375° C.

Composition (per cent. Al by weight).	Parameter.	Composition (per cent. Al by weight).	Parameter.
100	4·080 Å.	44	4·055 Å.
98	4·068	41	4·053
95	4·066	33	4·037
80	4·065	25	4·028
61	4·069	15	4·016
54	4·058	10	4·015
48	4·059		

is greater, and that of the γ-phase less, than at 350° C. The change in the parameter of the γ-phase is so small that the whole drop across the region of pure solid solution is almost within the range of the experimental error. This makes it impossible with this method to fix a definite limit to the solubility of zinc in aluminium at this temperature, but it appears to be very small. The parameter

remains at a constant value (4·067 Å.) from approximately 98 per cent. to 60 per cent., when it changes to a lower value (4·058 Å.) and remains at this value till approximately 45 per cent. aluminium, which marks the β-($\beta+\gamma$) boundary. The pure β-region extends at this temperature from 45 to about 19 per cent. aluminium, the parameter decreasing almost linearly over this range. The parameter remains constant in the ($\alpha+\beta$) region at 4·015 Å. The photographs taken of alloys in this region exhibit both cubic and hexagonal structures, the hexagonal lines predominating in the alloy containing 10 per cent. aluminium.

Photographs of alloys at 430° *C.*—These were taken with a view to fixing the β-($\beta+\gamma$) boundary at this temperature.

Fig. 10.

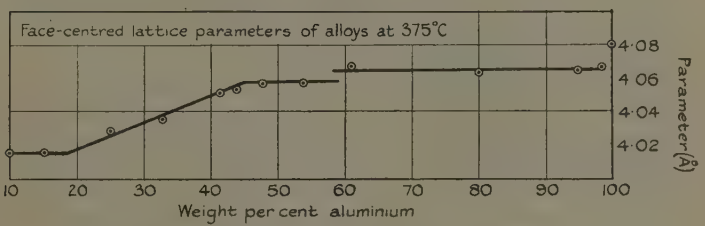

The photographs taken are reproduced in fig. 11 (Pl. XIV.), the measurements of which gave 47 per cent. as the approximate limit of the aluminium saturated β-phase at 430° C.

Conclusions.—With alloys that were annealed and quenched from different temperatures and photographed at room temperature, the results of X-ray analysis corroborate the accepted equilibrium diagram of the system. This statement applies to alloys removed from the β-region.

The examination of the alloys at the temperature of annealing reveals several changes from the accepted diagram. The modifications needed below the transformation temperature are but slight. The present results place the limit of solubility of the γ-phase at 250° C. between 79 and 80 per cent. aluminium. This differs slightly from

Hanson and Gayler's diagram, but agrees with that of Tanabe. The range of solubility of the α-phase is found to be about the same as that given by Hanson and Gayler.

The more serious modifications occur above the transformation temperature. In the first place the X-ray data suggest that this temperature lies between 300° C. and 310° C., which is higher than that previously recorded by any of the investigators of this system. At temperatures above 300° C. the extent of the γ-phase is found to be much reduced, and what was previously regarded as pure γ-phase has been shown to consist of a mixture of the two face-centred cubic structures with slightly different parameters.

After this investigation was completed a paper by Schmidt and Wassermann * appeared in which it is stated that the compound Al_2Zn_3 does not exist, and that the β- and γ-phases at high temperatures are almost identical face-centred cubic lattices, being separated from one another by a gap of immiscibility. The present results confirm these statements.

The present results also show that the extent and position of the β-region are somewhat different from those given in previous diagrams. In order that the β-phase should extend to the composition suggested here it seems necessary that the solidus must have the shape given to it by Rosenhain and Archbutt, and by Bauer and Vogel, in the earlier diagrams, and by Isihara in a more recent publication.

Sources of error.—There are two main sources of error in the investigation ; these arise from the measurement of the temperature and from volatilization of zinc when the alloy is at high temperature for a long period. We have already referred to the uncertainty arising from the temperature measurement, which is due to the fact that the estimation of temperature is made from the current which passes through the heating coil. However careful the adjustments are so as to ensure that the junction of the thermocouple is exactly in the position on the axis of the coil where the X-rays strike the specimen, one is never certain that the same conditions obtain when the specimen is being exposed as when the thermo-

* Schmidt and Wassermann, *Metallwirtschaft*, xi. p. 386 (1932).

couple was in position inside the coil, and the calibration of the ammeter was carried out. We made several observations of the temperatures under various conditions, from which it was concluded that the temperature could be estimated by this method to within $\pm 5°$ C.

The second source of error, namely, loss of zinc by volatilization, is more serious, as it may affect the final result in various ways. The general procedure was to analyse a portion of the powder prepared from the ingot and to mount some of this powder on the fibre for the X-ray exposure. The amount used on the fibre was insufficient to carry out an accurate chemical analysis, and even if the composition of the heated specimen could be determined accurately, it could not be guaranteed that the composition found represented that of the surface granules which are mainly responsible for the X-ray reflexions. In this connexion we may refer to a result obtained with the alloy AgMg in a previous investigation *. This alloy, when lightly etched, yielded a spectrum corresponding to pure silver. The same effect may possibly occur by the volatilization of one of the components of an alloy.

But there are other considerations which are somewhat reassuring that the above effect does not, in the present investigation, produce serious errors. One is that the lines in all the photographs taken at high temperatures are very sharply defined. If a change in composition were taking place in the reflecting layers we should expect to find the lines losing definition. Another fact bearing on this emerged from an investigation on the interdiffusion of zinc and copper, when it was found that below the melting-point of zinc, interdiffusion takes place exceedingly slowly, and it is to be expected that the reverse process of volatilization takes place equally slowly below this temperature (416° C.); the observations recorded in this investigation were mainly conducted at temperatures below the melting-point of zinc.

An attempt was made to estimate the amount of volatilization of zinc by heating sufficient quantities of powders of several alloys spread in thin layers on glass sheets in a furnace through which a slow current of nitrogen was passed as in the actual experiment when

* Owen and Preston, Phil. Mag. ii. p. 1266 (1926).

the specimen was exposed to the X-rays. Chemical analysis before and after the operation, which was carried out at 350° C. for 10 hours, showed that the loss of zinc amounted to 0·2 and 0·6 per cent. for alloys containing 25 and 60 per cent. aluminium respectively. But as already stated, this did not give definite information concerning the surface layer of the granules exposed to the X-rays, and in any case the conditions of experiment were not exactly the same as those obtaining when the exposure was made.

To improve the method it is desirable that the time of exposure be so diminished that no appreciable amount of volatilization can take place, and that enough powder be irradiated to allow a chemical analysis to be made on the actual specimen. It would also be a step forward if the investigation could be continued with a precision camera. The width of the lines would then provide a severe test on the amount of volatilization taking place. Now that the structures of the various phases have been determined, it is intended to continue the investigation with a modified precision camera, suitable for high temperature work, when it is hoped that the exposures may be reduced and the accuracy of measurement increased.

Summary.

An account is given of a preliminary survey of the aluminium-zinc system, in the course of which alloys covering a wide range of composition have been examined by the powder-spectrum method. It was found that only alloys below the eutectoid transformation temperature could be investigated by quenching from the desired temperature. These alloys were examined with both spectrum and precision cameras. The results showed that at 250° C. the system consists of the following regions : (1) α-phase (close-packed hexagonal structure) consisting of alloys which contain less than about 2 per cent. aluminium by weight ; the atomic volume of the α-phase alloys changes from 15·109 Å. for pure zinc to 15·164 Å. for the alloy saturated with aluminium. (2) $(\alpha+\gamma)$ region extending from about 2 per cent. to 80 per cent. aluminium. (3) γ-phase (face-centred cubic structure), consisting of alloys which contain more than 80 per cent. aluminium. The parameter of the γ-phase changes from

4·0406 Å. for pure aluminium to 4·0345 Å. for an alloy containing 80 per cent. aluminium.

To investigate alloys above the eutectoid transformation a special technique was developed by which X-ray spectrum photographs could be taken at high temperatures. The structure of alloys varying in composition from pure zinc to pure aluminium have been investigated at different temperatures ranging from 290° C. to 450° C.

The transformation temperature is found to lie between 300° C. and 310° C., which is higher than that recorded by previous investigators.

The β-phase is a solid solution having a face-centred cubic structure. At 375° C. it extends from 19 to 45 per cent. aluminium, the corresponding parameters being 4·016 Å. and 4·058 Å.

In the $(\beta+\gamma)$ region two face-centred cubic lattices of different parameters exist together.

At the higher temperatures the parameters of the γ-phase alloys indicate a much smaller range of solubility of zinc in aluminium than that given in most of the thermal diagrams hitherto published.

The results of X-ray analysis closely resemble the results of Hanson and Gayler and of Tanabe for alloys quenched from high temperatures in regions of the equilibrium diagram removed from the β-region, but there seem to be definite departures from the diagram when the alloys are examined at high temperatures.

XXXV. *Electron Diffraction Experiments with Graphite and Carbon Surfaces.* *By* R. O. Jenkins, *A.R.C.S., B.Sc.* *

[Plates XV.–XVII.]

THESE experiments have been performed with various types of graphite surfaces with a view of determining its inner potential, if any, and of understanding the mechanism of graphite polish and lubrication. The behaviour of amorphous carbon when polished has also been studied to amplify X-ray and electron diffraction researches into the crystal structure of carbon.

* Communicated by Prof. G. P. Thomson, M.A., F.R.S.

The electron diffraction camera used in this research was of the type designed by Prof. G. P. Thomson for use with fast electrons *. A high tension supply, which gave about $\frac{1}{2}$ milliamp. at 30,000 volts, was used. This consisted of an induction coil with mercury make and break feeding a two electrode Metalix valve, the anode of which was connected through a water resistance to the cathode of the discharge-tube. A condenser of ·002 mfd. capacity was shunted from the valve anode to earth, while the voltage across the discharge-tube was measured by a spark-gap between two spheres whose diameter was 5 cm.

Theory.

The electron beam selected by the two slits in the anode hits the specimen surface at a small angle. Owing to their wave-length, $\lambda = \frac{h}{mv}$ (De Broglie), the electrons are diffracted at the crystal surface according to the Bragg relation $n\lambda = 2d \sin \theta$, where d is the distance between the Bragg planes and θ the angle of diffraction. Combining these two relations with the camera dimensions equation (i.) is obtained :

$$d = \frac{L\sqrt{150}}{x\sqrt{V}} \times 10^{-8} \text{ cm.}, \quad . \quad . \quad . \quad . \quad \text{(i.)}$$

where L is the length of the camera, V the voltage of the discharge, and x the distance of the diffracted spot from the undeviated beam.

If there is an inner potential the electron beam is refracted on entering the surface of the specimen and the diffracted spot takes up a different position on the photographic plate from that indicated by equation (i.). Bethe † has shown that in such cases

$$\mu = \sqrt{1 + \frac{\phi}{V}},$$

where ϕ is the inner potential and V the voltage of the discharge.

* Thomson and Fraser, Proc. Roy. Soc. vol. cxxviii. A, p. 641 (1930).
† Bethe, *Naturwissenschaften*, xv. p. 787 (1927) ; xvi. p. 333 (1927).

Using this relation together with the Bragg and De Broglie relations the following equation may be derived :

$$x^2 = x_0^2 - \frac{4\phi L^2}{V}, \quad \ldots \quad \text{(ii.)}$$

where x_0 is the theoretical distance of the spot from the undeflected position as calculated from equation (i.) and x is the observed distance. This refraction effect only alters the component distance in a plane perpendicular to the surface of the specimen.

To obtain refraction the surface must be very flat, with no projections more than a few atoms high, so that the electron beam enters and leaves the crystal through the same or a parallel lattice plane. If there are projections the electron beam will pass through these, and a transmission pattern without any refraction effect will be observed.

Results with Natural Graphite.

Diffraction patterns due to large flakes of natural graphite occurring in a quartz formation have been photographed and measured. These show a structure agreeing with that assumed by Debye and Scherrer *, and also an inner potential which has been calculated.

The main cleavage plane which formed the surface of the specimen consists of carbon atoms at the corners of hexagons. The electron beam may have two positions symmetrical to this surface :

(i.) perpendicular to the hexagon sides ;

(ii.) parallel to the hexagon sides.

Photographs were taken with the crystal in both these positions. Owing to the fact that the cleavage surface was not a perfect plane, but was slightly convex, the pictures obtained show a series of orders of the (002) spacing along a line perpendicular to the shadow of the edge of the crystal. This is the equivalent of a rotation picture. Rows of side-spots were also obtained with one or two faint Kikuchi lines, and no trace of Kirchner-Raether surface lines, showing that the spots were true Bragg spots (Pl. XV. figs. 1 & 2).

* Debye and Scherrer, *Phys. Zeit.* xviii. p. 297 (1917).

The central row of spots showed a distinct refraction effect. To obtain the value of the inner potential the square of the distance between the diffracted spot and the undeflected spot was plotted against the square of the order number. From equation (ii.) it will be seen that the slope of the resulting straight-line graph should give the square of the distance between the first-order spot and the undeflected spot if no refraction had taken place. The intercept on the y-axis is the quantity $\frac{4\phi L^2}{V}$, from which the value of ϕ, the inner potential, was obtained. By substituting the square root of the slope of the graph for x in equation (i.) the (002) spacing was obtained.

The perpendicular distance between the rows of side-spots and the centre row of spots was due in azimuth (i.) to a lattice distance of $\frac{3}{2}a$, where a is the side of the hexagon, while in azimuth (ii.) the lattice spacing is $\sqrt{\frac{3}{2}}a$.

Any possibility of the voltage being inaccurate was eliminated owing to the fact that two rings appeared on each plate, due to very small fragments of graphite on the surface of the specimen. These rings corresponded exactly to the lattice spacings in graphite which give the strongest rings in X-ray pictures.

The following table gives a summary of the plates taken, using natural graphite :—

Azimuth.	Discharge voltage (K.V.).	Calculated (002) spacing (Å.U.).	Inner potential (volts).	Hexagon side (Å.U.).
1.....	28·5	3·38	10·7	1·44
1.....	36·8	3·40	10·9	1·44
1.....	33·1	3·41	10·4	1·50
1.....	29·6	3·38	10·6	1·44
1.....	38·4	3·36	10·8	1·40
2.....	39·0	3·47	10·4	1·43
2.....	44·2	3·39	11·1	1·42
2.....	43·0	3·41	10·8	1·44

The mean values for the above figures are as follows :—

(002) lattice spacing	3·40Å.U.
Hexagon side a	1·44Å.U.
Inner potential	10·7 volts.

The latest values for the first two quantities according to Ewald and Herrmann in Landolt and Börnstein's tables are 3·35 Å.U. and 1·43 Å.U. The previous value due to Debye and Scherrer for the first quantity was actually 3·40 Å.U. As a matter of interest the inner potential was also calculated from the data, assuming the value 3·35 Å.U. The value so obtained for the inner potential was 11·0 volts.

An additional measurement of the hexagon side was obtained by a transmission picture through a very thin flake of graphite, which accidentally was bent up from the edge of one of the specimens. This gave a pattern which consisted of spots at the corners of a series of rhombi with angles 60° and 120°. The distance between adjacent spots on the pattern corresponds to a lattice spacing of $\frac{3}{2}a$ (a=the hexagon side). The following details of one of the plates gives a value for a:

Voltage of discharge 41·0 KV.
Rhombus side on photograph 1·13 cm.
Lattice spacing deduced $= \frac{3}{2}a = 2{\cdot}15$ Å.U.
Hence $a = 1{\cdot}43$ Å.U.

Graphite and Carbon Surfaces.

Polycrystalline Graphite Surfaces.

Graphite surfaces of a polycrystalline and unorientated nature were prepared and their diffraction patterns photographed. A piece of graphited arc electrode was rubbed on ground glass, kept wet with absolute alcohol, until a small amount of fine graphite powder was obtained. This was mixed with a drop of alcohol and poured on to a small flat piece of ground-glass. The graphite and alcohol was then spread evenly by placing another piece of ground-glass over the top of the mixture and slowly drawing it off the surface of the first piece. When the alcohol had evaporated the glass was left with an even coating of graphite. Using this as a specimen, a good ring pattern showing no orientation was obtained. The lattice spacings corresponding to each ring were calculated, and were in good agreement with those obtained by Hull * using X-rays (Pl. XVI. fig. 3).

A specimen was prepared in a similar fashion using colloidal graphite suspended in water (marketed as

* Hull, Phys. Rev. x. p. 692 (Dec. 1917).

Aquadag by E. G. Acheson, Ltd.) instead of the powder and alcohol as previously. A similar diffraction pattern was obtained, except that the rings were not quite so sharp as with the previous specimen. This was due to the smaller crystal size having reduced the resolving power. From the reduction in resolving power the minimum crystal size of the colloidal graphite was of the order of 150 lattice spacings, or 60 millimicrons.

An interesting point concerning these ring patterns was the appearance of the (002) ring. F. Trendelenburg * only obtained this very faintly with electron diffraction, using a transmission arrangement. In the case of the specimen made with ordinary graphite this ring was only just visible, but in the case of the Aquadag specimen it appeared quite strongly, showing slight orientation of these planes in the surface of the specimen.

Polished Graphite Surfaces.

Polishing of these surfaces was then effected by rubbing gently with a pad of cotton-wool, giving only a dozen strokes. The diffraction pattern was then completely altered, the rings having almost disappeared, leaving a central row of strong diffuse spots corresponding to the orders of the cleavage lattice plane, and also two faint series of side-spots in rows parallel to the central row (Pl. XVI. fig. 4). The spots actually were arcs of circles subtending about 10° at the central spot. This pattern was due to the crystals all having orientated into a position with their main cleavage plane in the plane of the specimen surface. The rows of side-spots were analogous to the inner rows obtained in the single crystal work. The rows nearer the centre were due to the same planes which gave side-spots in azimuth (i.), while the outer row corresponded to those in azimuth (ii.).

Owing to the surface not being perfectly flat the refractive-index effect was hardly observable. The (002) spacing calculated from the central orders was, however, about 4 per cent high for the first order, decreasing with increasing order. This would be due to an effective inner potential of a small fraction of a volt.

From the diffuseness of the spot it was apparent that polishing had reduced the crystal size considerably as well

* F. Trendelenburg, 24 Feb. 1933, *Naturwissenschaften*, viii. p. 176 (1933).

as orientating the crystals. The approximate thickness of the crystals after polishing, as deduced from this diffuseness, was 100 Å.U. Diffraction photographs were taken with a specimen made by pencilling a piece of ground-glass with a graphite arc electrode, and exactly similar patterns were obtained.

Another polished graphite surface was made by rubbing a piece of this electrode on ground-glass moistened with alcohol till a flat surface was obtained. A final polish was given to the electrode surface with the ground-glass dry, leaving the graphite with a mirror surface apart from slight pits due to the underlying grain structure. The diffraction pattern from this specimen was similar in every respect to the other polished graphite surfaces. Polishing was then continued for an hour on dry ground-glass. The diffraction pattern then showed that the crystal size had been further reduced to about 25 Å.U., while the orientation was still quite marked.

Polish on Amorphous Carbon.

Debye and Scherrer * originally stated that amorphous carbon was in reality graphite with a very small crystal size. The effect of polish on amorphous carbon was therefore tried, to see if it would behave in any way analogous to graphite. A piece of amorphous arc carbon was polished on ground-glass for the same time as the first arc electrode specimen. A flat mirror surface was obtained, though not quite so bright as with graphite. The diffraction pattern obtained from this specimen showed three strong diffuse rings corresponding to the strongest ones in graphite patterns, but showing practically no selective orientation as in the case of polished graphite with a similar crystal size (Pl. XVII. fig. 5).

Polishing was continued for about an hour on dry ground-glass, and a diffraction pattern again taken. There had been no reduction in crystal size as deduced from the width of the rings, but the orientation of the cleavage plane in the plane of the specimen had appeared to a marked degree, though not quite as complete as in the case of graphite (Pl. XVII. fig. 6).

The explanation which seems most likely is that the grains of amorphous carbon consist of aggregates of very

* *Phys. Zeit.* xviii. p. 300 (1917).

small graphite crystals (of the order of 100 Å.U. thickness) bound together fairly tightly. The initial polish only smooths the surface of the specimen without damaging these aggregates, which would have no tendency to selective orientation. The subsequent polishing knocks the small graphite crystals out of the aggregates without reducing the crystal size. The small crystals, being similar to graphite, tend to orientate with their cleavage plane in the plane of the specimen. Thus, when the final diffraction pattern was taken the surface layer was composed almost entirely of these small crystals and gave a pattern similar to graphite.

Diffraction patterns exactly similar to the unorientated carbon rings were obtained from a piece of ground-glass smoked in a benzene flame, and also from a piece of chemists' charcoal smoothed on ground-glass.

Experiments with Oildag.

E. G. Acheson, Ltd., claim that if a metal bearing surface is lubricated with oil containing colloidal graphite in suspension an adsorbed graphite film is formed on the bearing surfaces which reduces friction losses, and, by stopping metal-to-metal contact, prevents metal "picking up" from the surfaces. While mechanical tests substantiate the claims of better lubrication, the actual existence and state of such an adsorbed film can only be found by an electron diffraction method. With this aim experiments were made using Oildag as supplied by E. G. Acheson, Ltd.

A specimen of Swedish iron had its face ground flat and then polished on progressively finer grades of emery-paper, and a flat iron table 2 inches in diameter was prepared in a similar manner. Keeping the table lubricated with Oildag, the specimen was rubbed backwards and forwards for about three hours. The specimen was then cleaned thoroughly with three washings of benzene, while the friction face was also swabbed with cotton-wool soaked in benzene. Diffraction patterns showed both graphite and iron rings. Although the strongest iron and graphite rings were not resolvable, the relative intensities of the strong rings and the occurrence of certain fainter rings showed that an adsorbed graphite surface had been formed on the metal. Further washings

in alcohol and ether failed to remove this film, as the graphite ring system was not eliminated from the pattern.

A similar film was formed on a piece of polished nickel. In this case the strong graphite rings were resolvable from those due to nickel. These films of graphite were of a crystal size comparable with the size of the crystals in the colloidal suspension in oil.

To obtain some idea of the behaviour of such a "graphoid" film under conditions of heavy stress or inadequate lubrication these surfaces were given a hard rubbing with a pad of clean dry cotton-wool. Diffraction patterns taken of the modified surfaces showed that the rings due to graphite had broadened and had a considerable tendency to strengthen towards the centres in the case of those due to orders of the (002) spacing, while the rings due to the metal had been nearly suppressed.

This would seem to indicate that under conditions of stress the film covers the metal entirely, while the crystals are reduced in size. At the same time the crystals tend to orientate, so that the main cleavage planes are in the plane of the specimen. The film then prevents metal-to-metal contact, while the slip between the two bearing surfaces takes place along the cleavage planes of the graphite rather than at the metal surface or in the metal itself.

Summary.

From the work that has been described the following facts have been deduced.

Natural graphite has an inner potential of 10·7 volts. This value, assuming the X-ray value for the (002) spacing, becomes 11·0 volts.

Any attempt to polish a graphite surface causes the crystals to take up an orientated position with the main cleavage plane (001) in the plane of the specimen, as well as reducing the crystal size.

In the case of carbon the polishing breaks up the aggregates of very small graphite crystals comprising the grains of carbon, and only after the surface is largely composed of these small crystals broken off from the aggregates does the usual orientation appear. As these crystals are already so small very little reduction in size takes place during polishing.

Finally, the existence of adsorbed graphite films on metal has been proved, and that friction reduces crystal size and causes orientation of the graphite crystals in this layer has also been shown.

In conclusion, I would like to express my appreciation to Professor G. P. Thomson, F.R.S., who suggested the subject for research and made many valuable suggestions in the course of the work.

The Imperial College of Science and Technology, London.
November 1933.

XXXVI. *The Structure of Oxide Films on Nickel.* *By* G. D. Preston, *B.A.* (*From the National Physical Laboratory* *.)

THIN films of nickel oxide, separated from the metal by electrolytic corrosion, have been examined by the electron diffraction method by Darbyshire †, who found that the films were structurally identical with nickel monoxide in massive form. The diffraction pattern corresponded with the usual face-centred cubic crystal lattice of side 4·17 Å. In the present investigation the oxide film has been examined without removing it from the surface. It is evidently a matter of some importance to know whether the anodic corrosion alters the structure of the film, and as a result of these experiments it appears that in the case of nickel the detached film has the same structure as the film on the metal.

Specimens were prepared by bending nickel sheet 0·12 mm. in thickness round three sides of a square section rod about 2 cm. in length and 0·4 cm. side. One side of the bent sheet was polished on a medium grade emery paper until flat, the scratches running along the length of the face. The metal rod was then removed and the nickel inserted in the holder of the electron diffraction apparatus, which held the sheet at one end by a small screw. The end remote from the clamp

* Communicated by Sir J. E. Petavel, K.B.E., D.Sc., F.R.S.
† Trans. Faraday Soc. vol. xxvii. p. 657 (1933).

was then inserted in a small hydrogen flame until about 0·5 cm. of the sheet was red hot. This treatment results in the production, about the centre of the specimen, of a system of interference fringes. Close to the clamp the metal is apparently unchanged, and about 0·5 cm. along the specimen a faint yellow tint is apparent, which changes in a distance of 4 mm. to a blue tint, and then to grey. A second system of colours narrower than the first then appears, and is followed by a region of blackness.

Specimens prepared in the above manner have been examined at different parts of the interference pattern. To facilitate the placing of the specimen in the electron beam one of its sides was covered with a little calcium tungstate. When the specimen was moved in the apparatus the fluorescence of this side showed the point at which the electron beam struck it. The interference fringes were roughly perpendicular to the long axis of the specimen, so that the narrow electron beam could be brought approximately on to any desired part of the system of interference colours.

No diffraction rings could be observed on the fluorescent screen in the electron diffraction apparatus, nor could any diffuse scattering be observed. The proper adjustment of the specimen in the beam was thus rather difficult, and had to be carried out by moving it perpendicularly to its prepared surface until the electron beam was partly obscured, and then rotating it through a small, angle. In a preliminary series of exposures it was found that diffraction lines of uniform intensity extending over nearly a semicircle could be photographed. As no orientation of the film was present the apparatus was fitted with a diaphragm, so that strips 2 cm. in width of the pattern were received in the photographic plate. Five such exposures could be made successively without refilling the camera. Imperial ("Special") lantern plates have been used.

Tables I., II., and III. contain part of the results obtained in one series of exposures. The first column of Table I. gives the values of $\sin\theta$ for a photograph from the "white," *i. e.*, apparently unaltered metal. In the second column are the corresponding values of the interplanar spacings d. To these have been assigned the indices hkl listed in the third column, and the last

column contains the values of the crystal parameter calculated from each line by the relation

$$a = d\sqrt{h^2+k^2+l^2}.$$

The mean value 3·50 Å agrees within the limits of error with the parameter of nickel as determined by X-ray investigation, the accepted value being 3·517±0·001Å *. Reflexions from the planes (222), (400), and (331) are absent. The first, third, and last lines have spacings closely agreeing with the lines (200), (311), and (333) of NiO (see Table III.), but it seems highly probable that we have here diffraction by the scratched nickel surface as observed by Germer †. Table II. contains

TABLE I.

White 64 K.V. $\lambda = 0{\cdot}0469$ Å.

I.	Sin θ.	d.	hkl.	a.
		Å.		Å.
m	0·0116	2·02	111	3·50
w	$0{\cdot}0137_5$	$1{\cdot}70_5$	200	3·41
m	$0{\cdot}0188_5$	1·24	220	3·52
m	0·0220	$1{\cdot}06_5$	311	3·53
w	0·0297	$0{\cdot}78_9$	420	3·53

Mean $a = 3{\cdot}50 \pm 0{\cdot}05$ Å.

a similar list of observational data obtained from the yellow part of the oxide film. The values of "a" agree, within about 1 per cent., with a face-centred cubic structure of side 4·11 Å. This figure agrees with that found by Darbyshire for the spacing of the film removed from the metal by electrolytic corrosion. It is about 2 per cent. smaller than the value usually given for NiO, but, although this is possibly due to some inaccuracy in the voltage measurement, the agreement between Darbyshire's figure and that here obtained may have some significance. Table III. contains similar data for a photograph from the blue region of the film.

* Neuberger, *Gitterkonstanten*, 1931, *Z. f. Krist.* lxxx. p. 103 (1931).
† Phys. Rev. xliii. p. 724 (1933).

TABLE II.

Yellow 62 K.V. $\lambda = 0{\cdot}0477$ Å.

I.	Sin θ.	d.	hkl.	a.
		Å.		Å.
w	0·01160	$2{\cdot}04_5$	200	$4{\cdot}09_5$
s	0·0162	$1{\cdot}46_5$	220	4·15
w	$0{\cdot}0195_5$	$1{\cdot}21_5$	311	4·03
			222	4·21
s	0·0261	0·910	420	4·07
m	$0{\cdot}0282_5$	0·841	422	4·12
w	0·0348	0·682	600	$4{\cdot}09_5$
			442	
w	0·0384	0·619	622	4·10

Mean $a = 4{\cdot}11 \pm 0{\cdot}05$ Å.

TABLE III.

Blue 62 K.V. $\lambda = 0{\cdot}0477$ Å.

I.	Sin θ.	d.	hkl.	a.
		Å.		Å.
w	$0{\cdot}0101_5$	2·34	111	$4{\cdot}05_5$
m	0·0116	$2{\cdot}04_5$	200	$4{\cdot}09_5$
m	$0{\cdot}0162_5$	1·46	220	4·13
w	$0{\cdot}0195_5$	$1{\cdot}21_5$	311	4·03
			222	4·21
s	$0{\cdot}0260_5$	0·912	420	4·08
m	$0{\cdot}0282_5$	0·891	422	4·12
w	0·0304	0·781	333	4·06
			511	
w	0·0348	0·682	600	$4{\cdot}09_5$
			442	
w	$0{\cdot}369_5$	0·643	620	$4{\cdot}06_5$
w	0·0384	0·619	622	4·10

Mean $a = 4{\cdot}10 \pm 0{\cdot}04$ Å.

Similar results have been obtained from other parts of this specimen. The second yellow band gave diffraction lines of the oxide with a spacing of 4·00 Å. Another specimen heated in a small gas flame gave the same type of evidence, the spacing being about 4·10 Å. In this case a photograph from part of the specimen recorded as " white " gave lines of the oxide pattern with a spacing of 4·05 Å.

The evidence described above shows that the coloured films on heated nickel consist of NiO and that the oxide film is detectable by the electron diffraction method when it has a thickness insufficient to produce a visible coloration. The limit of the yellow in the interference pattern cannot be accurately determined, but it appears that the film extends beyond the point at which it ceases to show interference colours.

If we assume that the colours exhibited by the oxide film are produced by interference in a thin plate, and that they are viewed at normal incidence, then the thickness of the film at the yellow may be estimated. The refractive index of NiO for blue light is 2·39 *, so, taking a wave-length of 4000 Å., the thickness ($\lambda/2\mu$) is approximately 800 Å., or about 200 crystal units. The measurements quoted above are not sufficiently precise to show any variation of spacing with film thickness even if such variation should be present in films of so many atoms thickness.

Summary.

Films of nickel oxide prepared on the surface of a nickel sheet so as to produce a number of parallel interference bands have been examined by the electron diffraction method. The crystal structure of the film is found to be identical, within the limits of error of observation, with massive NiO having a rock-salt type of lattice of approximately 4·10 Å. parameter.

I have great pleasure in acknowledging the assistance of Dr. L. L. Bircumshaw during these experiments, and of Mr. G. Glaysher in the design and construction of the apparatus employed. My thanks are also due to Dr. C. H. Desch for his interest in and encouragement of this work.

10th October, 1933.

* Groth, ' Chemische Krystallographie,' i. p. 71.

XXXVII. *Raman Effect in the Study of Chemical Reactions.* *By* S. Parthasarathy *.

[Plate XVIII.]

1. Introduction

THE Raman Effect has found much useful application in the elucidation of molecular structure and also in the following up of some physico-chemical changes, as examples of which can be cited the transformation of α-hydrogen into the β-variety, electrolytic dissociation, and thermal dissociation. So far, however, it has not been used in the study of chemical reactions, and the present paper is one describing three typical chemical reactions, namely, (1) one where the reaction is reversible and the equilibrium is therefore displaceable with temperature, (2) another where one of the resulting products of reaction attacks the original substance and two wholly different products are obtained as a consequence, and (3) a third where the reaction is unidirectional. The above are exemplified in (1) acetic acid and ethyl alcohol, (2) ethyl alcohol and excess of acetic anhydride, and (3) acetic anhydride and water.

Incidentally some chloro-compounds have been included for investigation.

2. The Raman Spectra.

The method for obtaining the Raman spectra is the one after Wood, namely, bringing the mercury lamp close to the tube of liquid and focussing the scattered light on to the slit of spectrograph. Special precautions were as usual taken to avoid the extraneous light. Both the Fuess glass spectrograph and Hilger's constant deviation spectrograph were used at different times.

The frequencies obtained in each case are given below. The letters *a*, *b*, *c*, *d*, *e*, *f*, *g*, and *h* indicate the exciting lines of the mercury arc, and stand respectively for 3650·1, 3654·8, 3662·9, 4046·6, 4077·8, 4339·2, 4347·5, and 4358·3 Å.U. B and D stand for broad and diffuse lines respectively.

* Communicated by the Author.

3. Results.

1. *Acetic acid.*—242 ($\frac{1}{2}$) band *h* ; 446 (1) *h* ; 602 (1) *dh* ; 621 (3) *dh* ; 872 (2) *dh* ; 893 (5) *dh* ; 1014 (1) *h* ; 1221 (1) *dh* ; 1278 (1) *dh* ; 1366 (2) *dh* ; 1433 (3) D *dh* ; 1663 (2) *h* ; 2944 (8) *abdeh* ; 2996 (1) *dh* ; 3031 (1) *dh*.

It is found that the Raman lines in this acid are comparatively sharper than those in formic acid. The band at $\triangle\nu$ 242 is reported for the first time. The Raman spectrum of this liquid is also obtained at a temperature of 95° C., and the two frequencies 2996 and 3031 are found to get diffuse.

2. *Acetic anhydride.*—352 (4) *h* ; 417 (1) *h* ; 526 (1) *dh* ; 556 (2) *dh* ; 626 (2) *dh* ; 665 (5) *dh* ; 778 (3) *dh* ; 808 (5) *dh* ; 888 (2) B *h* ; 1014 (4) *dh* ; 1438 (6) D *dh* ; 1777 (4) *h* ; 1817 (4) D *h* ; 2941 (10) *dh* ; 3003 (6) *dh* ; 3063 (6) *dh*.

This liquid has been investigated by Thatte and Ganesan. Some close doublets have, however, been recorded as unresolved lines by these authors.

3. *Ethyl acetate.*—379 (5) *h* ; 634 (6) *dh* ; 788 (1) *dh* ; 842 (4) *dh* ; 924 (1) B *dh* ; 998 (2) *dh* ; 1043 (2) *dh* ; 1110 (3) *dh* ; 1398 (0) *h* ; 1447 (4) *dh* ; 1735 (4) *h* ; 2881 (3) *dh* ; 2935 (8) *abdh* ; 2971 (4) *dh*.

There is good agreement between the values given above and those obtained by Dadieu and Kohlrausch and Ghosh and Kar for this liquid.

4. *Ethyl alcohol.*—270$\pm$40 (1) band *h* ; 427 (1) *h* ; 885 (4) *deh* ; 1049 (4) *defgh* ; 1272 (2) *dh* ; 1448 (3) *dh* ; 2882 (3) *dh* ; 2928 (6) *abdh* ; 2971 (4) *dh* ; 3330$\pm$20 (2) band *a*.

The band at $\triangle\nu$ 270 is reported for the first time.

5. *Chloral.*—204 (2) *h* ; 248 (2) *h* ; 275 (3) *h* ; 322 (2) *h* ; 383 (1) *h* ; 406 (1) *h* ; 444 (8) *dh* ; 504 (0) *h* ; 554 (0) *h* ; 622 (2) *dh* ; 730 (2) *dh* ; 851 (2) *dh* ; 993 (0) *h* ; 1358 (1) *dh* ; 1568 (1) *h* ; 1757 (2) *h* ; 2862 (4) D *d*.

6. *Chloral hydrate (solid).*—223 (2) *h* ; 272 (2) *h* ; 313 (2) *h* ; 421 (4) *h* ; 513 (1) D *h* ; 590 (4) *h* ; 726 (0) *h* ; 1007 (2) *h* ; 1555 (1) *h* ; 1675 (1) *h* ; 2947 (2) *d*.

Chloral and chloral hydrate have been investigated by other authors, and their results are in good agreement with those reported here. Some new frequencies in both of them are, however, recorded by the author.

7. *Monochloracetic acid* (*solid*).—242 (3) *h* ; 294 (3) *h* ; 333 (3) *h* ; 426 (4) *h* ; 575 (4) *h* ; 648 (0) *h* ; 789 (2) *h* ; 991 (1) *h* ; 1235 (2) *h* ; 1366 (1) band *h*.

8. *Trichloracetic acid* (*solid*).—250 (1) *h* ; 286 (1) *h* ; 327 (1) *h* ; 453 (2) *h* ; 600 (2) *h*.

Ghosh and Kar have investigated these two acids in concentrated solution *.

4. Reactions, and Discussion of their Results.

(a) *Ethyl Alcohol and Acetic Acid Mixtures.*

The Raman spectra of a simple mixture alone and then of an esterified mixture are obtained and compared with the result for pure acid and pure alcohol. For preparing the esterified mixture the simple mixture in the right proportion of acid and alcohol was kept in a flask over a water-bath with a reflex condenser for about ten hours, when the reaction was supposed to be complete.

The main frequencies, with the changes observed in them, are given below. The numbers within brackets give the relative intensities of the lines in the same spectrogram.

Acid	..	621	893	1433 D.	1663	2944
Alcohol	..	..	885	1448 (sharp)	..	2928
Mixture	...	628 D	888	1445 (sharp)	1710	2928
Esterified mixture.	379 (5)	632	886 (10) 842 (4)	1448	1720	2937
Pure ester	379 (5)	634	842 (4)	1447	1735	2935

(In the case of C-H frequencies only the central intense line is given in the above cases, except for acetic acid, for which there is only one in that region.)

It will be noted from the above table that the main change is observed in the characteristic frequency of the C=O bond. The value increases from 1663 in the acid to 1710 even in the simple mixture, and undergoes

* For references see "Bibliography on the Raman Effect" by S. C. Sirkar in the Indian Journ. of Physics, vii. p. 431 (1933), together with an earlier one, Indian Journ. of Physics, v. p. 257 (1931).

a further increase as we pass on to the esterified mixture. It is interesting to note that, although such a marked change occurs in the position of this line on merely mixing the two liquids, the strong lines 379 and 842 which are characteristic of pure ester do not make their appearance until the mixture is esterified. It is therefore suggested that before the stable binding between the alcohol and the acid with the formation of the COC group characteristic of the ester takes place an intermediate stage in the reaction occurs in the simple mixture itself, resulting in some kind of a loose addition between the two molecules at the C=O group. It may also be noted here that the C=O frequency in the esterified mixture is distinctly less than the corresponding value in the pure ester, a result which may be attributed to the presence of water in the former.

Indeed, the mixture is simply an addition compound, and not a stable one, as is evidenced by the absence of $\triangle\nu$ 379 in it, which is a characteristic frequency, representing the transverse oscillation of oxygen in the C-O-C group. And the nature of this compound is also supported by the non-appearance of the lower frequency of 842, characteristic of the C-C vibration in the ester.

Such a shift of 1735 in ester to 1720 in the esterified mixture is due to the fact that the latter contains water also. It is simply a question of the hydrolysis of the ester when it is expected to undergo changes. It is very striking to note here that, while addition of water to acetic acid enhances the C=O frequency, the same addition to ester lowers it. Probably this is connected with the fact that water functions in different ways in the two cases.

The amount esterified can be easily computed at any stage from the relative intensities of 842 and 886, bearing in mind at the same time that both alcohol and acid contribute to 886. In a particular case studied by the author after keeping the mixture under reflex for about ten hours the mixture was found to be esterified to about 40 per cent. only.

(b) *Acetic Anhydride and Ethyl Alcohol.*

The spectra of the pure liquids and of the mixtures in the molecular ratio 1 : 1 and 1 : 2 of the anhydride

and alcohol were obtained (see Pl. XVIII.). The spectrum of the first mixture showed characteristic lines of ethyl acetate by the shifting of $\triangle\nu$ 352 to 379, by the appearance of $\Delta\nu$ 841, in the shifting of 665 to 633, by the weakening of 808 and also the strengthening of $\Delta\nu$ 890, and appearance of the frequency 605, two very characteristic lines of acetic acid only and not of either of the two liquids taken, to anything in the order of intensity. The reaction has therefore proceeded to ethyl acetate and acetic acid. The second spectrogram shows unmistakably the greater strengthening of the frequency 891, with all the other characteristic lines of ethyl acetate. Since this mixture was made up by the further addition of alcohol to the first mixture evidently instead of more ester being formed an equilibrium mixture between the remaining acid and alcohol has been formed, and this is indicated by the more intense line of 891, since otherwise $\Delta\nu$ 842 will be much the more intense one. Both alcohol and acid give frequencies about this region with little difference in their values.

(c) *Acetic Anhydride and Water.*

The spectra were taken of the pure liquids and of mixtures of these in the molecular ratio 2 : 1 and 1 : 1. The most characteristic change is the sudden strengthening of $\Delta\nu$ 888, due to freshly formed acetic acid molecules. Another is the appearance of frequency 621, characteristic of the acid, while the Raman frequency 665 gradually tends to disappear in proportion as 621 makes its appearance. The measurement of relative intensities of two such lines in any mixture, as we have here, will enable us to measure the extent of reaction, and here of hydrolysis. Since the reaction is unidirectional the changes are gradual, all the frequencies of the anhydride being transformed slowly into those of acetic acid.

5. Conclusion.

One marked reaction is that of ethyl alcohol and acetic acid. Esterification can be followed up easily by a study of the intensities of certain characteristic frequencies. It may be pointed out here that the above furnishes us with a means of determining the equilibrium constant at any particular temperature; and it is

well known that when two such constants are determined at two different temperatures it is easy to evaluate the heat of reaction, entropy of reaction, etc. The method is limited only by the limitations and errors in the measurement of intensities of spectral lines. The author hopes to overcome these difficulties and study some more typical reactions quantitatively.

The author thanks Sir C. V. Raman, F.R.S., N.L., for facilities offered for work at the laboratory of the Indian Association for the Cultivation of Science, Calcutta. The above work was carried out over two years ago, but owing to some unavoidable delay it could not be published earlier.

2 Anand Building,
Mahim, Bombay.
14th July, 1933.

XXXVIII. *A Unified Field Theory.*—II. *Gravitation.* *By* D. MEKSYN, *Ph.D., D.Sc., Imperial College of Science, London* *.

§ 1. *Introduction and Summary.*

IN a previous communication we have suggested that a unified gravitational and electromagnetic field associated with two particles can be represented in an eight-dimensional space whose me ric satisfies Einstein's gravitational equations $G_{\mu\nu}=0$; and we have shown that, in fact, such space describes an electrostatic and constant magnetic fields.

The aim of this paper is to show that our equations provide the solution of two-body problem in the General Theory of Relativity. The obtained result is very similar to the classical one.

According to the latter the motion of gravitating particles M, m is equivalent to a uniform rectilinear motion of their centre of gravity, and a motion of a particle of reduced mass $\frac{m\mathrm{M}}{m+\mathrm{M}}$ in a gravitational field due to mass $\mathrm{M}+m$; we obtain exactly the same result.

* Communicated by Prof. R. H. Fowler, M.A., F.R.S.

I. The Metric of a Gravitational Field.

§ 2. *First Approximation.*

Einstein's gravitational tensor in its usual rotation is

$$G_{\mu\nu}=-\{\mu\sigma,\alpha\}[\rho\nu,\alpha]g^{\sigma\rho}+\{\mu\nu,\alpha\}[\rho\sigma,\alpha]g^{\sigma\rho}$$
$$+\tfrac{1}{2}g^{\sigma\rho}\left(\frac{\partial^2 g_{\rho\sigma}}{\partial x_\mu \partial x_\nu}+\frac{\partial^2 g_{\mu\nu}}{\partial x_\rho \partial x_\sigma}-\frac{\partial^2 g_{\mu\sigma}}{\partial x_\rho \partial x_\nu}-\frac{\partial^2 g_{\rho\nu}}{\partial x_\mu \partial x_\sigma}\right). \quad (1)$$

For the first approximation we need only the last term We shall show that the following form of ds^2 satisfies the equations (1):

$$\left.\begin{aligned} ds^2=&m\left(1-\frac{2M}{r}\right)dx_4{}^2-m\left(1+\frac{2M}{r}\right)(dx_1{}^2+dx_2{}^2+dx_3{}^2)\\ &+2.\frac{2Mm}{r}(dx_1dx_5+dx_2dx_6+dx_3dx_7+dx_4dx_8)\\ &+M\left(1-\frac{2m}{r}\right)dx_8{}^2-M\left(1+\frac{2m}{r}\right)(dx_5{}^2+dx_6{}^2+d_7{}^2),\\ r^2=&(x_1-x_5)^2+(x_2-x_6)+(x_3-x_7)^2, \end{aligned}\right\} \quad (2)$$

where m has the coordinates x_1, x_2, x_3, x_4.

We shall show that without the cross terms we cannot satisfy the gravitational equations, even in the first approximation.

Consider the equation $G_{11}=0$. We have

$$G_{11}=\tfrac{1}{2}g^{\sigma\rho}\left(\frac{\partial^2 g_{\sigma\rho}}{\partial x_1{}^2}+\frac{\partial^2 g_{11}}{\partial x_\rho \partial x_\sigma}-\frac{\partial^2 g_{1\sigma}}{\partial x\,\partial x_1}-\frac{\partial^2 g_{\rho 1}}{\partial x_1 \partial x_\sigma}\right), \quad (3)$$

and let the fundamental tensor be

$$\left.\begin{aligned} g_{44}=m(1-\alpha),\quad g_{11}=g_{22}=g_{33}=-m(1+\alpha),\\ g_{88}=M(1-\beta),\quad g_{55}=g_{66}=g_{77}=-M(1+\beta), \end{aligned}\right\} \quad (4)$$

Remembering that $\dfrac{\partial}{\partial x_1}=-\dfrac{\partial}{\partial x_5}$ we can easily show that the second term is equal to

$$\tfrac{1}{2}g^{\sigma\rho}\frac{\partial^2 g_{11}}{\partial x_\rho \partial x_\sigma}=-\tfrac{1}{2}\left(\frac{1}{m}+\frac{1}{M}\right)\left(\frac{\partial^2 g_{11}}{\partial x_1{}^2}+\frac{\partial^2 g_{11}}{\partial x_2{}^2}+\frac{\partial^2 g_{11}}{\partial x_3{}^2}\right).$$

We have now only to prove that the remaining terms are cancelled out.

The only terms that survive are those for which $g^{\sigma\rho}$ have like indices. We obtain accordingly the following expression:

$$\tfrac{1}{2}\Big(g^{11}\frac{\partial^2 g_{11}}{\partial x_1^{\,2}}+\ldots+g^{88}\frac{\partial^2 g_{88}}{\partial x_1^{\,2}}-g^{11}\frac{\partial^2 g_{11}}{\partial x_1^{\,2}}-g^{11}\frac{\partial^2 g_{11}}{\partial x_1^{\,2}}$$
$$-g^{55}\frac{\partial^2 g_{15}}{\partial x_1\partial x_5}-g^{55}\frac{\partial^2 g_{15}}{\partial x_1\partial x_5}\Big).$$

Making use of the values (4) for the g's we notice that the terms with the subscripts running from one to four are mutually cancelled out, as in the case of Einstein's theory; and we are left with the equation

$$\frac{\partial^5\beta}{\partial x_1^{\,5}}-\frac{1}{\mathrm{M}}\frac{\partial^2 g_{15}}{\partial x_1^{\,2}}=0,$$

whence

$$g_{15}=\mathrm{M}\beta.$$

It is clear that owing to symmetry we must also have $g_{15}=m\alpha$, whence we are led to the form (2).

The rest of the equations can be treated in a similar way.

§ 3. *Second Approximation.*

We need only the second approximation of the components g_{44}, g_{88}, g_{48}.

In order to find g_{44} we consider the equation $\mathrm{G}_{44}=0$. Written out in full it is

$$\left.\begin{aligned}\mathrm{G}_{44}=&-\tfrac{1}{4}g^{a\lambda}\Big(\frac{\partial g_{4\lambda}}{\partial x_\sigma}+\frac{\partial g_{\sigma\lambda}}{\partial x_4}-\frac{\partial g_{4\sigma}}{\partial x_\lambda}\Big)\Big(\frac{\partial g_{\rho\alpha}}{\partial x_4}+\frac{\partial g_{4\alpha}}{\partial x_\rho}-\frac{\partial g_{\rho 4}}{\partial x_\alpha}\Big)g^{\sigma\rho}\\&+\tfrac{1}{4}g^{\pi\lambda}\Big(\frac{\partial g_{4\lambda}}{\partial x_4}+\frac{\partial g_{4\lambda}}{\partial x_4}-\frac{\partial g_{44}}{\partial x_\lambda}\Big)\Big(\frac{\partial g_{\rho\alpha}}{\partial x_\sigma}+\frac{\partial g_{\pi\sigma}}{\partial x_\rho}-\frac{\partial g_{\rho\sigma}}{\partial x_\alpha}\Big)g^{\sigma\rho}\\&+\tfrac{1}{2}g^{\sigma\rho}\Big(\frac{\partial^2 g_{\rho\sigma}}{\partial x_4^{\,2}}+\frac{\partial^2 g_{44}}{\partial x_\rho\partial x_\sigma}-\frac{\partial^2 g_{4\sigma}}{\partial x_\rho\partial x_4}-\frac{\partial^2 g_{\rho 4}}{\partial x_4\partial x_\sigma}\Big)\end{aligned}\right\}\quad\ldots\quad(5)$$

In evaluating this expression we have to bear in mind that our next approximation is of the order $\frac{1}{r^2}$, and, hence, we need in our equations only terms of the order $\frac{1}{r^4}$; also, our tensor is independent of x_4 and x_8.

We consider separately the three terms.

First Term.—Multiplying out, we find

$$-\tfrac{1}{4}g^{\alpha\lambda}g^{\sigma\rho}\left(\frac{\partial g_{4\lambda}}{\partial x_\sigma}\frac{\partial g_{4\alpha}}{\partial x_\rho}-\frac{\partial g_{4\lambda}}{\partial x_\sigma}\frac{\partial g_{\rho 4}}{\partial x_\alpha}-\frac{\partial g_{4\sigma}}{\partial x_\lambda}\frac{\partial g_{4\alpha}}{\partial x_\rho}+\frac{\partial g_{4\sigma}}{\partial x_\lambda}\frac{\partial g_{\rho 4}}{\partial x_\alpha}\right). \quad (6)$$

To our order of approximation we need to retain only components of $g^{\mu\nu}$ with two like indices. The second term in (6) vanishes, because λ can be only 4 or 8, hence α must have the same values; but $\dfrac{\partial g_{\rho 4}}{\partial x_4}=\dfrac{\partial g_{\rho 4}}{\partial x_8}=0$; in the same way the second term vanishes. Interchanging in the fourth term the dummy indices σ and ρ for λ and α, we obtain that the fourth term is equal to the first one. Finally, (6) becomes

$$-\tfrac{1}{2}g^{\alpha\alpha}g^{\sigma\sigma}\frac{\partial g_{4\sigma}}{\partial x_\sigma}\frac{\partial g_{4\alpha}}{\partial x_\sigma}. \quad . \quad . \quad . \quad . \quad . \quad . \quad (7)$$

The only values that α can take are four and eight.

Making use of (2) we easily find that (7) is equal to

$$\frac{2(\mathrm{M}+m)^2}{r^4} \quad . \quad . \quad . \quad . \quad . \quad . \quad . \quad (8)$$

Second Term is equal to

$$-\tfrac{1}{4}g^{\alpha\lambda}g^{\sigma\rho}\frac{\partial g_{44}}{\partial x_\lambda}\frac{\partial g_{\rho\alpha}}{\partial x_\sigma}-\tfrac{1}{4}g^{\alpha\lambda}g^{\sigma\rho}\frac{\partial g_{44}}{\partial x_\lambda}\frac{\partial g_{\sigma\alpha}}{\partial x_\rho}+\tfrac{1}{4}g^{\alpha\lambda}g^{\sigma\rho}\frac{\partial g_{44}}{\partial x_\lambda}\frac{\partial g_{\rho\sigma}}{\partial x_\alpha}. \quad (9)$$

The second term in (9) is equal to the first one, as can be seen by interchange of dummy indices σ and ρ; and so the first two components become

$$-\tfrac{1}{2}g^{\alpha\lambda}g^{\sigma\rho}\frac{\partial g_{44}}{\partial x_\lambda}\frac{\partial g_{\rho\alpha}}{\partial x_\sigma}. \quad . \quad . \quad . \quad . \quad . \quad . \quad (10)$$

To evaluate (10) we notice that if $\lambda=1$ then $\alpha=1$, and ρ and σ can be either $\rho=\sigma=1$ or $\rho=\sigma=5$.

Continuing in the same way we find that (10) consists of twelve terms: and by making use of (2), we find that (10) is equal to

$$-\frac{2(m+\mathrm{M})^2}{r^4} \quad . \quad . \quad . \quad . \quad . \quad . \quad . \quad (11)$$

The term

$$\tfrac{1}{4}g^{\alpha\lambda}g^{\sigma\rho}\frac{\partial g_{44}}{\partial x_\lambda}\frac{\partial g_{\rho\sigma}}{\partial x_\alpha} \quad . \quad . \quad . \quad . \quad . \quad . \quad (12)$$

can also be easily evaluated. We notice that $\lambda=\alpha$, and

$$g^{\sigma\rho}\frac{\partial g_{\rho\sigma}}{\partial x_\alpha}=g^{\sigma\sigma}\frac{\partial g_{\sigma\sigma}}{\partial x_\alpha}=2\left(\frac{1}{m}+\frac{1}{\mathrm{M}}\right)\left(\frac{\partial}{\partial x_\alpha}\frac{2\mathrm{M}m}{r}\right). \quad . \quad (13)$$

Making use of (13) and (2), we find that (12) is equal to

$$\frac{2(m+\mathrm{M})^2}{r^4} \quad . \quad . \quad . \quad . \quad . \quad . \quad . \quad . \quad (14)$$

This is exactly equal and opposite to (11); or the second term in (5) vanishes.

Third Term.—The only surviving components are

$$\tfrac{1}{2}g^{\sigma\rho}\frac{\partial^2 g_{44}}{\partial x_\rho \partial x_\sigma} \quad . \quad . \quad . \quad . \quad . \quad . \quad . \quad (15)$$

Now let g_{44} be equal to

$$g_{44}=m-\frac{2\mathrm{M}m}{r}+\frac{\mathrm{A}}{r^2} \quad . \quad . \quad . \quad . \quad . \quad . \quad (16)$$

It is easily seen that for the second approximation $\frac{\mathrm{A}}{r^2}$, we must take $g^{\sigma\rho}$ with like indices, but in the terms

$$\frac{\partial^2}{\partial x_\rho \partial x_\sigma}\left(-\frac{2\mathrm{M}m}{r}\right)$$

we have to put not only $\rho=\sigma$, but also $\rho=1$, $\sigma=5$; $\rho=2$ $\sigma=6\ldots$; as, however, $g^{15}=g^{26}=g^{37}$, and $\frac{2m\mathrm{M}}{r}$ satisfies Laplace's equation all these terms vanish, and (15) becomes

$$-\tfrac{1}{2}\left(\frac{1}{m}+\frac{1}{\mathrm{M}}\right)\left(\frac{\partial^2}{\partial {x_1}^2}+\frac{\partial^2}{\partial {x_2}^2}+\frac{\partial}{\partial {x_3}^2}\right)\frac{\mathrm{A}}{r^2} \quad . \quad . \quad (17)$$

Combining (17) and (18), we obtain the equation

$$\tfrac{1}{2}\left(\frac{1}{m}+\frac{1}{\mathrm{M}}\right)\nabla^2\left(\frac{\mathrm{A}}{r^2}\right)=\frac{2(\mathrm{M}+m)^2}{r^4}, \quad . \quad . \quad (18)$$

or

$$\mathrm{A}=2m\mathrm{M}(m+\mathrm{M}). \quad . \quad . \quad . \quad . \quad . \quad (19)$$

To find g_{88} we have to solve the equation $\mathrm{G}_{88}=0$; but as (19) is symmetric in m and M we can see at once that the additional term in g_{88} will be equal to (19).

In order to find g_{48} we have to solve the equation $\mathrm{G}_{48}=0$. The solution of this equation is almost a complete repetition of the solution of $\mathrm{G}_{44}=0$ and need not

be given here. The final result is that the term in g_{48} is equal to

$$-\frac{2m\mathrm{M}(m+\mathrm{M})}{r^2}, \quad . \quad . \quad . \quad . \quad . \quad (20)$$

or, it is opposite to (19).

We obtain finally the following values of g_{44}, g_{88}, g_{48} to the second order of approximation.

$$\left.\begin{aligned} g_{44}&=m\left[1-\frac{2\mathrm{M}}{r}+\frac{2\mathrm{M}(m+\mathrm{M})}{r^2}\right]\\ g_{88}&=\mathrm{M}\left[1-\frac{2m}{r}+\frac{2m(m+\mathrm{M})}{r^2}\right]\\ g_{48}&=\frac{2m\mathrm{M}}{r}-\frac{2m\mathrm{M}(m+\mathrm{M})}{r^2} \end{aligned}\right\} . \quad . \quad . \quad (21)$$

II. Motion of two Particles.

§ 4. *Reduction of the Fundamental Form.*

From (2) and (21) it is easily seen that the fundamental form can be written as

$$\left.\begin{aligned} ds^2=&m(dx_4{}^2-dx_1{}^2-dx_2{}^2-dx_3{}^2)\\ &+\mathrm{M}(dx_8{}^2-dx_5{}^2-dx_6{}^2-dx_7{}^2)\\ &+\left[-\frac{2m\mathrm{M}}{r}+\frac{2m\mathrm{M}(m+\mathrm{M})}{r^2}\right](dx_4-dx_8)^2\\ &-\frac{2m\mathrm{M}}{r}[(dx_1-dx_5)^2+(dx_2-dx_6)^2+(dx_3-dx_7)^2] \end{aligned}\right\} . \quad (22)$$

We make the substitution:

$$\left.\begin{aligned} x_1-x_5&=x, & (m+\mathrm{M})\xi&=mx_1+\mathrm{M}x_5,\\ x_2-x_6&=y, & (m+\mathrm{M})\eta&=mx_2+\mathrm{M}x_6,\\ x_3-x_7&=z, & (m+\mathrm{M})\zeta&=mx_3+\mathrm{M}x_7,\\ x_4-x_8&=t, & (m+\mathrm{M})\tau&=mx_4+\mathrm{M}x_8, \end{aligned}\right\} . \quad . \quad (23)$$

Combining (22) and (23), we obtain finally the following expression for (22):

$$\left.\begin{aligned} ds^2=&(m+\mathrm{M})(d\tau^2-d\xi^2-d\eta^2-d\zeta^2)\\ &+\frac{m\mathrm{M}}{m+\mathrm{M}}\left\{\left[1-\frac{2(m+\mathrm{M})}{r}+\frac{2(m+\mathrm{M})^2}{r^2}\right]dt^2\right.\\ &\left.-\left[1+\frac{2(m+\mathrm{M})}{r}\right](dx^2+dy^2+dz^2)\right\} \end{aligned}\right\} . \quad (24)$$

The expression (24) represents a fundamental form of a mass $(m+M)$ moving with a uniform rectilinear velocity, and a particle of mass $\frac{mM}{m+M}$ moving in a gravitational field due to mass $(m+M)$.

The expression in brackets is Einstein's fundamental form for a mass $m+M$, and so it will give us the correct value for the precession of perihelion.

Although Einstein's equations are not linear, we have obtained exactly the same result as the classical theory of gravitation.

The law of motion is again given by

$$\delta \int ds = 0,$$

which provides us also with the connexion between the two times. The method of solution of these equations is similar to the electrostatic case. (1st part, § 2.)

From (24) follows that the law of conservation for the centre of gravity holds good in the General Theory of Relativity; as it is known the centre of gravity lost its importance in the Special Theory of Relativity.

§ 5. *Summary.*

1. An eight-dimensional space-time whose metric satisfies Einstein's law of gravitation $G_{\mu\nu}=0$ describes the gravitational field due to two particles.

2. The law of motion of the two particles is a geodesic of its eight-dimensional space.

3. The general result is analogous to the classical case. Two particles m, M moving under the influence of their gravitational fields are equivalent to a particle of mass $m+M$, located in the centre of gravity and moving with a uniform rectilinear velocity, and a particle of reduced mass $\frac{mM}{m+M}$ moving in a gravitational field due to mass $m+M$.

4. Centre of gravity regains the same importance in our case as in the classical dynamics.

XXXIX. *The Ionization of Cæsium Vapour by Ultra-violet Light.* *By* Jakob Kunz *.

Abstract.

A new method has been applied for the determination of the photo-electric effect of cæsium vapour. The photo-electric current has been amplified by a G.E. F.P. 54 amplifier. The coulombs liberated per erg of the incident beam and the atomic ionization coefficient have been determined for wave-lengths between 3130 and 2400Å, and for three temperatures of 25°, 75°, and 125° C.

THE ionization of cæsium vapour by ultra-violet light has been investigated by several physicists and with different methods. The ionization produced by the absorption of ultra-violet light was detected by E. H. Williams and myself by a direct method, while Mohler, Foote, and Chenault applied an indirect space-charge method developed by Hertz and Kingdon. A beam of monochromatic ultra-violet light is made to pass between two electrodes in cæsium vapour at a given temperature. This is about the simplest possible photo-electric effect outside the ionization of hydrogen by means of Röntgen rays, and the results are important from the point of view of the quantum theory of light and wave mechanics. The latter especially leads to the result that the ionization efficiency should decrease in a monotonic way with increasing frequency, starting from the convergence frequency of the principal series. Lawrence and Edlefsen obtained results in qualitative agreement with wave mechanics, while Foote, Mohler, and Chenault, Little and F. W. Cooke obtained a very pronounced minimum in the ionization curve. The direct method used by Little and Cooke in our laboratory suffers from two difficulties. Cæsium vapour deposits on the walls of the glass and on the electrodes, forming a conducting layer at higher temperatures and emitting thermions. It is necessary to separate the thermions from the photo-

* Communicated by the Author.

electrons. For this purpose I have indicated in the 'Physical Review' * a new method which allowed the separation of these negative charges. The beam of light is interrupted rapidly, and the two electrodes of the ionization chamber are connected to a condenser through which an intermittent charge passes while a direct current due to thermions is checked. In this way the thermionic disturbance is eliminated, and at lower temperatures the layer of cæsium on the glass wall is non-conducting. The readings can be taken at ease, while they were very difficult and even painful in the older method.

The Experimental Arrangement.

We were only interested in the ionization curve beyond the convergence frequency, and decided therefore to use the mercury arc instead of the hydrogen source. A quartz capillary water-cooled mercury arc was used as a source of ultra-violet light. This arc gave a very intense concentrated light, with fluctuations that were short in comparison with the inertia of the remainder of the apparatus. A variable resistance was in series with it across a 110 volt d.c. line, and the current was 2·4 amperes.

With one Hilger quartz spectrograph it is difficult to obtain monochromatic light of sufficient purity. We applied therefore two quartz spectrographs in series, and obtained very good monochromatic light. An image of the arc was formed by a condensing lens upon the slit of a single prism constant deviation monochromator. The slit of the Hilger E_2 was placed at the focus of the first spectrograph. A sliding shutter allowed the beam to be cut off. The light of the desired wave-length was then sent through the ionization tube by means of another lens. The slits on the collimators of the spectrographs could be made sufficiently wide so that the ensuing beams were sufficiently strong and still monochromatic. On a plate over-exposed for the given line there were no traces of any other lines of the mercury spectrum.

The ionization tube was longer than the one used by Cooke. The electrodes of platinum were 19·5 cm. long

* Phys. Rev. xxxix. p. 866 (1932).

and 22 mm. wide, with no additional guard-plates. Quartz windows were sealed to a pyrex-tube. In the preparation of the tube it was very necessary to heat it in a furnace to at least 300° C. for three hours before introducing the cæsium, in order to drive out the gases. A little gas ruins the photo-electric effect. The leads to the electrodes passed through well insulated plugs of hard rubber through the furnace. For each line the furnace carrying the tube had to be adjusted by a motion on a table.

In 1917 * I gave a method for the amplification of photo-electric current by means of audion-tubes. The

Fig. 1.

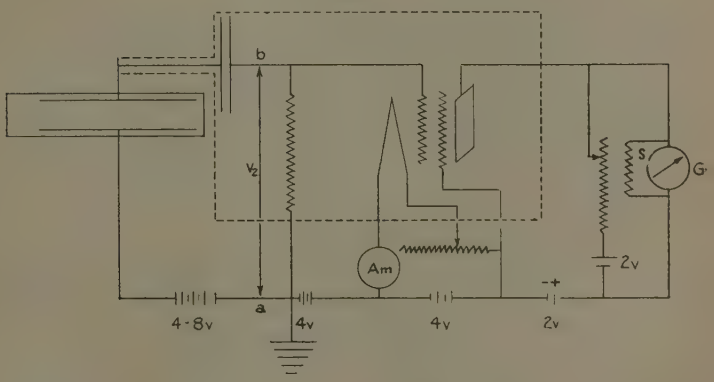

method has been perfected in different directions. The G. E. pliotron F.P. 54 especially proved to be an excellent amplifier for our purpose. It has been used by A. E. Whitford † for the photometry of stars. The diagram of the circuit is given by fig. 1.

The part of the circuit within the broken lines was inside a metallic box which was grounded. The lead from the ionization tube to the bias grid was also electrostatically shielded. The high resistance (HR) was made by pencil marks on hard rubber. The shunt S was an Ayrton-Mather universal shunt. The galvanometer had a figure of merit of $1{\cdot}69.10^{-9}$ at a distance of 1·5 m.

* Phys. Rev. x. p. 205 (1917).

† 'Astrophysical Journal,' lxxvi. p. 213 (1932).

Two storage batteries gave the voltage for the F.P. 54 circuits. The potential across the ionization cell was obtained from B batteries. The condenser used in the beginning with an interrupted beam of light was indicated by C. It was soon found, however, that we obtained only a ballistic throw of the galvanometer, and that readings of constant deflexion could be taken without the use of the condenser. These deflexions were quite steady. The results obtained with and without the condenser, were in close agreement. In order to calibrate the amplifier the high resistance was disconnected, and the ionization leads were replaced by the apparatus shown in fig. 2.

Fig. 2.

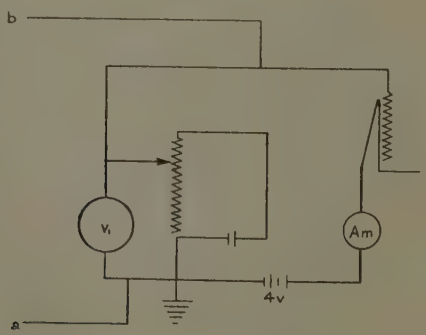

The potentials were so chosen that we were using the straight-line part of the grid voltage—plate current characteristic. Then the voltage V_2 of the photo-electric current between the points a and b was determined by the voltage V_1 of the calibration apparatus, and the corresponding deflexions of the galvanometer are given by

$$\frac{V_1}{V_2} = \frac{d_1}{d_2}.$$

The photo-electric current was then determined by $iR = V_2$.

The spectrum energy was measured by means of a quartz potassium photo-electric cell, which was calibrated against a Coblentz thermopile; the thermopile in turn was calibrated by a Hefner lamp. The resistance both

of thermopile and galvanometer was about 12 ohms. The photo-electric current was measured by a quadrant electrometer. The photo-electric cell was calibrated over the region between 3130 Å. and 2537 Å. against the thermopile. The sensitivity curve of the photoelectric potassium cell was then plotted.

The energy of each line passing through the cæsium vapour was measured by the photo-electric cell just after or before the ionization current was measured. The potassium cell was placed a short distance from the slot in the plate-holder; after the reading of the electrometer deflexion the cell was removed, and the beam of light allowed to pass through a lens into the cæsium cell, which was in the same relative position as the thermopile during the calibration.

The ionization current in cæsium was measured for several lines from 2400 Å to 3130 Å for each of the three temperatures 24°, 75°, and 125° C. Curves were plotted of the ratio of coulombs per erg against wave-length and also of the ionization coefficient k against wave-length. k is given by the relation

$$k = \frac{i}{e} \frac{h\nu}{\mathrm{I}_\nu \mathrm{N} \mathrm{V}},$$

where

i=ionization current,

e=charge of ion,

I_ν=ergs/cm.^{2},

N=number of atoms per cm.^{3},

V=volume of illuminated gas.

The value of i was obtained from the calibration of the amplifying circuit and the galvanometer deflexion. It was not necessary to use the maximum amplification; indeed, at a temperature of 25° C. and for a wave-length of 3130 Å the measured current i_2 was $=3{\cdot}41.10^{-7}$, while the ionization current was $3{\cdot}38.10^{-11}$, so that the amplification was only 10^4.

I_ν is the energy entering the cæsium tube if the volume is replaced by the length of the electrodes in the tube, the energy being corrected for absorption and reflexion from the quartz windows. Cooke's data were

used. N was found from the pressure on the assumption that cæsium vapour acted as a perfect gas.

$$pv=NkT\,;\ v=1.$$

p was calculated from the relation

$$\log_{10} p=7{\cdot}1650-\frac{3\,966}{T}\,.$$

Results.

In general the shapes of the curves agree with those obtained by Little, Cooke, Mohler, and Boeckner. The atomic ionization coefficient k has a maximum value at the ionization limit of 3184 Å., then decreases with increasing frequency, until a minimum is reached at about 2800 Å., and then increases again. This effect appears at all temperatures. For 3130 Å. at 125° C. $k=2{\cdot}10.10^{-19}$; while Mohler and Boeckner obtained $1{\cdot}85.10^{-19}$ by photo-ionization and $3{\cdot}0.10^{-19}$ by absorption, and Cooke 2 to $3{\cdot}6.10^{-19}$. For lower temperatures k depends on the pressure calculation. If, however, the experimentally determined value * of vapour pressure at 75° is taken instead of the computed value then k is nearly the same as that at 125°.

The coulomb-erg curves in all three temperatures show the effect as previously stated. The lower the temperature the less pronounced the rise becomes near 3184 and the minimum seems to be shifted toward the longer wave-length. As the wave-length decreases the ionization increases again at all temperatures. The shape of this curve agrees very well with that obtained by Braddick and Ditchburn † for the absorption of cæsium in this region. The results were obtained with much greater ease than in the previous investigation in our laboratory. Beyond 125° C., however, we could not raise the temperature because of the large increase in conductivity of the cell; and when it was once conducting we were unable to remove the conductivity by heating the central part of the tube and cooling the cæsium reservoir. The results are plotted in the curves of figs. 3, 4, and 5; they represent the relation between

* Rowe, Phil. Mag. iii. p. 545 (1929); Scott, *ibid.* xlvii. p. 32 (1924).
† 'Nature,' Jan. 28, 1933.

Fig. 3.

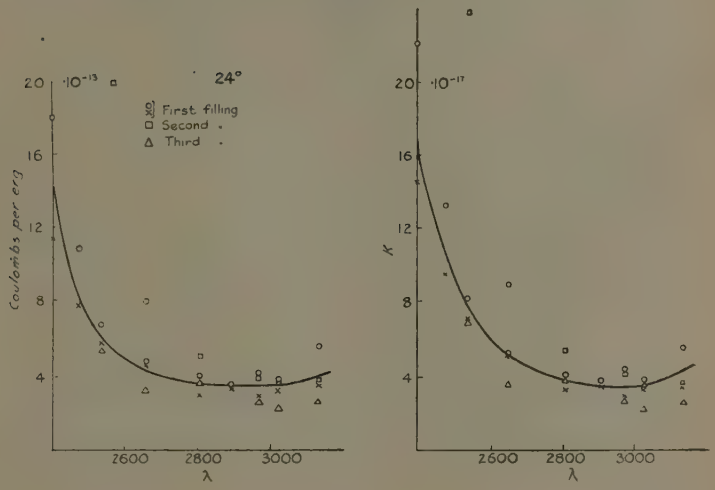
·10⁻¹³
24°
First filling
Second
Third
Coulombs per erg
20
16
12
8
4
2600
2800
3000
λ
·10⁻¹⁷
K

Fig. 4.

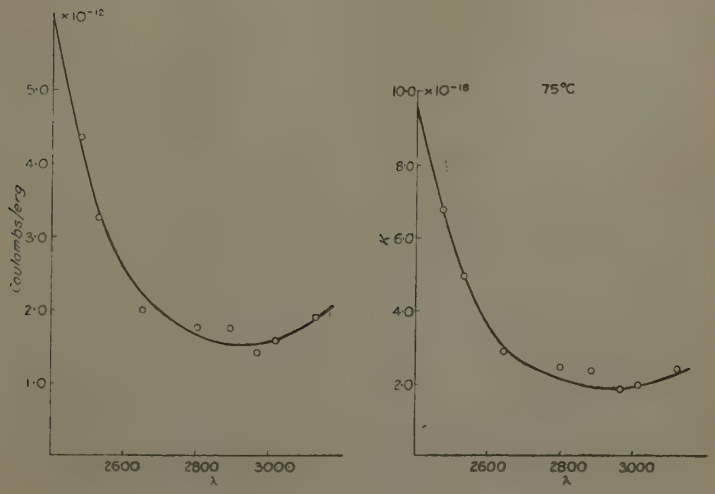
×10⁻¹²
Coulombs/erg
5·0
4·0
3·0
2·0
1·0
2600
2800
3000
λ
10·0 ×10⁻¹⁸
75°C
K
8·0
6·0
4·0
2·0

coulomb/erg and wave-length and the atomic ionization coefficient k and wave-length. These curves show clearly the influence of temperature on these relations.

Fig. 5.

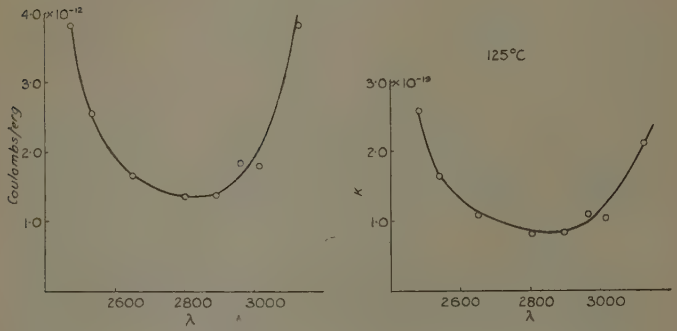

From these curves we took the data of the following table :—

$\lambda = 3130$ Å.

T.	k.	Coulombs per erg.
25	$4{\cdot}2.10^{-17}$	$3{\cdot}8.10^{-13}$
75	$2{\cdot}3.10^{-18}$	$1{\cdot}9.10^{-12}$
125	$2{\cdot}1.10^{-19}$	$3{\cdot}85.10^{-12}$

$\lambda = 2800$ Å.

T.	k.	Coulombs per erg.
25	$3{\cdot}8.10^{-17}$	$3{\cdot}6.10^{-13}$
75	$2{\cdot}2.10^{-18}$	$1{\cdot}65.10^{-12}$
125	$0{\cdot}85.10^{-19}$	$1{\cdot}35.10^{-12}$

$\lambda = 2537$ Å.

T.	k.	Coulombs per erg.
25	$8{\cdot}10^{-17}$	$6{\cdot}2.10^{-13}$
75	$5{\cdot}10^{-18}$	$3{\cdot}3.10^{-12}$
125	$1{\cdot}6.10^{-19}$	$2{\cdot}55.10^{-12}$

It is surprising to see that k varies with the temperature within rather wide limits. For low temperatures, however, k depends on the vapour pressure, which is determined by a curve, which only holds for higher temperatures; indeed, at low temperatures the vapour pressures measured and calculated do not agree with each other. It is very hard to eliminate all scattering of light, but special experiments showed that scattering was absent. If, however, a trace of scattering were present it would affect the value of k. The coulombs liberated per erg seem at first to increase with the temperature and then to remain nearly constant.

The investigation will be continued for higher frequency in order to find the second maximum of the sensitivity curve.

I am very much obliged to A. H. Daniels, Dean of the Graduate School of the University of Illinois, for a stipend for assistance in this work, and to Dr. H. Q. Fuller for his help.

XL. *The Half-value Period of Uranium II.*

By O. A. Gratias, *D.Phil* *.

RECENTLY the traditional value of $2 \cdot 10^6$ years for the half-value period of uranium II has been seriously questioned. The original value was obtained by assuming the correctness of the Geiger-Nuttall rule and applying it to Geiger's [1] [2] value for the range of the α-particles from uranium II. Owing to the long half-value period of uranium I and the small difference in range between the α-particles emitted by uranium I and uranium II the measurement of the latter offers considerable experimental difficulty, while it has long been recognized that the Geiger-Nuttall relation is only a rough approximation.

Later work on the subject has been along two main lines:—

(a) A redetermination of the range of α-particles from uranium II and empirical changes in the relationship

* Communicated by Prof. F. A. Lindemann, Ph.D., F.R.S.

between the range and the decay constant. The first of these determinations by Gudden [3] gave a very long half-value period of 10^8 years, but later work by Laurence [4], Kurie [5], Ziegert [6], and Bateson [7], using Wilson cloud chamber, ionization, and scintillation methods, showed that the range of the α-particles of uranium II is greater than the formerly accepted value, which suggests that the half-value period is about 10^4 years.

(*b*) A direct determination of the decay constant by measuring the number of α-particles emitted by a known number of uranium II atoms.

Walling [9], using a very strong source, estimated the number of α-particles by measuring the ionization current they produced in an α-ray electroscope, and obtained a value of $3.4.10^5$ years ; Collie [8], using a weak source and a direct counting method of measuring the α-particles, obtained a lower limit of 10^6 years.

The purpose of the present paper is to clear up the discrepancy between these two direct determinations. Collie's method, although it had the advantage that the original uranium X solution could be definitely shown to be free from uranium, suffered from the disadvantage that it was not possible to be sure that all the uranium II formed from the decay of the uranium X actually entered the solution as an ion which could be separated electrolytically.

In a friendly criticism Professor Hahn suggested that, in spite of the precautions taken to avoid this source of error, the possibliity of the formation of colloidal aggregates not electrolytically separable was a serious one. In the experiments to be described both methods of measurement were used on the same source, so that the proportion of uranium II left in solution after electrolysis could be obtained.

A strong source of uranium X was prepared, purified, and freed electrolytically from uranium. It was then placed in the cell used by Collie and allowed to decay into uranium II ; this was then separated electrolytically on to a platinum cathode, and the number of α-particles determined by means of an ionization chamber and amplifier as previously described. Meanwhile the electro-

lyte which contained the part of the uranium II not separated on to the platinum cathode was strongly acidified, the cerium and ionium removed by precipitation as fluoride in platinum vessels, and the activity due to uranium II measured with a Lindemann electrometer.

Preparation of Source.

The parent source [10] of 20 kg. of uranyl nitrate had been specially purified, and had been used continually for two years as a source of uranium X_1. The method of separating uranium X_1 was essentially that used in some previous work on uranium Y [11]. The equilibrium amount of uranium X_1 was concentrated from an ethereal solution of the parent source into a few c.c. of aqueous solution by means of a double ether method, and the radio elements of atomic number 90 separated out on a precipitate of 12 mg. cerium fluoride. After fusion with potassium hydrogen sulphate the cerium was precipitated as the carbonate, and dissolved up in a few c.c. dilute nitric acid. This uranium X_1 cerium nitrate solution was then evaporated to dryness to remove the free nitric acid, and the nitrate dissolved in 20 c.c. weak acetic acid, (2·5 c.c. glacial acetic acid per litre). This solution was filtered directly into the electrolytic cell [12], and the total activity of the uranium X_1 obtained by measuring an aliquot part of solution with a calibrated β-ray electroscope. In order to ensure that this uranium X_1 should be free from uranium at time $t=0$ the solution was electrolyzed twice for about eight hours, using a current of 50–60 m.a. per 100 sq. cm. of cathode surface. Collie has shown that any uranium present in such an acid solution under these conditions separates out on to a platinum electrode.

Results.

All α-ray activities are measured with an ionization chamber and a Lindemann electrometer. This arrangement proved to be twenty to thirty times as sensitive as an ordinary β-ray electroscope.

The uranium X_1 solution was left for 248 days, so that practically all (99·9 per cent.) had decayed into uranium II. The uranium X_1 at time zero had a β-ray activity of

1031·5 d.p.m., an amount in equilbrium with 4910 gm. of uranium.

Electrolytic Method.

In this method if all the atoms of uranium II present are separated on to the platinum cathode one would expect

$$\left(\text{using } \cdot 33 \text{ as the ratio of } \frac{\alpha\text{-particles observed}}{\text{total number of } \alpha\text{-particles emitted}}\right)$$

$$\frac{4\cdot 91 \times 6\cdot 06 \,.\, 10^{23} \times 10^{3} \times 4\cdot 9 \times 10^{-18} \,.\, 33}{3\cdot 275 \times 10^{-7} \times 238} \lambda \text{ } \alpha\text{-particles a second}$$

in the chamber, where λ is the decay constant of uranium II.

Substituting Collie's value of λ in the above one would expect to observe $6\cdot 1 \times 10^{13} \times 1\cdot 5 \times 10^{-14} \times 60 = 54\cdot 9$ α-particles a minute. With Walling's value of λ this comes out to be 237·9 p.p.m., and with Laurence's estimate 6222 p.p.m.

The platinum electrode was carefully cleaned and its natural leak observed. This was found to be 1·12 p.p.m. 0·365 gm. of standard uranyl acetate was then added from a small pipette, and the solution electrolyzed for 8 hours. The standard solution contained 500 m.g. of uranyl acetate per litre, so the above quantity would be expected to give 3 or 4 recorded α-particles per minute alone.

After the electrolysis the cathode was tested for α-particles, and found to have emitted 3761 particles in 80 minutes 10 seconds, or $4\cdot 69 - 1\cdot 12 = 3\cdot 57$ d.p.m. No β-ray activity was carried down.

Since all these α-particles can be attributed to the added uranium, either

(*a*) the uranium II produced by the decay of uranium X_1 was not separated by the electrolysis, or

(*b*) since it was emitting less than one α-particle per minute, its decay constant is less than $2\cdot 7 \,.\, 10^{-16}\,s^{-1}$, corresponding to a half-value period of $8\cdot 10^{7}$ years. The subsequent examination of the electrolyte showed that the former hypothesis is correct.

Ionization Method.

The acetic acid solution was poured into a platinum dish and the electrolytic cell washed out with hot concentrated HCl a number of times, in order to dissolve off any uranium II that may have been adsorbed on the glass. The ionium and uranium X_1 were separated from the solution by precipitating the cerium as fluoride. The uranium II filtrate was taken to dryness in a small platinum dish, and its activity carefully measured, using the electrometer and ionization chamber. No measurable β-ray activity was found associated with the uranium II film, while the β activity of the ionium uranium X_1 precipitate was 9·7 d.p.m.

The fluosilicic acid film containing the uranium II was weighed. Using the relation for equivalent thickness, *i. e.*, $\frac{\rho d}{\sqrt{A}}$ [14] =const. (where ρ, d, and A are respectively the density, thickness, and atomic weight of the element under consideration), and, using the fact that the stopping power of compounds is an additive property, this film was found to have an equivalent stopping power of ·82 mg. U_3O_8 per sq. cm. A film of U_3O_8 of this weight per sq. cm. was then made up, and the α-ray ionization measured with the electrometer made very sensitive. From this the total α-ray ionization of 4910 grams of uranium was calculated, and found to be $2{\cdot}56 \times 10^7$ divisions per minute.

The activity of the uranium II using the same sensitivity was 10·7 d.p.m. We thus have measures of the ionization produced by a given quantity of uranium and by an amount of uranium II formed by the decay of the UX in equilibrium with this uranium. To calculate the decay constant of uranium II we need to know as well the relative ionizing power of the α-particles from uranium and uranium II. These were obtained by assuming the ranges of uranium I and uranium II to be 2·58 cm. and 3·11 cm. at 0° C. respectively, corresponding to $1{\cdot}33.10^5$ ions per α-particle from U II and $1{\cdot}254.10^5$ ions from the α-particles from ordinary uranium (U I+U II).

If P_1, P_2, are the half-value periods of uranium X and

uranium II respectively, A_1 and A_2 the measured activities of the uranium and the uranium II, then we have that

$$P_2 = \frac{P \,.\, A_1 \,.\, 1{\cdot}33}{A_2 \,.\, 1{\cdot}254}$$

$$= 1{\cdot}7\ 10^5 \text{ years},$$

corresponding to a decay constant $\lambda = 1{\cdot}29 \,.\, 10^{-13} s^{-1}$.

Remarks.

It seems from the above results that the uranium II was not separated at all in the electrolytic method, and this in itself explains the discrepancy between Collie's and Walling's values for the half-value period. Although the value obtained is less than Walling's it is still much greater than the period deduced from the Geiger-Nuttall law using a range of 3·28 cm. at 15° C.

In conclusion, I have to thank Professor Lindemann and Mr. C. H. Collie for their advice and unfailing interest, as well as for the loan of some of the apparatus used in this work.

Summary.

The half-value period of uranium II has been measured and found to be $1{\cdot}70 \times 10^5$ years. The discrepancy between the two most recently determined measurements of the decay constant has been accounted for by using both an electrolytic method combined with a valve amplifier, and an ionization method using a Lindemann electrometer.

References.

(1) Geiger and Nuttall, Phil. Mag. xxiii. p. 439 (1912).
(2) Geiger, *Z. Physik*, viii. p. 45 (1921).
(3) Gudden, *Z. Physik*, xxvi. p. 110 (1924).
(4) Laurence, Phil. Mag. v. p. 1027 (1928).
(5) Kurie, Phys. Rev. xli. p. 701 (1932).
(6) Ziegert, *Z. Physik*, xlvi. p. 669 (1928).
(7) Bateson, Can. Journ. of Res. v. p. 567 (1931).
(8) Collie, Proc. Roy. Soc. A, cxxxi. p. 541 (1931).
(9) Walling, *Z. Physik, Chem.* x. p. 467 (1930).
(10) Gratias and Collie, Proc. Roy. Soc. A, cxxxix. p. 567 (1933).
(11) Gratias and Collie, Proc. Roy. Soc. A, cxxxv. p. 299 (1932).
(12) Collie, *loc. cit.*
(13) Walling, *loc. cit.*
(14) Meyer and Schweidler "Radioactivität," p. 103.

XLI. *A Theory of the Viscosity of Liquids.*—Part I. *By* E. N. da C. Andrade, *Quain Professor of Physics in the University of London* *.

1. *Introduction.*

THE inner mechanism of viscosity of liquids is a subject to which a certain amount of desultory attention has been given, but it may be said that so far no theory which is even moderately satisfactory has been put forward. The difficulties are obvious: so little is known of the properties of a liquid that even such comparatively simple problems as those offered by the specific heat and its variation with temperature and by the variation of volume with pressure are yet unsolved. Any attempt to build up a theory of liquid viscosity which shall be of any practical use must clearly be in the first case of a half empirical nature; any regularities among the experimental data which may be discovered must be allowed to influence the hypothesis more perhaps than would be the case in a phenomenon which, like the viscosity of gases, has a tolerably sure mechanical basis. In the theory which is now put forward attention will be directed not only to an expression which gives a close estimate of the absolute viscosity of a simple liquid near the freezing-point in terms of other experimental constants, but also to a very close agreement between experimental results and a formula developed for the variation of the viscosity of a liquid with temperature. There is, further, a relation between the viscosity and pressure which is satisfactory as long as the pressures are not too high. Even if the present theory should have to be modified account will have to be taken of these regularities.

The theory follows simple classical lines, no attempt having been made to introduce quantum conceptions. No doubt at a later stage it may be possible to give a quantum interpretation to the theory, but while the broad outlines of the problem are being considered it does not seem profitable to attempt this, as it is the general experience that a quantum treatment does not introduce substantial modification where liquids are concerned, but only refinements in certain respects.

* Communicated by the Author.

This opinion of the writer's can be supported by the following words of Professor Debye's *, written when other liquid properties were under discussion :—" If we are dealing with liquids, however, the interaction is so strong that a treatment .... more closely related to classical statistics seems profitable, and the impression prevails that quantum theory would not introduce essential changes in the principal results."

The mechanism of the viscosity of a liquid must be of quite another nature from that of the viscosity of a gas, as is clearly evinced, for instance, by the fact that the viscosity of a liquid decreases with rising temperature while the viscosity of a gas increases with rise of temperature. In a gas the tangential forces between two parallel layers are produced by the transport of the individual atoms from one layer to another, with a consequent transfer of momentum. Between collisions, the molecules are supposed to move freely over a distance large compared to the molecular size, and it is essential for the theory that disparity between mean free path and molecular diameter should exist. Nevertheless, owing to the success of the mechanism with gases, attempts have been made to apply it to liquids, although here there is, in the ordinary sense, no free path at all, the motion of a molecule being always in an intense field of intermolecular force.

Certain previous workers have recognized that friction by transport, as the gaseous mechanism may be called for shortness, is inadequate to explain liquid viscosity, among whom J. D. van der Waals, Jr., may be especially cited †. He has discussed various possible mechanisms—instantaneous transfer of momentum at collision ; the effect of orientation of dipolar molecules in the formation of what he calls " streaks " ; and, thirdly, the formation of spherical groups, elongated into ellipsoids when the liquid is in motion. Eventually, however, he considers forces of collision to be the only important factor ; he derives a somewhat complicated formula,

$$\eta = \frac{8\sqrt{\pi}}{15} n^2 \sigma^4 m^{\frac{1}{2}} k^{\frac{1}{2}} \frac{v}{v-b} T^{\frac{1}{2}} e^{-\epsilon/RT},$$

where σ is the diameter, m the mass of the molecule,

* P. Debye, ' Polar Molecules,' p. 77 (New York, 1929).

† " Koninklijke Akademie van Wetenschappen te Amsterdam," Proceedings, xxi. no. 5, 1918 ; no. 10, 1919.

n the number of molecules per sq. cm., k Boltzmann's constant, and ϵ represents the difference between the amount of potential energy that the molecules of the liquid possess on an average and the amount which they possess at the moment of a collision.

He attributes, however, little importance to the exponential term, and says that "at constant volume η must increase proportionately to $\sqrt{T}$." He attributes the lack of agreement with experiment to the fact that η is measured at constant pressure and not at constant volume; but there are, thanks to Bridgman, experimental data for the variation of viscosity of liquid with pressure which enable us to compare the viscosity at constant volume and different temperatures *. Experimentally $\frac{1}{\eta}\left(\frac{\partial \eta}{\partial T}\right)_v$ is always negative, whereas according to J. D. van der Waals it should be positive. Other comparisons of the formula with experiment will be found in his paper, but they are not very satisfactory. A very important point established by Bridgman is that η is not, even approximately, a function of volume alone; for isoamyl alcohol the viscosity at 30° is greater than that at the same volume at 75° by a factor which varies from 2·5 at the lower pressures to 6·6 at higher pressures, while for mercury at lower pressures, where the departure is relatively small, the factor is still 1·09. In general viscosity decreases when temperature and pressure are increased together in such a way as to keep the volume constant †.

Leon Brillouin ‡ has also given a theory of liquid viscosity in which the fundamental idea is that the impact of molecules gives rise to elastic waves, the effect of which is that neighbouring molecules are successively disturbed from their positions. The theory is an attempt to transfer the general theory developed by Einstein and Debye for the specific heats of solids and liquids to the field of liquid viscosity. He finds in the first place a *negative* coefficient of viscosity, which he explains by saying that the waves

* Summarized in P. W. Bridgman, 'The Physics of High Pressure' (London, 1931).

† See Bridgman, 'The Physics of High Pressure,' p. 352 (London, 1931).

‡ *Journal de Physique*, iii. p. 326 (1922).

diminish the *natural* viscosity of the liquid, to prove which he imagines a mechanism independent of the temperature if the specific volume is kept constant. His final formula gives that the viscosity is a function of the specific volume, and independent of the temperature, which is contradicted by Bridgman's results just cited; another result, which gives the temperature coefficient of viscosity in terms of the thermal conductivity and the velocity of sound, fails by a factor of nearly 5000 *.

An earlier attempt and references to the previous work of Jäger will be found in M. Brillouin's 'Viscosité des Liquides et des Gaz,' vol. ii. p. 119 *et seq.*

It will be seen, then, that none of the older attempts have led to results which can withstand comparison with experimental results, in particular with the recent high-pressure results of Bridgman, which enable viscosities at constant volume to be computed. Reference to some more recent workers will be made in connexion with particular points.

In general lack of agreement with experiment is the chief reproach that can be levelled against the older theories.

2. *General Basis of the Theory.*

I believe that the theory of liquids should be approached not, as has hitherto been done, from the point of view of the kinetic theory of gases, which was constructed to deal with matter where the spaces between the molecules are large compared with the size of molecules, but from the point of view of the solid state, the density of which is not markedly different from that of the liquid state of the same substance. The forces between molecules in the solid and in the liquid state cannot be very different. Support can be cited for this point of view; for instance, Lindemann's theory of fusion †, which has been remarkably successful in yielding values for the fundamental frequencies of simple solids which are in good accord with those found by other and widely different methods, supposes that melting takes place when the amplitude of the vibrations of the molecules about their equilibrium positions becomes a fixed large fraction of the average distance apart, σ, of the atoms.

* Bridgman, *loc. cit.* p. 354.

† *Phys. Zeitschr.* xi. p. 609 (1911).

The equilibrium is then disturbed and the substance becomes fluid, but clearly the liquid in the neighbourhood of its melting-point has much in common with the solid.

Let us consider a liquid moving in plane layers parallel to one another, there being a velocity gradient in the direction normal to the layers. I assume that the viscosity is due to a communication of momentum from layer to layer, as in Maxwell's theory of gaseous viscosity, but that this communication of momentum is not effected to any appreciable extent by a movement of the equilibrium position of molecules from one layer to another, but by a temporary union at the periphery of molecules in adjacent layers, due to their large amplitudes of vibration. The meaning of this union is considered in more detail a little further on. The molecules are considered, then, as behaving to a first approximation as if remaining each one in its original layer, and executing vibrations about a position in this, the equilibrium position changing very slowly. There is nothing against this in the known properties of liquids, diffusion being extremely slow. Consider, for instance, the one case where the self-diffusion, to use Maxwell's term, of a liquid has been measured, namely, that of liquid lead, where "marked" molecules are obtained by using the isotopic element thorium B, which can be detected by its radioactive properties *. The coefficient of diffusion is 2·2 sq. cm./day, so that

$$\frac{\overline{x^2}}{\tau} = 2\mathrm{D}$$
$$= \frac{4\cdot4}{86400}\ \mathrm{cm.^2/sec.}$$
$$= 5\cdot1\times10^{-5},$$

where $\overline{x^2}$ is the average value of the square of the distance travelled in time τ.

Accordingly the time taken to traverse in a given direction a distance of $3\cdot1\times10^{-8}$ cm., which is the average distance between centres of molecules as calculated from the density and molecular weight, is

$$= \frac{3\cdot1^2}{5\cdot1}\times10^{-11}$$
$$= 1\cdot89\times10^{-11}\ \mathrm{secs.}$$

* J. Groh and G. von Hevesey, *Ann. der Phys.* lxiii. p. 85 (1920).

If it is justifiable, as I shall contend, to take the frequency of vibration of an elementary substance in the liquid state as approximately equal to that of the same substance in the solid state, we may take the value of the time between collisions as given by the fundamental frequency, found for solid lead by the well-known methods usually cited in connexion with specific heat calculations. With the mean value, obtained from several methods *, of 2×10^{12} we have for the time between collisions $2{\cdot}5\times10^{-13}$ seconds, supposing that a collision takes place at each extreme libration, so that in the time $1{\cdot}89\times10^{-11}$ seconds 76 collisions will have taken place. This calculation rests directly upon experimental evidence, and shows that the assumption that the molecules may be considered as remaining in layers is a good first approximation.

Another method suggests itself for obtaining an estimate of the number of impacts taking place when the mean position of the centre of the molecule moves through the mean distance σ separating molecular centres in the liquid. This demands, however, some general assumption as to the method in which the slow displacement of the equilibrium position of the vibrating molecule is effected. If we suppose that the movement of the molecule takes place by n equal paths of unknown length l which succeed each other in random directions, we can, knowing the mean velocity v in such paths, obtain, as will be shown, an estimate of the (large) number of paths required, on the average, to take the molecule through the distance σ in time τ. The required velocity v can be found by equating the kinetic energy to $\frac{3}{2}k\mathrm{T}$.

We proceed to find n. To get v we have

$$\tfrac{1}{2}m\overline{v^2}=\tfrac{3}{2}k\mathrm{T},$$

where $\overline{v^2}$ is the average value of v^2. If we assume that the motion in each path is simple harmonic, then the mean velocity $\bar{v}$

$$=\frac{2\sqrt{2}}{\pi}\sqrt{v^2},$$

$$=\frac{4}{\pi}\sqrt{\frac{3}{2}}\sqrt{\frac{k\mathrm{T}}{m}}.$$

* Blom, *Annalen der Physik*, xlii. p. 1397 (1913).

It follows at once from a theorem of Lord Rayleigh's * that if we have a large number of consecutive paths of length l in random directions in three-dimensional space, then the probability of the end of the nth path lying between r and $r+dr$ is

$$\phi(r).dr=3\sqrt{\frac{6}{\pi}}\frac{n^{-\frac{3}{2}}}{l^3}e^{-r^2/\frac{2}{3}nl^2}r^2\,dr.$$

If we let $nl=d=\bar{v}\tau$, which is fixed in our case, then

$$\phi(r)=3\sqrt{\frac{6}{\pi}}\frac{n^{\frac{3}{2}}}{d^3}e^{-\frac{3}{2}\frac{r^2n}{d^2}}r^2.$$

We choose n so that $\phi(r)$, the probability that the centre of the molecule has moved through a distance σ, shall be a maximum, d being fixed.

Then
$$\frac{\partial\phi(r)}{\partial n}=0$$

gives
$$n=\left(\frac{d}{r}\right)^2.$$

The numerical values are $r=3{\cdot}1\times10^{-8}$ cm., $\tau=1{\cdot}89\times10^{-11}$ sec., T=616 abs.

$$d=\bar{v}\tau=\frac{4}{\pi}\sqrt{\frac{3}{2}}\sqrt{\frac{k\mathrm{T}}{m}}\tau$$
$$=29{\cdot}5\times10^{-8}.$$

whence
$$n=\left(\frac{29{\cdot}5}{3{\cdot}1}\right)^2=90.$$

This value compares very favourably with that of 78 obtained by the first method when the approximate nature of the assumptions is considered. It may be noted that, reversing things, this calculation enables us to make a rough estimate of the frequency of vibration of the lead atom directly, for if there are 90 impacts, estimated as above, in the time required to diffuse through $3{\cdot}1\times10^{-8}$ cm., viz., $1{\cdot}89\times10^{-11}$ sec., the frequency is $2{\cdot}4\times10^{12}$, as against, for instance, the value $2{\cdot}2\times10^{12}$, derived both by Einstein, from the compressibility, and by Grüneisen by consideration of the equation of state of solid bodies †.

* 'Theory of Sound,' vol. i. p. 40 *et seq.* (second edition, London, 1894); Phil. Mag. xxxvii. p. 321 (1919).

† C. E. Blom, *loc. cit.*

It is assumed that the arrangement of molecules in the liquid state is very like that in the solid state, and that consequently the average intermolecular force which acts on a given molecule as the result of the electric field of all neighbouring molecules is, on the whole, very little different from the average intermolecular force in the solid state. The essential difference between the liquid and solid state is not the magnitude of the intermolecular force, under which the molecule vibrates, but the amplitude of the motion. In the liquid state this is so large that the molecules come into contact at every extreme libration, a result of which is that they are disturbed and the "position of equilibrium," which in a solid is fixed, is in a liquid slowly displaced. The assumption is, then, that there is for a liquid molecule a vibration about a slowly displaced equilibrium position, with a frequency which is the same as that of the molecule in the solid state.

This view is supported by a consideration of the specific heat of elements in the solid and liquid phases near the melting point*. For most monatomic substances the atomic heat of the liquid at constant volume is within 10 per cent. of that of the solid, the value being about 3R, where R is the gas constant for the gram molecule. This implies that the potential energy of the atoms is about equal in the two states and that the atoms of the liquid in the neighbourhood of the melting point continue to execute approximately simple harmonic vibrations.

It is further assumed that when, at every extreme libration, the molecules of one layer come into contact with those of an adjacent layer at this contact they will, in general †, enter into a temporary union, the duration of which does not exceed the very brief time necessary for the molecules to acquire a common velocity of translation. The duration of this union must be very small compared to the period of vibration, and does not involve anything of the kind that is ordinarily called association. This sharing of velocities between molecules in adjacent

* L. G. Carpenter, 'Nature,' Jan. 9, 1932.

† While as a basis of calculation we shall assume that the temporary union takes place *at the temperature of melting* at *every* extreme libration, and while comparison with experiment confirms this hypothesis as a first approximation, it is possible, as discussed in the second part of this paper, that sharing of momentum takes place not in all, but in a large fraction of, the extreme librations.

layers will, of course, introduce viscous forces in the way explained in Clerk Maxwell's original theory of gaseous viscosity.

These two assumptions suffice to allow us to express the viscosity of a simple liquid in the neighbourhood of its melting-point in terms of experimental constants having nothing to do with viscosity measurements.

3. *Calculation of Viscosity of Simple Liquids in the Neighbourhood of the Freezing-point.*

The average distance by which a molecule leaves its position of equilibrium, speaking still as if the liquid were in the solid state, is difficult to define and calculate. Various hypotheses are possible: that throughout regions large compared with the molecule the molecules execute vibrations which are synchronous and parallel, but that the direction and epoch change slowly with regard to both time and space; that throughout such a region the molecules execute vibrations which are parallel but not synchronous; that the molecules execute vibrations about equilibrium positions with random directions and epochs. It is held by the writer, however, that there is at present too little known of the liquid state to render precise hypothesis profitable, and it may be recalled that even in the case of the viscosity of gases the formula

$$\eta = k\rho u_m \mathrm{L}$$

contains the constant k, which has been calculated correctly for monatomic gases (spherical, elastic, non-rotatory molecules) only *, while for other gases it has to be determined empirically.

All that will be sought then is to enquire how a formula may be derived which will give, *to a first approximation*, the viscosity of a simple liquid near to its freezing-point. For this purpose it does not matter whether we assume the local crystallization just discussed, with random directions of the crystal axes, or whether we consider layers of molecules parallel to the direction of shear, and assume the molecules to be moving in random directions. For simplicity we take the second case, and

* Chapman, Phil. Trans. ccxi. A, p. 433 (1912); ccxvi. A, p. 279 (1915); ccxvii. A, p. 115 (1917). Enskog, *Phys. Zeitschr.* xii. pp. 56 and 533 (1911); and 'Kinetische Theorie der Vorgänge in mässig verdünnten Gasen' (Upsala, 1917).

suppose as a first approximation that for molecules moving at right angles to the layers communication of momentum takes place at every extreme displacement of a molecule. We make the usual simplifying assumption that $\frac{1}{3}$ of the molecules are vibrating along each of three directions normal to one another. The number p of molecules in unit area of a layer is $\frac{1}{\sigma^2}$, where σ is the average distance between the centres of molecules. If n is the number of molecules per unit volume, then

$$\sigma = n^{-\frac{1}{3}} \quad \text{and} \quad p = n^{\frac{2}{3}}.$$

Supposing that communication of momentum takes place at every extreme libration, this means that a molecule of a given layer conveying momentum crosses a plane parallel to the drift twice in every complete vibration, and a molecule of the adjacent layer also crosses the plane twice in every complete vibration. This is clearly an extreme simplification, adopted in the absence of closer knowledge of the behaviour of adjacent liquid molecules.

If, then, there are ν vibrations a second, the transfer of momentum per unit time per unit area is

$$\frac{4}{3}\frac{1}{\sigma^2} \nu m \frac{dv}{dz} \sigma = \frac{4}{3} \nu m \frac{dv}{dz} \frac{1}{\sigma}$$

$$= \eta \frac{dv}{dz},$$

or

$$\eta = \frac{4}{3} \frac{\nu m}{\sigma} \quad . \quad . \quad . \quad . \quad . \quad . \quad (1)$$

The numerical factor 4/3 will, no doubt, have to be modified or more precisely justified when further experimental knowledge allows a more precise formulation of the condition of impact and use of more detailed calculation. It may be considered as analogous to the use of the factor 1/3 for k in the simple formula for the viscosity of gases already cited, which Enskog and Chapman have shown to be almost exactly 1/2 for monatomic gases treated rigorously, and of which the value cannot be calculated precisely for more complex molecules.

We now introduce the assumption that at the melting-point the frequency of vibration is equal to that in the solid state—that is, that when a solid is melted it still

retains in the liquid form sufficient of its crystalline character for the molecules to possess a frequency of vibration which is practically the same as that of the solid form at the melting-point. This is not so remote from the considerations of Lindemann's theory, already cited. There is fairly good experimental support for Lindemann's formula, which is widely accepted as giving at any rate a first approximation to the mechanism of melting. The formula is

$$\nu = C\sqrt{\frac{T_m}{AV_A^{\frac{2}{3}}}} \quad . \quad . \quad . \quad . \quad . \quad . \quad . \quad (2)$$

where ν is the fundamental frequency, T_m is the melting-point, A the atomic weight, and V_A the volume of a gram-atom at temperature T_m. Suppose that we substitute the frequency ν so found in the viscosity formula. Since

$$\sigma = \left(\frac{V_A}{N}\right)^{\frac{1}{3}},$$

and $m = \frac{A}{N}$, where N is Avogadro's number, we obtain from (1) and (2) for the viscosity η at the melting-point

$$\eta = \frac{4}{3}C\frac{(AT_m)^{\frac{1}{2}}}{(NV_A)^{\frac{2}{3}}} \quad . \quad . \quad . \quad . \quad . \quad . \quad . \quad (3)$$

The value of this constant C is $2{\cdot}8 \times 10^{12}$ *.

Substituting this and the value $6{\cdot}06 \times 10^{23}$ for N, we have

$$\eta = 5{\cdot}1 \times 10^{-4}\frac{(AT_m)^{\frac{1}{2}}}{V_A^{\frac{2}{3}}} \quad . \quad . \quad . \quad . \quad . \quad . \quad . \quad (4)$$

It must be emphasized that this formula does not contain any arbitrary constant, the $5{\cdot}1 \times 10^{-4}$ being ultimately derived from the best experimental values of ν for solids.

The following tables show the calculated and experimental results for elementary substances, of which the

* This is the usually accepted value, as given by Grüneisen, *Annalen der Physik*, xxxix. p. 257 (1912). Lindemann, in his original paper, gives a somewhat smaller value; Blom, *Annalen der Physik*, xlii. p. 1397 (1913), gives $3{\cdot}1 \times 10^{12}$. The value is found by a comparison with the values of ν obtained from specific heats, elastic constants, and by other methods (see, in particular, Blom, *loc. cit.*), and thus represents the tolerably concordant results of a considerable body of experiment. Whether $2{\cdot}8$ or $3{\cdot}1 \times 10^{12}$ is adopted as the value does not affect our general conclusions.

viscosity of the liquid form in the neighbourhood of the melting-point can be found from published experimental data.

In view of the fantastic discrepancies * between the values of the viscosities of liquid metals obtained by different workers, a word is necessary as to the values here set down, which are given to two significant figures only, to emphasize that no very high precision can be claimed. In general the values of Arpi and of Majima are very much lower than those of other workers. Arpi's work has been criticized by Plüss on grounds that seem to the present writer to be well justified †. An account of Majima's work is not at present accessible to the writer.

TABLE I.

Metal.	η cal.	η obs.	Crystal structure.
Mercury	·021	·021	Approx. close packed.
Lead	·025	·028	Close packed.
Tin	·019	·020	Close packed, distorted.
Copper	·038	·038	Close packed.
Antimony	·015	·024	Rhombohedral hexagonal; not close packed.
Bismuth	·018	·023	

On the other hand, the work of Sauerwald and his collaborators shows careful checking against mercury and consistent results with different instruments, and in the case of tin the value agrees fairly well with those of Plüss. In the case of bismuth a group of Plüss's values fall well in line with those of Sauerwald and Toepler taken over a wider range, but two of Plüss's points at lower values fall right off the curve, and have

* The epithet may be allowed in view of such facts as the following:—For bismuth at 300° C. Majima (Bull. Inst. of Phys. and Chem. Research, 1924, quoted in 'Tables Internationales,' vol. vi. 1, p. 56) gives, as the value of 100 η, 1·416, while Sauerwald and Toepler (*Zeitschr. für anorganische Chemie*, clvii. p. 117, 1926) give 1·679; at 600° C. the former gives 1·219, the latter ·998, so that while at 300° C. Sauerwald and Toepler's value exceeds Majima's by 18·5 per cent., at 600° C. Majima's value exceeds the other by 21·9 per cent. Majima's value for antimony at 650° C. is about half that of Bieniass and Sauerwald (*Zeitschr. für anorganische Chemie*, clxi. p. 51, 1927). Arpi's value for tin at 300° C. is 1·08, as against Sauerwald and Toepler's 1·68 and Plüss's 1·62 (interpolated). Many other examples will reveal themselves to him who examines the data.

† *Zeitschr. für anorganische Chemie*, xciii. p. 1 (1915).

been neglected. Sauerwald and Toepler's value for lead agrees pretty well with Fawsitt's *. I have, then, after careful examination of the methods used, placed my faith in the value of Sauerwald and his collaborators, which are incidentally, the most recently obtained and are in rough agreement with the values of Plüss † for the metals bismuth and tin, which have been examined by both. To extrapolate to the value at the melting point, which is generally some tens of degrees below the lowest temperature for which a measurement was made, I have used the exponential formula $\eta = Ae^{\frac{C}{T}}$, plotting $\log \eta$ against $1/T$, when T is the absolute temperature, which gives a tolerably straight line ‡.

The agreement between calculation and experiment for the first four metals is surprisingly satisfactory—in fact much closer than one has a right to expect considering the approximate nature of the assumptions. It may be said to be within experimental error. The values of κ found by different methods vary somewhat: if, for instance, Blom's average value from different methods of $1{\cdot}08 \cdot 10^{15}$ is taken for lead, instead of $1{\cdot}8 \cdot 10^{12}$ found from Lindemann's formula with $C = 2{\cdot}8 \cdot 10^{12}$, the calculated viscosity in the above table becomes ·028. For antimony and bismuth the agreement is less good than for the first four metals. This is in itself an interesting point. For the first four metals the crystal structures approximate to close-packing. Supposing that, as we have assumed, the crystal structure is locally and temporarily reproduced in the liquid form near the melting point, then our assumptions will clearly be more nearly true for these metals than for metals such as antimony and bismuth, when the structure is in both cases rhombohedral hexagonal, and far from close packed.

The monatomic metals are clearly the best substances on which to test the theory. I have, however, carried out the calculation with liquids which have diatomic molecules, at any rate in the gaseous form, namely, the liquid halogens, chlorine, bromine, and iodine, and liquid

* Journ. Chem. Soc. xciii. p. 1209 (1908).

† Since this was written a paper by V. H. Stott, Proc. Physical Society, xlv. p. 530 (1933), has appeared, in which the same conclusion is reached. "It has been assumed that the experiments of Sauerwald and Toepler are substantially correct, this assumption being based upon a critical study of their method."

‡ See Part II.

oxygen and hydrogen. The latter are of special interest on account of their very low viscosity. It makes little difference whether in the formula we put for A and V_A the values for a monatomic or a diatomic molecule in the liquid state, since the latter case gives the same result as the former except for a factor $2^{\frac{2}{3}} = 1{\cdot}12$. In the following the monatomic values have been used.

The values for the halogens are extrapolated, by the logarithmic formula already cited, from the values of Stewart and Johnson *. A value of 8·1, instead of 5·1, for the constant in (4) gives tolerable agreement.

As regards the viscosities of liquid oxygen and hydrogen only one determination, that of J. E. Verschaffelt †,

Table II.

Liquid	Melting-pt. abs.	Viscosity at melting point.	
		Calculated.	Observed.
Chlorine	171	·0070	·0103
Bromine	265·7	·0088	·0138
Iodine	386	·0132	·0232
Oxygen	54	·0025	·0049
Hydrogen	14	·00034	·00013

exists, namely, at 90° abs. for oxygen ($\eta = ·0049$) and at 21° abs. for hydrogen ($\eta = ·00013$), temperatures which are respectively 67 per cent. and 50 per cent. above the melting point. The viscosities at the melting point must undoubtedly be higher than those shown above. No method suggests itself for estimating the temperature variation of the viscosity of liquid oxygen and hydrogen, since the molecules are so different from any considered in the second part of this paper.

No great significance is attached to the calculation in the case of these diatomic gases, but the table suffices to show that the values given by the formula follow roughly the experimental values, especially indicating the low value for liquid oxygen and a much lower one for liquid hydrogen.

* Journ. Amer. Chem. Soc. lvii. p. 754 (1925).

† Comm. Phys. Lab. Leyden, cliii. *b*, p. 16 (1917).

While Lindemann's formula has been used in order that the viscosity may be expressed in terms of the melting-point, atomic weight, and atomic volume, the agreement between the calculated value and the experimental value of the viscosity of elementary liquids at the melting-point is clearly not dependent on its use. The value of the frequency ν, found in any other way, may be introduced into formula (1) without altering the general result.

No great emphasis is placed by the writer on the surprising closeness of the agreement for the first four substances in Table I., which is within 10 per cent. or less, for this agreement depends upon the exact value given to the constant in formula (1). This constant, as already discussed, may have to be modified when more precise methods of calculation are available, although no very large change is to be anticipated. What it is desired to stress is that the calculated result is of the right order and that it not only places the viscosities of the closely packed liquids in the right sequence of magnitude, but also gives their relative magnitude.

The question of the variation of viscosity with temperature and pressure will be discussed in the second part of the paper.

XLII. *On the Volume of the Meniscus at the Surface of a Liquid.*—Part III. *By* Alfred W. Porter, *D.Sc., F.R.S., F.Inst.P., Emeritus Professor in the University of London* *.

In October 1932, p. 694 of this Journal, I published the results of calculations of the volume of a meniscus for different radii of cylindrical and conical tubes, based partly upon Bashforth and Adams's Tables and partly upon the calculations made by the late Lord Rayleigh, which were applicable to much larger radii. These latter were, however, applicable only to a zero angle of contact. I was able, however, to obtain values for other angles in a tentative way by making use of the property that the curves of volume against radius become asymptotic to easily calculated straight lines.

* Communicated by the Author.

I have since extended Rayleigh's calculations to other angles and have applied them to determine the value of $V/\pi\beta^3$ for each ten degrees contact angle for values of r/β

Fig. 1.

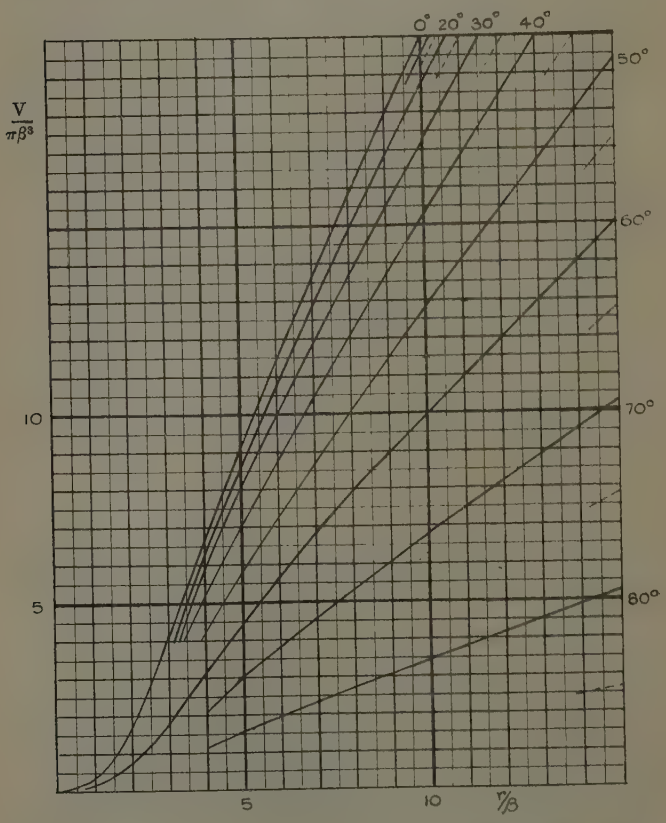

up to 10, where the curves become practically coincident with their asymptotes. It may be noted that Rayleigh's formulæ become more accurate the *higher* the radius, and they hold down to $r/\beta=6$. I applied them in Part I. (*loc. cit.*) down to the value 5, but I have since found

that they give somewhat too high a value at that abscissa. The tables of Bashforth and Adams do not extend further than $r/\beta = \sqrt{10}$, so that the intervening

Fig. 2.

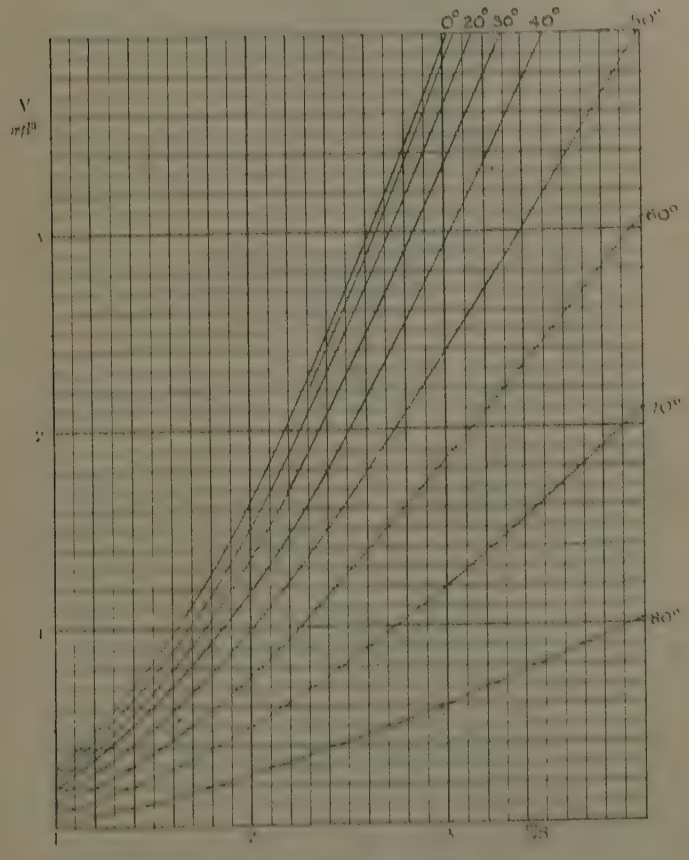

gap has still to be filled up graphically, but this can be done with considerable reliability.

The results of these new calculations are shown in figs. 1 and 2. The following rectangular coordinates are given for those who may choose to construct the figures on a scale more suitable to their own use: —

TABLE I.

$X = r/\beta$, $Y = V/\pi\beta^3$.

	0°.	10°.	20°.	30°.	40°.	50°.	60°.	70°.	80°.
X	0·4815	$0·4749_7$	$0·4551_3$	$0·4218_5$	$0·3755_2$	$0·3170_6$	0·2480	$0·1703_8$	$0·0867_4$
Y	$·0340_5$	·03311	·02678	$·0188_2$	$·0112_6$	$·0054_9$	$·0019_8$	$·0004_3$	$·0002_9$
X	$·8852_9$	$·8755_9$	$·8450_2$	$·7916_8$	$·7139_4$	$·6114_6$	$·4849_5$	$·3371_1$	·1730
Y	·2031	$·1912_6$	·1600	$·1178_1$	$·0743_9$	$·0383_1$	·0146	$·0033_1$	$·0002_2$
X	2·1688	$2·156_7$	$2·116_7$	$2·042_8$	$1·926_2$	$1·754_8$	$1·499_4$	$1·159_9$	$0·6581_2$
Y	1·9862	$1·982_2$	$1·737_8$	$1·451_6$	$1·085_9$	$0·716_3$	$0·370_3$	$0·121_3$	0·0120
X	2·407	2·395	2·355	2·280	2·162	1·987	1·734	1·362	0·801
Y	2·520	2·423	2·208	1·874	1·442	0·975	0·532	0·189	$0·021_3$
X	2·605	2·593	2·552	2·477	2·359	2·182	1·924	1·540	0·935
Y	2·948	2·873	2·599	2·245	1·759	1·220	0·690	0·263	0·033
X	2·773	2·761	2·720	2·645	2·526	2·349	2·089	1·696	1·059
Y	3·349	3·261	2·998	2·582	2·047	1·443	0·843	0·338	0·047
X	2·919	2·907	2·867	2·792	2·673	2·495	2·233	1·834	1·174
Y	3·709	3·613	3·333	2·887	2·309	1·651	0·986	0·413	0·063
X	3·165	3·152	3·112	3·037	2·918	2·740	2·476	2·071	1·380
Y	4·326	4·221	3·912	3·416	2·768	2·021	1·250	0·559	0·098

Table II.

Angle of contact. r/β.	0°.	5°.	10°.	15°.	20°.	25°.	30°.	35°.	40°.	45°.	50°.	55°.	60°.	65°.	70°.	75°.	80°.
							Values of h/β.										
·5	...	...	...	...	...	...	...	...	...	...	...	...	0·16	0·12	0·09	0·07	0·05
1·0	0·86	0·79$_5$	0·74	0·68	0·63$_5$	0·57$_5$	0·54	0·48	0·44	0·39$_5$	0·36	0·32	0·26	0·22	0·18	0·12$_5$	0·07
1·5	1·11	1·04	0·96	0·89$_5$	0·83$_5$	0·76	0·70$_5$	0·65	0·57$_5$	0·52$_5$	0·46	0·41$_5$	0·34$_5$	0·30	0·23$_5$	0·17	0·10$_5$
2·0	1·26	1·18	1·11	1·04	·96	·90	·83$_5$	·77	·69$_5$	·63$_5$	·56	·50	·42$_5$	·36	·29	·22	·15
2·5	1·35	1·27	1·20$_5$	1·14	1·07$_5$	1·00	·93	·86	·79	·71$_5$	·64	·56$_5$	·50	·41$_5$	·34	·24$_5$	·16
3·0	1·43	1·36	1·29$_5$	1·22	1·15	1·07$_5$	1·00	·92	·84	·76	·68	·60	·52	·44	·36	·27	·18
4·0	*1·54*	*1·45*	*1·36*$_5$	*1·28*$_5$	*1·21*	*1·13*	*1·05*	·97	·89	·80$_5$	·72$_5$	·63	·54	*·45*	·36$_5$	·27	*·18*$_5$
5·0	1·57$_5$	1·48	1·39$_5$	1·30$_5$	1·23$_5$	1·15$_5$	1·07$_5$	·98	·90	·82$_5$	·74$_5$	·65	·56	·46$_5$	·37$_5$	·28	*·19*
6·0	1·57	1·47$_5$	1·38	1·30$_5$	1·23	1·15	1·07	·98$_5$	·90	·82	·74	·65	·56	·46$_5$	·37$_5$	·28	·18$_5$
7·0	1·55	1·46	1·37	1·29$_5$	1·22	1·14$_5$	1·07	·98$_5$	·90	·82	·74	·64$_5$	·55	·46	·37	·27$_5$	·18
8·0	1·53	1·44$_5$	1·36	1·28$_5$	1·21$_5$	1·14	1·06	·97$_5$	·89$_5$	·81	·73	·64	·55	·46	·37	·27$_5$	·18
9·0	1·52	1·43$_5$	1·35	1·28	1·21	1·13	1·06$_5$	·97	·89	·80$_5$	·72$_5$	·63$_5$	·54$_5$	·45$_5$	·37	·27$_5$	·18
10·0	1·51	1·42$_5$	1·34	1·27	1·20	1·12$_5$	1·05	·97	·89	·80$_5$	·72$_5$	·63$_5$	·54$_5$	·45$_5$	·37	·27$_5$	·18
20·0	1·445						1·02$_5$						·53$_5$				
∞	1·414	1·35$_7$	1·28$_5$	1·22	1·15	1·08	1·00	·92$_5$	·85	·77	·69	·60$_5$	·52	·44	·35	·26$_5$	·17$_5$

To avoid misunderstanding it may be necessary to repeat that the volume of the meniscus is the volume contained by the surface, the tangent to it at its centre and the wall of the vessel. It therefore contains water in the case of water and gas in the case of mercury.

To make use of the tables it is necessary to know the value of β (*i. e.*, the square root of the capillary constant) and the angle of contact in addition to the radius of the tube. For mercury β varies from 0·18 to 0·19 cm.; hence the following possible values at about 20° C.:

β	·18	·182	·184	·186	·118	·19
$n\beta^3$....	$\cdot0183_3$	$\cdot0189_4$	$\cdot0195_7$	$\cdot0202_3$	$\cdot0208_8$	$\cdot0215_6$

In this paper (as in Rayleigh's papers) the capillary constant is β^2—(surface tension divided by the gravitational acceleration and by the difference of the densities of the liquid and the superincumbent vapour). It is half the value usually adopted on the Continent.

Unfortunately the angle of contact is subject to variation, especially in the case of mercury, even for the same specimen in the same tube. Still more unfortunately it is nearly impossible directly to measure this angle. It can be inferred, however, from the height, h (or the reduced value h/β) of the meniscus.

By aid of Rayleigh's formulæ I have calculated the values of the acute angle of contact for various values of h/β and r/β. These are recorded in Table II. along with values calculated with the aid of Bashforth and Adams's Tables. It will be noticed that h/β takes a maximum value in the neighbourhood of $r/\beta = 5$. This table applies to all liquids when the value of β appropriate to the particular liquid and vessel is employed. When the angle is thus determined (from Table II.) the value of $V/n\beta^3$ can be obtained from figs. 1 or 2.

It may be observed that in the case of mercury, when only a rough measure is required, twice r/β gives the radius in millimetres and twenty times $V/(n\beta^3)$ gives the meniscus volume in cubic millimetres. These numbers are somewhat in excess of the values for average specimens of mercury.

Example: $r/\beta = 5$ means a radius in the case of mercury of about 10 mm.; if the observed h is 2 mm., h/β must be about unity; hence the angle of contact is about

35°; whence from fig. 1 $V/\pi\beta^3 \doteq 7{\cdot}5$, and consequently $V \doteq 150$ mm.^{3}.

An important historical case can be cited in illustration of the need of the determination of V. The late Lord Rayleigh carried out a series of investigations on Boyle's Law for various gases. In the last of these papers ('Collected Papers,' v. p. 230 (1905)) he expresses surprise at the accuracy obtainable being much less than he expected. He says: "I had supposed that an error of 3 parts in 100,000 (at the outside)....was as much as was to be feared. As it is, I do not believe that the discrepancies can be explained as due to errors of temperature or of pressure or of volume so far as the readings are concerned. But it is possible that a variable contact between mercury and glass in the lower chamber of the first manometer may have affected the volume in an uncertain manner, though care was taken to obviate this as far as could be." This was written ten years before his own great paper on wide tubes; and no measurements appear to have been made on the variation of the capillary height, h.

The values for air obtained on different days for the numbers which, according to Boyle's Law, should be unity were 1·00035, 1·00016, and 1·00018. The tables given in the present paper show that a variation of the contact angle from 40° 60° must lead to a variation in these numbers of ±·00012. The actual extreme range is ·00019. In the absence of measurements of the angle or of h it is impossible, however, to pursue this examination further; but it appears probable that Rayleigh had hit upon the correct explanation of the variation of his results.

Experimentalists in general appear to be under the illusion that by selecting a sufficiently wide tube the complications arising from capillarity will be reduced indefinitely, and theorists have not done much to disillusion them. When volume measurements are being made it is important to realize that the volume of the meniscus *increases* continuously with the radius becoming infinite for an infinite radius. In fact, as soon as the curves on fig. 1 can be confounded with their asymptotes

$$\frac{V}{\pi\beta^3} \doteq 2\frac{r}{\beta}\cos i,$$

which clearly increases proportionately to r/β

XLIII. *Notices respecting New Books.*

Hydrodynamics. By Sir Horace Lamb. Sixth Edition. [Pp. 738.] (Cambridge University Press, 1932. Price 45*s.* net.)

Every four years ago there appeared Lamb's 'Treatise on the Mathematical Theory of the Motion of Fluids.' This modest volume has grown into the stately work which, by its one word title, proclaims itself *the* the authority of the generation on what has become one of the most important studies of the generation. Rarely does a book on a scientific subject, which is growing with ever increasing pace, acquire the undisputed standing enjoyed by Lamb's 'Hydrodynamics.' The interval between successive editions has diminished from sixteen years to eight years. One turns to this book, not merely for the well-digested classical treatment of the subject, but also for the most recent developments of a period in which hydrodynamical theory has found most important applications in aviation and in the theory of the tides: and the author does not merely reproduce or condense these later researches, his own treatment adds suggestiveness and criticism that often stimulate to further study.

The author draws attention to the fact that the classical hydrodynamics "often referred to with a shade of depreciation, is here (in aeronautics) found to have a widening field of practical applications." This reference to the so-called Prandtl theory of the aerofoil is an interesting vindication of the applied mathematician's study of idealized problems, such as do not appear to correspond to problems as found in nature. The "perfect fluid," in which viscosity does not exist and which can slide freely over rigid boundaries, seems so unlike what we see in water or air, that it was a surprise to both mathematicians and engineers to discover that, for the treatment of the aerofoil with the vastly complicated motions in the fluid round it, some simple ideas of elementary hydrodynamics combined with the theory of conformal transformation sufficed to afford a remarkably accurate reproduction of the main features of the resistance observed.

This suggests that possibly Sir Horace Lamb is himself somewhat inclined to refer with more than "a shade of depreciation" to what appears to be a very remote representation of fluid motion, but which may nevertheless possess valuable features, namely, the discontinuous motion theory of the resistance produced by a rigid barrier. Apart from the sheer beauty of the mathematical methods, particularly as developed by Levi-Civita, it is a fact that one or two interesting properties of the cambered aerofoil do emerge, like

the forward movement of the centre of pressure as the angle of incidence of the cambered aerofoil is diminished, until a stationary position of the centre of pressure is obtained, when, with further diminution of the angle of incidence, the centre of pressure moves back.

Lamb's 'Hydrodynamics' has long been the accepted standard treatise on the subject both inside and outside English speaking countries, and there can be no doubt that for decades to come it will occupy an honoured place among those books in the mathematician's library to which he turns daily. It is hardly possible to "review" a new edition of a standard treatise which is so well known to all workers in hydrodynamics. Suffice it therefore to say that this great work has been brought further up to date, and is a reliable guide to the fundamental principles, to the mathematical processes, as well as to the main developments of the modern study of the motions of fluids.

Number, the Language of Science. By Tobias Dantzig. (London: George Allen and Unwin, Ltd., 1930. Price 10*s.* net.)

This is a fascinating book about mathematical ideas as exhibited by the evolution of the number concept. Perhaps the best description of the author's aim is that formulated by the author himself: "... our school curricula, by stripping mathematics of its cultural content and leaving a bare skeleton of technicalities, have repelled many a fine mind. It is the aim of this book to restore this cultural content and present the evolution of number as the profoundly human story which it is."

And the author certainly succeeds in his aim. Starting from the primitive attempts at an arithmetical process with various bases, Professor Dantzig discusses the decimal base and becomes more than lyrical about the discovery of zero — "one of the greatest single achievements of the human race." After a chapter on the romantic quest of properties of individual numbers, which, born in religious mysticism, passed through a period of erratic puzzle-solving and then became a real science in the modern theory of numbers, and a discussion of the nature of mathematical induction which involves the tacit assumption that every number has a successor, so that a process must be capable of indefinite repetition, and the concept of infinity emerges as a mathematical necessity, the author deals with mathematical symbolism, and then attacks the main conceptions that characterize the evolution of number.

The progress from the irrationals of the Greeks to the transcendental numbers of the nineteenth century is described under the title of "The Unutterable." Then comes the

ideas of the infinitesimal, involving continuity and the admission of the validity of infinite processes. The author returns to consider the Cartesian representation of numbers and the evolution of complex numbers, and then deals with aggregates, leading on to Cantor's theory and his assertion that there is no last transfinite number.

The book concludes with a table of "milestones in the evolution of the number concept," a very interesting résumé of what the author shows to have been an exciting history covering twenty-five centuries. The style is somewhat florid, and often suggests that the author is out to make an impression. The story of the old lady who objected to stained glass windows because she wanted her glass "the way the Lord made it" only spoils the account of the discovery of transcendentals, and Kronecker's famous phrase: "God made the integer, the rest is the work of man." But, on the whole, the book is eminently readable, both to the layman and to the mathematical specialist.

Collision Processes in Gases. By F. L. Arnot. [Pp. 104 + 37.] (Methuen. Price 3*s*.)

This is yet another of that useful little series of pocket monographs under the general heading "Methuen's Monographs on Physical Subjects."

Dr. Arnot is well qualified to write on the experimental aspect of the subject of collision processes in gases, since for several years he has devoted his attention to a section of this field, both at the Cavendish Laboratory and in the University of St. Andrews, where he is now a lecturer in Natural Philosophy.

The preface points out that attention is focussed, in this book, on single collisions such as are to be expected in gases at very low pressures—and that "the main object is to assist those who are about to begin experimental work . . . . with atoms and molecules of a gas at low pressures."

The opening chapters on critical potentials are accordingly of a rather simple character, but the author soon gets down to a description in general terms of the subject after this introduction.

The scope of the book is sufficiently indicated when it is said that the subjects treated include probabilities of electron excitation and ionization of atoms by electrons, with the inevitable discussion of scattering and effective atom cross-sections. Collisions between atoms and photons, and atoms and atoms also receive some attention.

The monograph can be recommended to students unreservedly.

[The Editors do not hold themselves responsible for the views expressed by their correspondents.]

% Al.

Fig. 1.

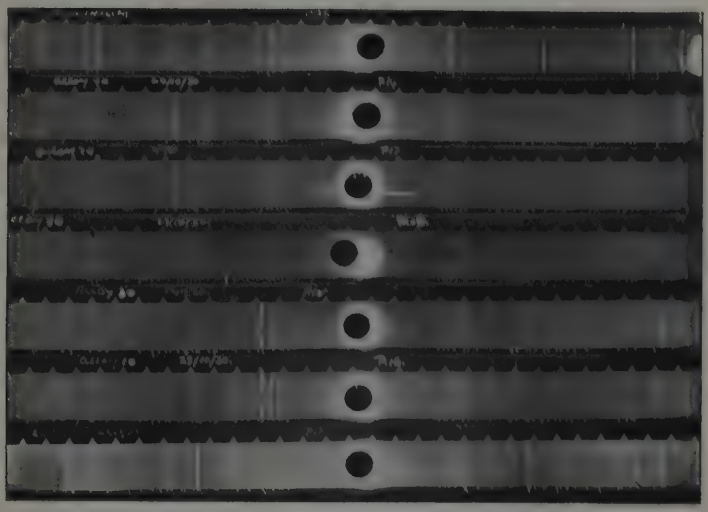

Spectrum photographs of Al Zn alloys annealed at 250° C. and quenched.

Fig. 4

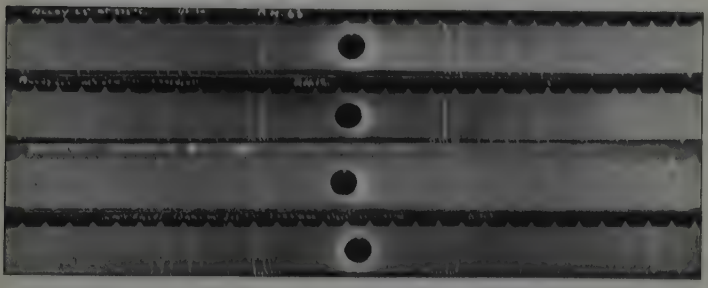

Spectrum photographs of alloy 25

1. Sample at 375° C. during exposure—β-phase structure.
2. Sample at 310° C. during exposure—β-phase structure.
3. Sample quenched from 375° C.; exposure at atmos. temp. $(\alpha + \gamma)$ structure.
4. Sample quenched from 375° C.; exposure at atmos. temp.; $(\alpha + \gamma)$ structure.

% Al. Fig. 6.

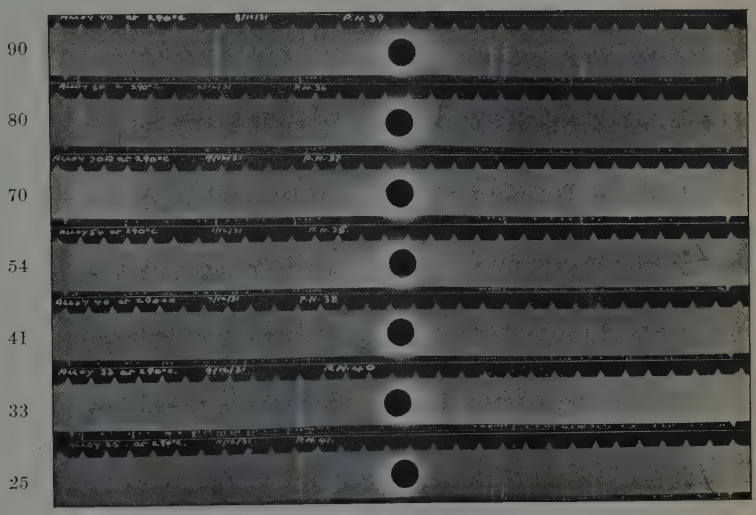

Spectrum photographs of alloys at 290° C. during exposure.

% Al. Fig. 7.

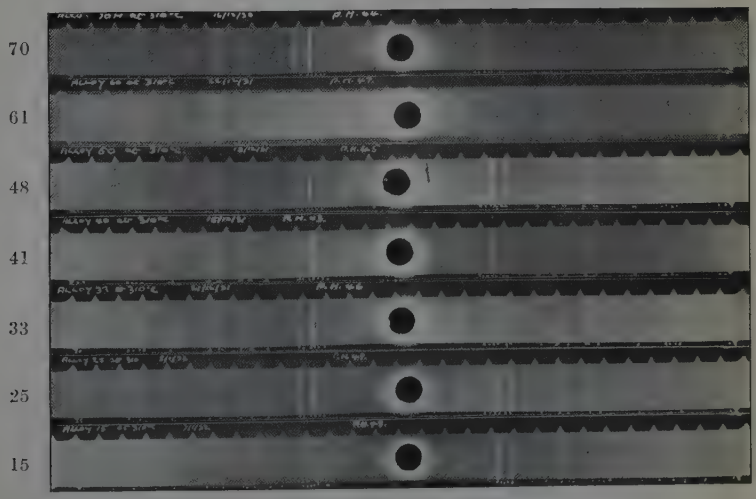

Spectrum photographs of alloys at 310° C. during exposure.
(Note duplex structure of alloys 40 and 50.)

% Al. Fig. 8.

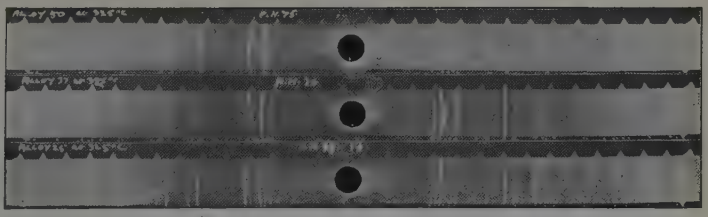

Spectrum photographs of alloys at 325° C. during exposure.
(Showing duplex structure.)

% Al. Fig. 9.

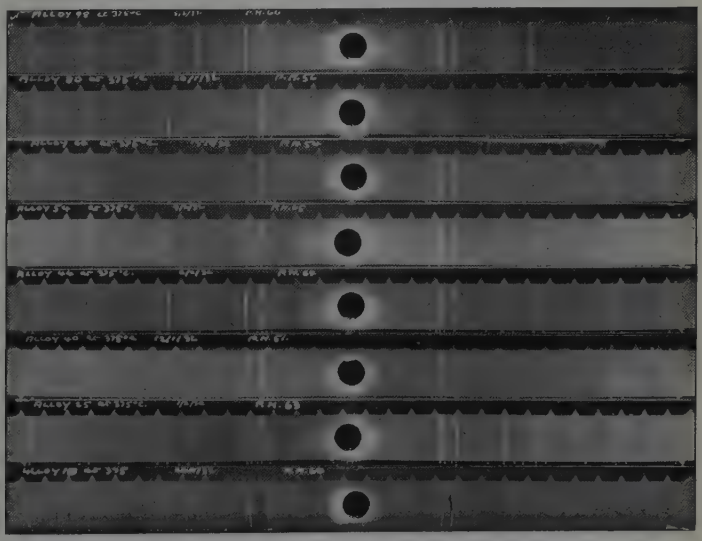

Spectrum photographs of alloys at 375° C. during exposure.

% Al. Fig. 11.

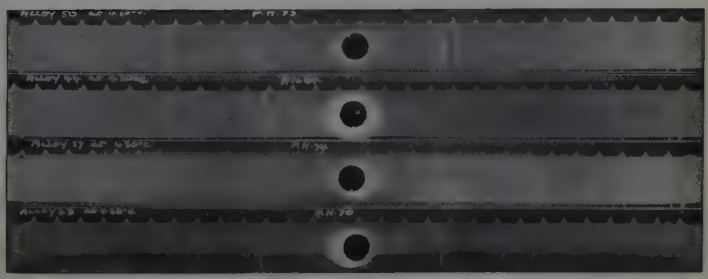

Spectrum photographs of alloys at 430° C. during exposure.

FIG. 1.

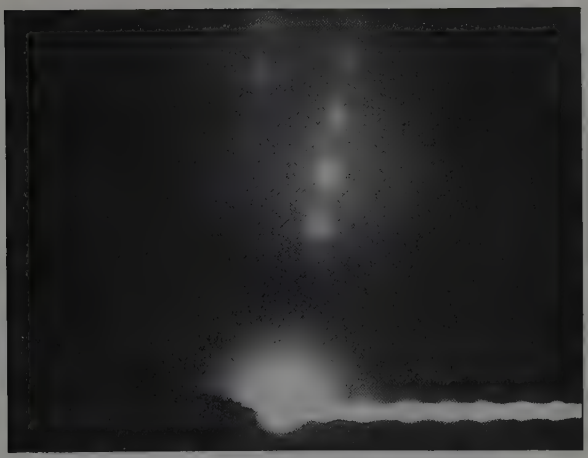

Natural graphite, azimuth 1.

FIG. 2.

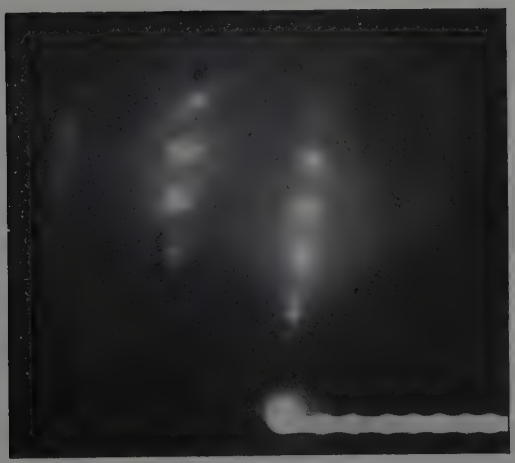

Natural graphite, azimuth 2.

FIG. 3.

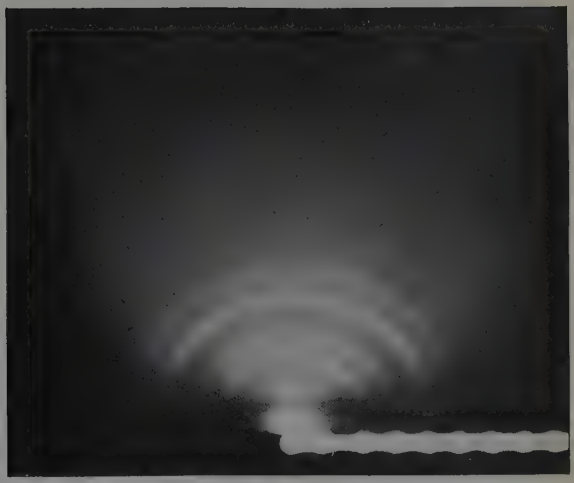

Unorientated graphite ring-pattern.

FIG. 4.

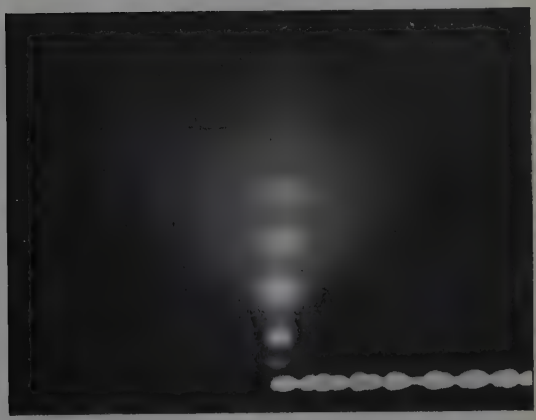

Typical orientated polish-pattern.

FIG. 5.

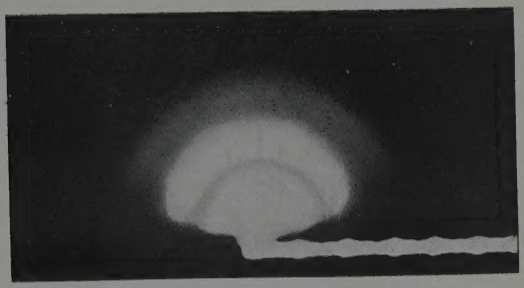

Unorientated rings due to carbon after initial polish.

FIG. 6.

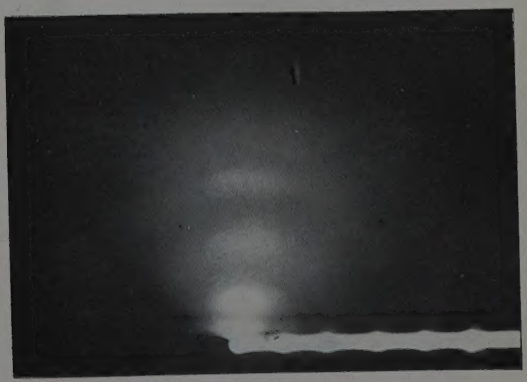

Orientated pattern due to carbon after continued polishing.

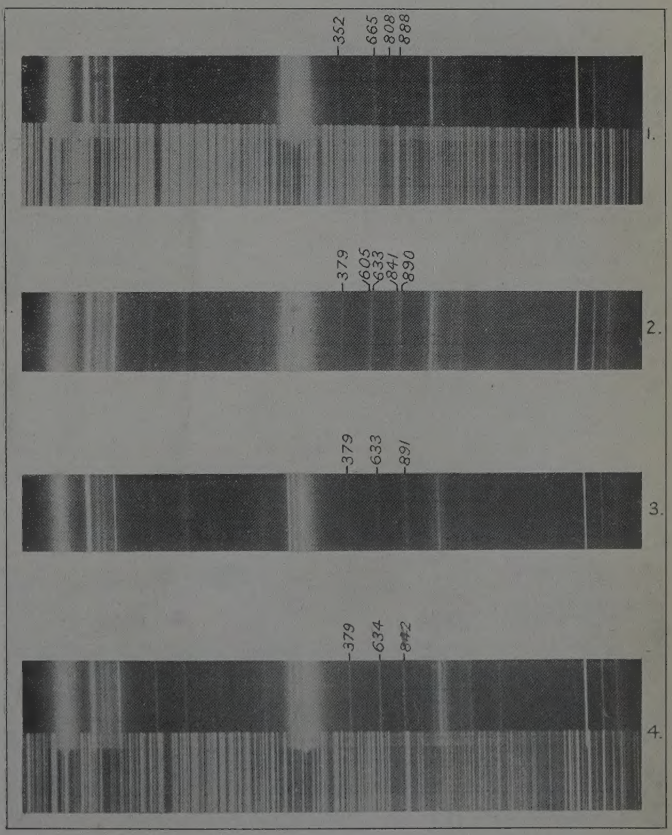

Raman spectra.

FIG. 1.—Acetic anhydride.
FIG. 2.—Acetic anhydride + ethyl alcohol in 1 : 1 molecular ratio.
FIG. 3.—Acetic anhydride + ethyl alcohol in 1 : 2 molecular ratio.
FIG. 4.—Ethyl acetate.